NUMERICAL SIMULATION AND OPTIMIZATION OF TRIPLE SUPERTWIST NEMATIC LIQUID CRYSTAL DISPLAYS

John Patrick Fogarty

B.S. Physics, University of Wisconsin-Madison, 1988

M.S. Physics, University of Wisconsin-Milwaukee, 1992

A dissertation submitted to the faculty of the

Oregon Graduate Institute of Science & Technology

in partial fulfillment of the

requirements for the degree

Doctor of Philosophy

in

Applied Physics

March, 1998

The dissertation " Numerical Simulation and Optimization of Triple Supertwist Nematic Liquid Crystal Displays" by John Fogarty has been examined and approved by the following Examination Committee

Raj Solanki, Dissertation Adviser
Associate Professor

Reinhart Engelmann
Professor

Anthony E. Bell
Associate Professor

Terry Scheffer
In Focus Systems, Inc.

ACKNOWLEDGMENTS

I would like express special thanks to my supervising professor Dr. Raj Solanki for his continuing support in my effort to finish this dissertation.

I would like to thank Dr. Terry Scheffer for his help in this dissertation and for providing the opportunity to work with him as a research intern at Motif Inc. and In Focus Systems Inc. His deep understanding of LCD behavior and in all topics related to display technology were extremely valuable in my efforts to focus on the many issues involved in this dissertation research.

I would also like to thank the good people at Motif and In Focus for the support of my research fellowship. The benefits of working in the display industry and the practical experience it provides can not be matched with purely theoretical investigations. Special thanks to Maria Holmes, who was very helpful in the fabrication of LCD devices used in my investigation. I would also like to thank Arlie Connor for unique insight into the design of TSTN displays.

Thanks also to Dr. Reinhart Engelmann and Dr. Anthony Bell for being on my thesis committee.

This dissertation is dedicated to Paula, Katie and Jack

TABLE OF CONTENTS

LIST OF ACRONYMS

AC	-	Alternating Current
AM	-	Active Matrix
AMLCD	-	Active Matrix Liquid Crystal Display
CIE	-	Commission Internationale de l'Eclairage
CRT	-	Cathode Ray Tube
DC	-	Direct Current
DSTN	-	Double Super-twisted Nematic
EL	-	Electroluminescent
EO	-	Electro-optic
FED	-	Field Emission Display
HTP	-	Helical Twisting Power
ITO	-	Indium Tin Oxide
LC	-	Liquid Crystal
LCD	-	Liquid Crystal Display
LED	-	Light Emitting Diode
OLED	-	Organic LED
PC	-	Polycarbonate
PVA	-	Polyvinyl Alcohol
RGB	-	Red, Green, Blue
rms	-	root mean square
SBE	-	Super-twisted Birefringence

SMPTE	-	Society of Motion Picture and Television Engineers
SR	-	Selection Ratio
STN	-	Super Twisted Nematic
SVGA	-	800 x 600 resolution
TFT	-	Thin Film Transistor
TN	-	Twisted Nematic
TSTN	-	Triple Super-twisted Nematic
UCS	-	Uniform Color Space
VGA	-	640 x 480 resolution
XGA	-	1024 x 768 resolution

LIST OF SYMBOLS

A	-	Absorption
d	-	Cell Gap Thickness
$\vec{D}$	-	Induced Electric Dipole
$\Delta\varepsilon$	-	Dielectric Anisotropy
Δn	-	Optical Anisotropy or Birefringence
$\vec{E}$	-	Electric Field
ϕ	-	LCD Twist Angle
$k_{\perp}$	-	Perpendicular Transmittance
$k_{\parallel}$	-	Parallel Transmittance
k_{11}	-	Splay Elastic Constant
k_{22}	-	Twist Elastic Constant
k_{33}	-	Bend Elastic Constant
λ	-	Wavelength
R_d	-	Dichroic Ratio
T_{10}	-	Fall Time
T_{90}	-	Rise Time
T_{cp}	-	Clearing Point Temperature
V_{10}	-	Threshold Voltage
V_{90}	-	Saturation Voltage
ξ	-	Electro-optic Curve Steepness

LIST OF TABLES

LIST OF FIGURES

ABSTRACT

NUMERICAL SIMULATION AND OPTIMIZATION OF TRIPLE SUPERTWIST NEMATIC LIQUID CRYSTAL DISPLAYS

John Patrick Fogarty

Oregon Graduate Institute of Science & Technology

Supervising Professor: Raj Solanki

An optimization process was undertaken for Triple Supertwist Nematic (TSTN) subtractive color stacked liquid crystal displays. An optical model for an arbitrary liquid crystal cell has been developed. This model, which is based on the Jones matrix method for light propagation through non-depolarizing elements, has been modified to account for the high voltage behavior of Supertwist nematic devices. The model has been used to characterize and optimize liquid crystal cells for use in a subtractive color stack. The simulation has been designed with a graphical user interface to ease the optimization process. Subtractive color display systems have been studied and compared to additive color systems so as to obtain a benchmark for LCD display performance. A process for optimization of the LCD displays has been developed. Liquid crystal displays have been fabricated and characterized so that the modeled optimization could be compared with experimental measurements. The results of the comparison demonstrate that modeling using a simplified Jones calculus model is effective and efficient as compared to the two other approaches which require extensive numerical computation.

1 INTRODUCTION

Flat panel displays have become an increasingly important part of the electronic display market. The conventional CRT is not currently in danger of losing its share of the desktop display market because of its low cost and superior picture quality, but if the current trends continue, flat panel and projection displays will not only create new markets but also begin to erode the dominance of the CRT in its current markets. The portable and large area display market is in a constant state of flux as new technologies develop and become cheaper to produce. Currently the portable or compact electronic display market is dominated by only a few technologies, Electroluminescent Displays (EL) , Field Emission Displays (FEDs), AC and DC Plasma displays, and Liquid Crystal Displays (LCDs)[1].

Electroluminescent (EL) displays, both DC powder and AC thin film are slowly gaining market share, especially in military, avionics and other niche markets. These technologies have shown promise but have several disadvantages, particularly cost. The advantages of EL displays are their wide viewing angle, high contrast, rugged construction and excellent temperature range. The original monochrome designs based on ZnS:Mn (yellow-orange) had good luminous efficiency but efforts to produce comparably efficient phosphors covering the green and blue primaries have not been entirely successful [2]. Another problem with EL displays is the cost associated with the high voltage drivers needed to address the display as well as the complicated electronics. EL displays have been limited in the commercial market to only 5% of their total production because of the

relatively high cost, their high power consumption and their inability to produce bright full color displays. Also starting to appear on the market is organic EL or OLED. These films are made of organic molecules which operate at low voltages (3-20V) [3].

Another emerging technology is the field emission display (FED) which is essentially a flat CRT made from an array of electron emitters. These displays are hampered by a complex manufacturing process although at least one major corporation has recently invested heavily in its development. The lack of initial interest in the technology has lead to high cost and very small incremental improvements in the technology until recently. Currently FEDs have only been produced in small sizes and with only moderate resolution[1].

Plasma displays, both AC and DC, also have problems although the possibility of making large area displays has been proven and developers are beginning to take an interest in this technology. The main problem area for plasma displays is the generally complex panel structure and cost associated with the high voltage drivers required [4]. Plasma displays also suffer from relatively poor contrast typically only 30:1 or worse. Recently, there have been several demonstrations of low volume runs of AC plasma displays with screen diagonals as high as 42 inches. At least four manufactures have committed to high volume manufacturing of these displays although the market is not yet proven and costs are not expected to drop dramatically.

The commercial market for portable and compact displays has been dominated by liquid crystal displays (LCDs)[1]. LCDs are successful because of their low cost, low power consumption and their ability to produce bright full color displays. One reason for the continued success of LCDs in the market is the amount of interest that developers have shown in the technology. As LCDs evolved from watches and calculators to high information content displays, the main problem that had to be overcome was the lack of a steep electro-optic curve which meant that they were limited in the number of rows that

could be multiplexed [5]. In the early 1980s two different solutions were developed. Some researchers concentrated on developing extrinsic addressing methods using thin film transistors at each pixel to control the voltage across the pixel elements. This Active Matrix (AM) technique was expensive and complicated, but produced displays with excellent contrast and good viewing angle as well as video speeds. Another solution was based on the discovery that the steepness of the electro-optic response could be increased if the twist of the nematic liquid crystal was made greater than 90° [6]. This type of display called the Supertwist Nematic (STN) was the first full sized LCD to enter the laptop computer market and because of the low cost of production, STN displays still comprise a good portion of that market [4]. The continued popularity of STNs is due to their low cost and increasingly high performance.

Regardless of the type of display, there are two methods used to obtain color in display systems [7]. The first and most common method is the additive color method. This method uses the traditional additive primaries, red, green, and blue, and combines them either spatially or temporally so that the viewer perceives this combination as a single complex color or grayshade. The second method is the same as that used in color photography and is known as the subtractive color method. In this system, the three subtractive primaries, cyan, magenta, and yellow, are combined in series to produce a complex color or grayshade. The additive color method is particularly suited for emissive displays such as CRTs and Electroluminescent displays where RGB subpixels can be readily made by patterning three additive primary phosphors into pixel triads to obtain a full color display.

In a transmissive display such as an STN, however, the additive color method is not necessarily the best solution and the subtractive color method offers several advantages [8]. One of the most important advantages is the possibility of higher transmission. In an additive system, each sub pixel blocks at least two thirds of the

visible spectrum, which means that even in the white state in which all of the sub pixels are on, the display absorbs two thirds of the light. For a display using a polarizer, the maximum transmission would be 16.6%. The subtractive system on the other hand blocks none of the spectrum when each of the cells is selected leading to a rough theoretical transmission of 50% for a display with ideal polarizers. Of course there are other losses due to incomplete polarization, reflection, and interpixel gaps so that a typical additive system usually only realizes about 4.5 - 6.5 % transmission while subtractive color designs have been developed with transmissions as high as 14.0 %. This increased transmission is especially important for portable displays where battery life is a concern. It is also important for contrast when it is not possible to completely eliminate ambient light in projection applications. Another advantage is in the reduction of "jaggies" when diagonal lines are drawn. Additive designs that use color filters only make use of one of the sub pixels when primary colors are displayed leading to an unattractive jagged effect in diagonally drawn lines. Subtractive displays use the full pixel to display the desired color, which leads to better perceived resolution.

Because of the importance of subtractive color liquid crystal display systems, especially in projection applications, an in-depth study of modeling and optimization of subtractive color displays, specifically the Triple Supertwist Nematic (TSTN) [9], was undertaken.

This thesis is divided into 7 chapters, after this introduction, Chapter 2 has a brief introduction to liquid crystal displays, both Supertwist (STN) and twisted nematic (TN). Chapter 3 contains a review of methods of achieving color in LCD systems and the merits of each system as well as an in-depth investigation of the various subtractive color designs. Chapter 4 is a review of the Jones calculus method of LCD modeling and a description of computer simulation based on the Jones calculus that was developed. Chapter 5 is a description of compensation methods in STNs and the process used to

compensate and optimize subtractive color LCD systems with the use of a graphical modeling program developed during the course of this investigation. Also included are examples of the use of the optimization process and comparisons of optimized and unoptimized systems.

2 REVIEW OF STN AND TN DISPLAYS

Liquid crystal displays (LCDs) first became commercially available in the early 1970s [10] as low information content watch and calculator displays. Since that time, the performance of LCDs has rapidly improved leading to the high information content color displays found in today's notebook computers and portable devices. LCDs have many advantages, including low power consumption, as well as versatility which enables their use in projection as well as direct view applications. Soon the LCD may even replace the CRT as the choice for desktop monitors because of its light weight and small footprint.

Twisted Nematic (TN) LCDs are capable of producing high contrast displays in direct drive applications [11]. However, the TN effect has difficulty producing a high contrast ratio at the high multiplex ratios found in high information content passively addressed displays [12]. This problem is due to the very shallow electro-optic curves that the TN LCDs exhibit, and the low selection ratio afforded by the rms drive schemes. At first, it was thought that these limitations could be overcome by finding new classes of liquid crystal material that had elastic constant ratios that would provide steeper electro-optic curves, but while some improvements did take place, it was apparent that materials capable of high multiplexing in the TN mode would likely not be found. In the 1970's, there were attempts to make instrument displays with limited pattern drive schemes which only allowed the simultaneous display of only one pixel per column, but these attempts fell far short of consumer expectations and were eventually abandoned[13].

During the mid 1980's, several major developments occurred. One development was that of using active substrates for the TN displays to allow for high multiplexing[14].

These active substrates use thin film transistors (TFTs) that are capable of delivering and holding a voltage at a pixel without significant crosstalk. The results were unparalleled, highly multiplexable displays but because of low yields, they were very expensive to produce and availability was limited. Another development was the discovery of the Supertwist Birefringence Effect (SBE), later known as the Supertwist Nematic Effect [15] (STN), which will be the focus of this dissertation. The STN effect was discovered as a result of computer modeling which showed that the electro-optic curve could be made steep, even infinitely steep with twists in the nematic layer between 180° and 270°. This development made it possible to use standard addressing techniques and achieve a high contrast ratio in a high information content passive matrix display.

2.1 Liquid Crystals

Liquid crystals have been studied since the second half of the 19th century. The first report of the liquid crystalline phase was made by Austrian botanist Friedrich Reinitzer in 1888 [16]. Most liquid crystals have the unique property that they flow and take the shape of their container like isotropic liquids, but they also have an orientational order like that found in crystalline solids. This unique behavior can be considered a partial melting where upon reaching a certain temperature, the LC molecules lose positional order but maintain orientational order. Upon further heating to a temperature known as the clearing point, T_{cp}, the LC finally loses its orientational order as well and enters the isotropic phase of an ordinary liquid.

While there are many classes of liquid crystals, only two classes of liquid crystal have been shown to be suitable for flat panel displays, smectics and nematics[16]. Ferroelectric LCDs use smectic liquid crystals which are rod like molecules that not only have orientational order, but also have a degree of one dimensional positional order. TN

and STN LCDs use the nematic liquid crystal which have only orientational order. For some applications nematic liquid crystals are commonly doped with small amounts of optically active chiral molecules which give them an intrinsic pre-twist. Cholesteric liquid crystals are nematic liquid crystals that have a built-in chiral component and therefore require no doping in order for the director to twist.

The average preferred direction of the long axis of the molecules in a local region of a nematic liquid crystal is described by a unit vector $\hat{n}$ called the director or local optic axis as shown in Figure 2.1.

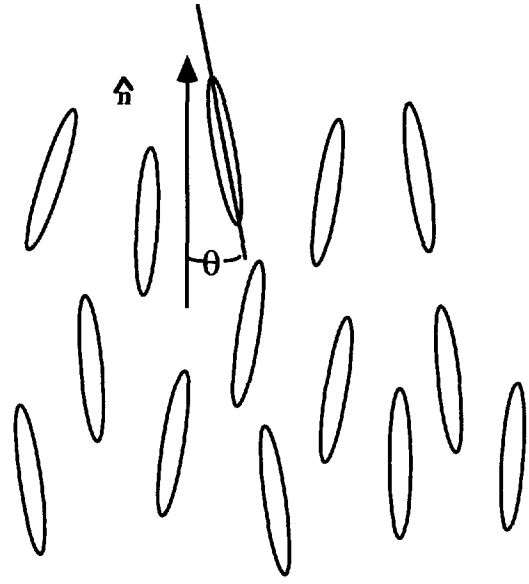

Figure 2.1 A representation of a nematic liquid crystal and the molecular director $\hat{n}$ associated with the liquid crystal and the angle θ with respect to the local molecular director.

The degree of orientation of nematic liquid crystal molecules is described by an order parameter S, defined by the average value of a function of the angle θ between the molecular axis and the local optic axis $\hat{n}$ [16].

$$S = \frac{1}{2}\langle 3\cos^2\theta - 1\rangle \qquad (2.1)$$

The order parameter S is temperature dependent and as the LC approaches the clearing point, it becomes less and less ordered until at T_{cp}, S abruptly drops to zero.

The long range orientational order of the nematic ordering of the molecules leads to anisotropies in many of the liquid crystalline properties, the dielectric constant anisotropy and optical anisotropy being the most important for the understanding of LCDs. The dielectric constant anisotropy is what allows electrical fields to reorient the molecules while the optical anisotropy is what accounts for the change in optical properties when the molecules reorient. The dielectric anisotropy $\Delta\varepsilon = \varepsilon_{\parallel} - \varepsilon_{\perp}$, is the difference in the dielectric constant parallel and perpendicular to the director. If the dielectric anisotropy of the LC is positive, the director will align parallel with the electric field while a negative dielectric anisotropy makes the molecules align perpendicularly with the electric field.

Optical anisotropy or birefringence $\Delta n = n_e - n_o$ is the difference between the principle refractive indices parallel and perpendicular to the director. The ordinary refractive index n_o corresponds to an "ordinary" ray with the electric vector oscillating perpendicular to the director or optic axis. The extraordinary index n_e corresponds to the "extraordinary" ray which has its electric vector oscillating parallel to the optic axis. For typical nematic liquid crystals, Δn lies in the range $0.06 < \Delta n < 0.25$. For comparison, Δn of quartz is 0.0091 and Δn of calcite is 0.172[17].

2.2 Passive Matrix Display Cell

A passive matrix liquid crystal display cell consists of a thin layer (~ 4-10 μm) of liquid crystal material sandwiched between two transparent substrates, typically glass but possibly plastic. The substrates are treated with several thin film coatings. The first coating is usually an ion migration barrier layer of SiO_2 to prevent sodium ions from

migrating from the soda-lime glass during high temperature processing. Next there must be a layer of indium tin oxide (ITO) or some other suitable transparent electrically conductive film. The LCD manufacturer generally purchases the glass with the barrier layer and ITO already applied. The ITO glass is then covered with an insulating topcoat, usually SiO_2-TiO_2 to prevent conductive particles from causing shorts between the two layers of ITO in the display cell. A rubbed polyimide or other surface alignment layer is then used to align the liquid crystal molecules at the surface. Some electro-optic effects require that the molecules have an initial tilt or pretilt at the surface which can be accomplished by controlling the chemical composition and processing of the polyimide alignment layer. Both the topcoat and polyimide layers are generally applied using an offset printing method. Figure 2.2 shows a cross-section of a typical STN LCD display.

Two of these coated substrates are brought together and glued with either spherical or fiber spacers separating them. The liquid crystal material then fills the gap between the two substrates.

The transparent conductor is patterned, so that specific areas of the display can be addressed with information. In most cases, the ITO is patterned in horizontal lines on one substrate and vertical lines on the other substrate creating a matrix of display elements known as pixels where the top and bottom electrodes overlap. With this type of passive matrix there are MxN addressable pixels with only M+N electrical connections where M is the number of columns and N is the number of rows in the display. The pixels are not entirely independent though since many pixels share a common electrode. The challenge in addressing passive matrix displays is developing drive schemes which allow the pixels to be independently switched even though they may share common electrodes.

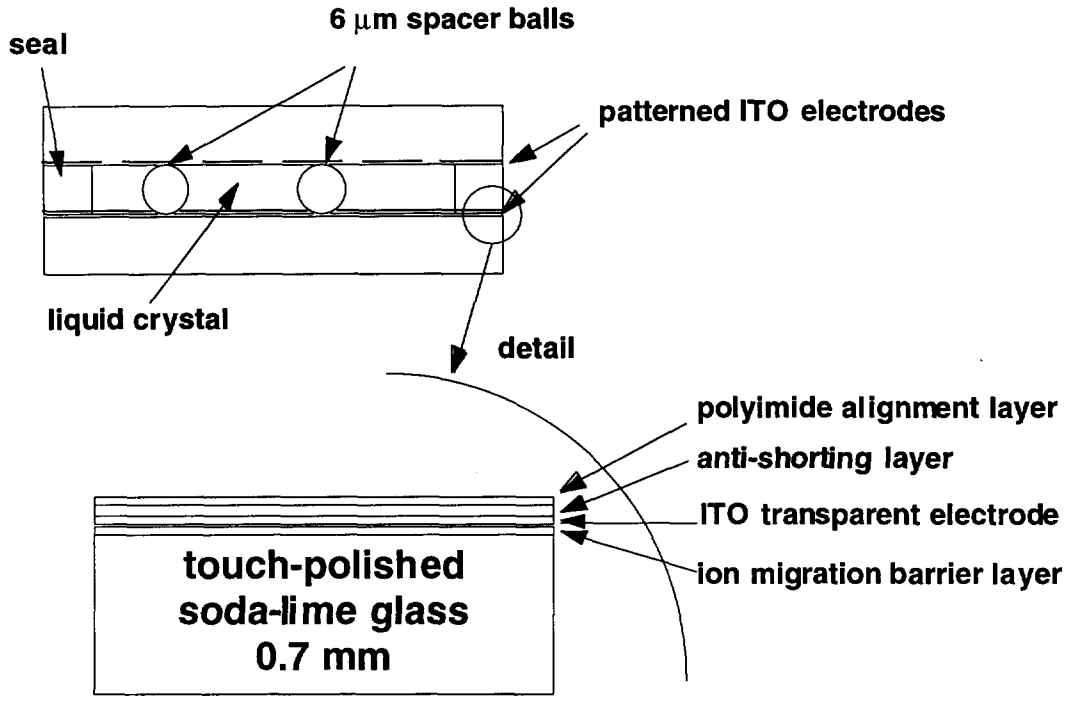

Figure 2.2 The cross-section of a typical STN LCD display cell.

2.3 Response of Liquid Crystals to Electric Fields

Thin layers of ferroelectric liquid crystals have a spontaneous permanent electric polarization and therefore respond differently to positive and negative applied electric fields. There is no permanent polarization of the electric dipoles in the molecules of nematic liquid crystals and so the TN and STN electro-optic effects are polarity independent. To see this, consider the nematic molecules where the induced dipole is proportional to the electric field ($\vec{P} \propto \vec{E}$). The induced dipole then interacts with the electric field so that we have an interaction which depends on $\vec{E}^2$. In practical drive schemes, there must be no net DC voltage across the pixel because DC voltages tend to cause irreversible electro-chemical reactions which reduce the life of the display and may

lead to temporary image retention. Typical STN and TN display response times are in the 20-200 ms range and are directly proportional to the square of the cell thickness. These response times are slow compared to the frame period of the addressing signal and tend to have an integrating effect, such that the optical state of nematic liquid crystal displays is determined by the average value of $\vec{E}^2$ or equivalently the rms value of the voltage across the pixel. We can define the electro-optic behavior of an LCD in the normally black mode by three main parameters[18]:

- Threshold voltage (V_{10}): The voltage for which the display is 10% on as measured optically.
- Saturation voltage (V_{90}): The voltage for which the display is 90% on as measured optically.
- Response times (T_{90} and T_{10}): The time that the liquid crystal device takes to reach 90% on from full off (rise time) and the time it takes to reach 10% on from full on (fall time).

From these another more useful parameter can be obtained, the steepness of the electro-optic curve $\zeta = (V_{90})/(V_{10})$ for normally black mode and $\zeta = (V_{10})/(V_{90})$ for normally white mode shown in Figure 2.3. The steepness of the electro-optic response curve is determined by the cell geometry and the LC material constants. There are three relevant liquid crystal elastic constants for a TN or STN display: the splay elastic constant k_{11}, the twist elastic constant k_{22} and the bend elastic constant k_{33}. For STN displays, steeper electro-optic behavior can be obtained by an increase in the ratio k_{33}/k_{11}, and also by decreasing the ratio k_{22}/k_{11}.

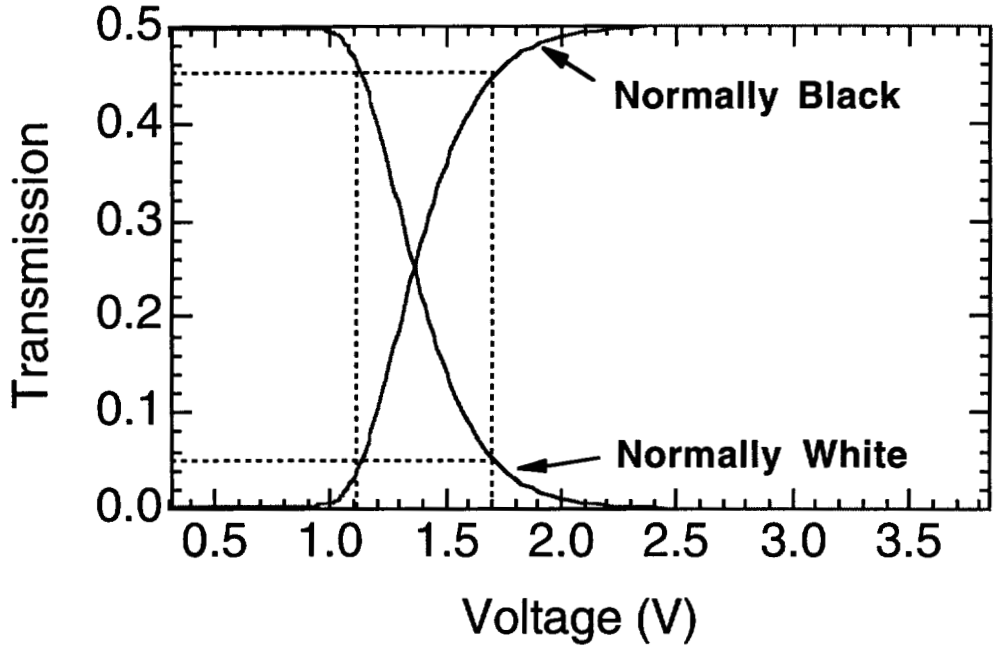

Figure 2.3 Showing a typical TN Electro-optic curve and two of the curve parameters, V_{10} and V_{90} in both the normally white and normally black modes assuming ideal polarizers. Notice that the two curves are complementary.

In a now famous paper, Alt and Plesko showed that for rms responding devices addressed with voltage modulation, there is a limitation to the on to off rms voltage ratio that can be achieved across a pixel [19,20]. This is of course due to the fact that each display element in a matrix display is not truly independent because of the shared electrodes. The maximum selection ratio, SR, i.e., the ratio of the select voltage V_{on} or V_{sel} to the nonselect voltage V_{off} or V_{ns} is given by

$$SR = \frac{V_{on}}{V_{off}} = \sqrt{\frac{\sqrt{N}+1}{\sqrt{N}-1}} \quad , \tag{2.1}$$

where N is the number of rows in the matrix display. This known as the "iron law of rms multiplexing" because it was later shown that, for all intents and purposes, this is the best

that can be done regardless of the types of addressing waveforms chosen. The steepness of the EO curve should be tailored to the multiplex ratio. Empirically, we find that for an STN device to operate with high contrast and transmission, (ζ-1) should be equal to about half of (SR-1)[21]. Figure 2.4 shows the way in which the selection ratio decreases as the number of multiplexed lines is increased.

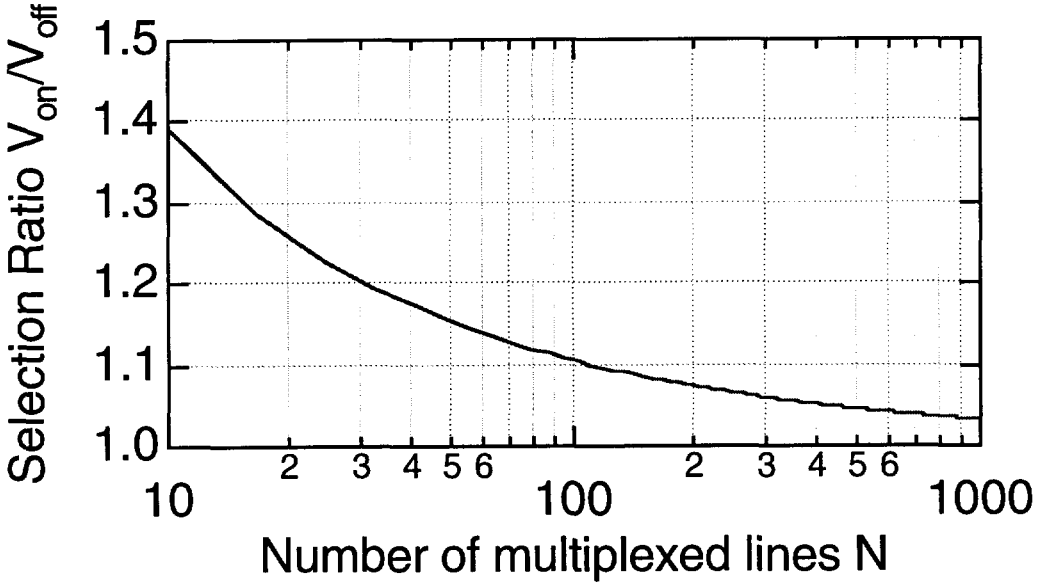

Figure 2.4 Selection ratio as a function of multiplexed lines for rms responding devices

2.4 Twisted Nematic Field Effect

Depending on the way in which a liquid crystal cell is constructed, there are different ways in which the electro-optic behavior of the device may manifest it self. One of the earliest liquid crystal effects discovered was the twisted nematic field effect. The twisted nematic LCD is made with the alignment layers treated to give the molecular axis of the liquid crystal material very small tilt or pretilt on the order of 2° - 4° . TN displays require a sufficient pretilt in the cell in order that tilt domains are not formed

while maintaining a low enough pretilt so that the sharpness of the electro-optic curve is not reduced for a multiplexed display. The substrates are assembled with the rubbing directions of each substrate perpendicular to each other, resulting in a uniform 90° twist in the liquid crystal material between the substrates. The 90° twist in the LC layer behaves like a waveguide. Incident light will rotate its polarization by 90° in step with the twisted structure provided that the plane of polarization of the incident light is either perpendicular or parallel to the director at the surface of the cell, and the product Δn^*p is large compared to the wavelength of the light (Mauguin condition, Chapter 4), where p is the pitch of the liquid crystal defined by the length over which the director rotates by 360°. In the case of a 90° twist cell, the pitch is just four times the thickness of the cell. When linearly polarized light is incident on the display cell, the light will emerge linearly polarized in an orthogonal direction. When a sufficiently strong (3x threshold) electric field is applied, the directors of the liquid molecules tend to align in the direction of the field so that 90° twist in the structure is lost and the polarization will not be rotated at all.

Twisted nematic cells may operate in one of two modes, the positive contrast mode or normally white, and the negative contrast mode or normally black. In the normally white mode, neutral polarizers are placed on the top and bottom of the cell aligned either parallel or perpendicular to their respective directors at the surfaces as in Figure 2.6. This state is normally white since unpolarized light incident on an undriven cell will become linearly polarized upon passing though the input polarizer and will then undergo a complete 90° rotation where it is passed by the output polarizer. When a pixel in the cell is activated, meaning that an electric field has been applied across the pixel, the light that passes from the input polarizer is not rotated and the output polarizer analyzes (blocks) all of the light leaving a dark pixel. The normally black mode of operation is achieved by placing the input and output polarizers parallel to each other which gives the

complementary mode. Figure 2.3 shows an example of the electro-optic characteristics of a typical TN device for normally black and normally white modes. One important thing to realize with regards to the normally white mode of operation is that when the cell is in the select state, there remains a thin transition layer of liquid crystal on both the top and bottom substrates which are anchored along the rubbing directions. This leaves, in effect, two equivalent uniaxial birefringent layers which exactly compensate each other since they are oriented at 90° with respect to each other. The compensation of these two layers is what gives the normally white mode contrast ratios in the 100-200 range. Figure 2.5 shows the contrast ability of each mode as a function of the voltage applied to the select state. The normally white mode is the standard in today's active matrix, high information content displays. Some low information content passive TN displays such as those found in calculators and watches also use the normally white mode while others such as those found in automobile clocks and radios use the normally black mode.

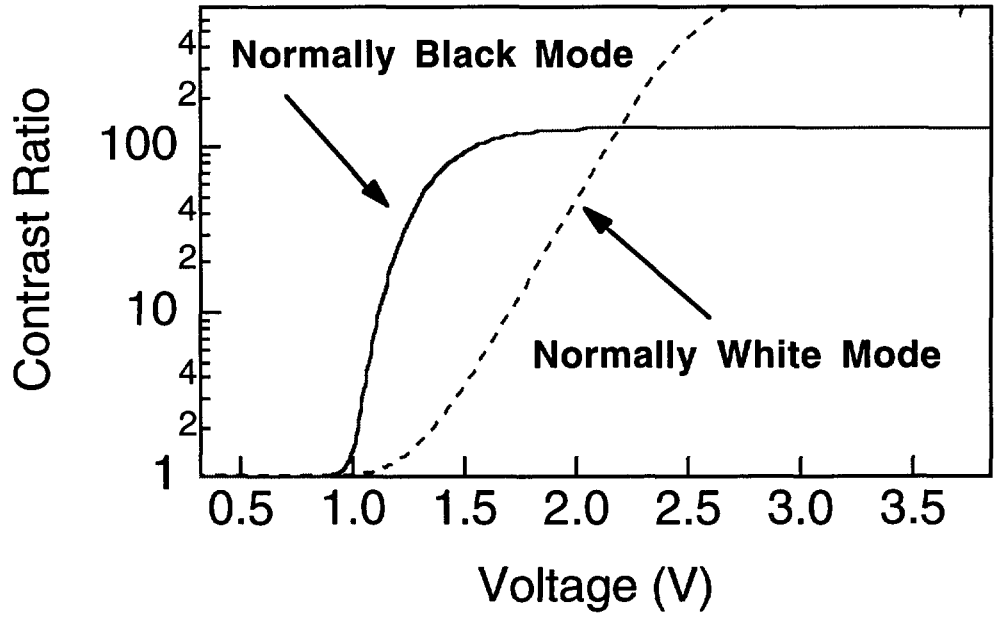

Figure 2.5 Contrast ratio as a function of voltage for the normally black and normally white modes. Notice that the contrast of the normally white mode can be better, but only with higher voltage drivers.

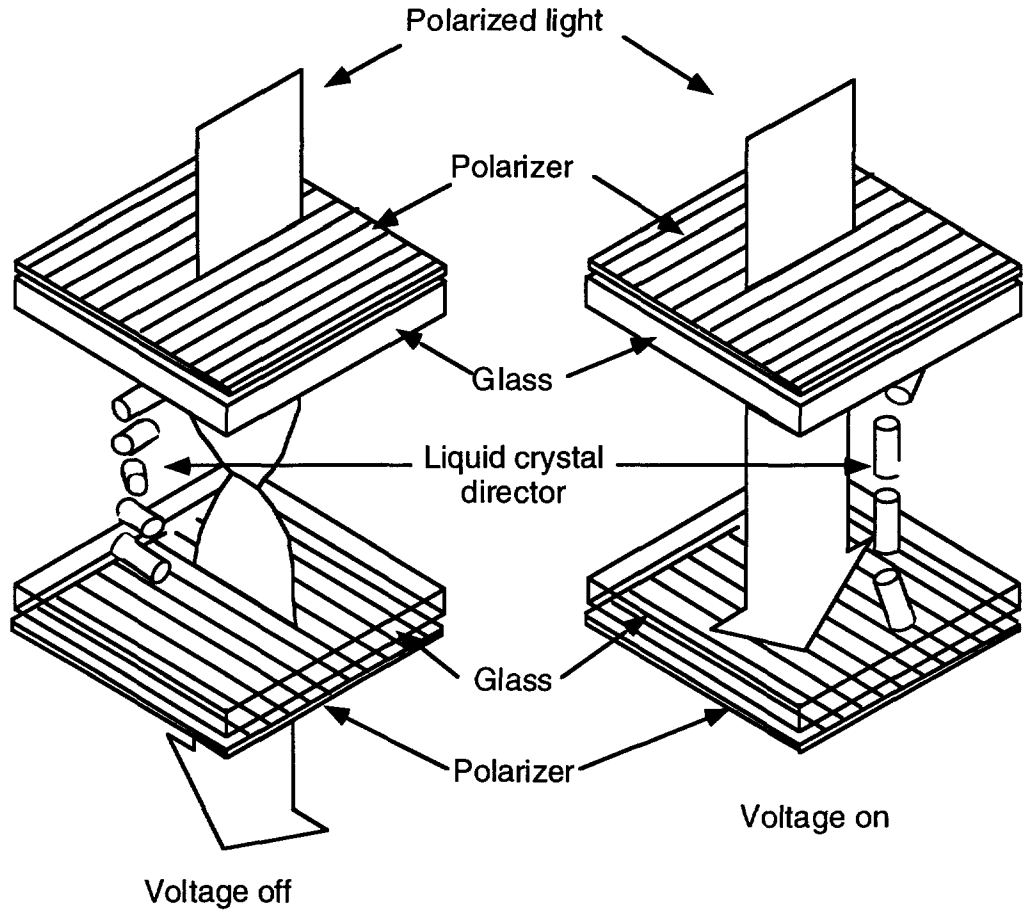

Figure 2.6 A TN cell operating in the normally white mode. In the off state, the local optic axis undergoes a continuous 90° twist. In the on state, the optic axis is oriented parallel to the applied electric field in the center of the layer.

2.5 Supertwist Birefringence Effect

Another important liquid crystal effect is the supertwist birefringence effect. It was discovered in early 1980's that the steepness of the electro-optic curve of an LCD is highly dependent on the twist of the liquid crystal and that displays could be designed with infinitely steep and even double valued electro-optic curves if the twist of the LC was greater than 240° for some LC materials[5]. In a typical Supertwist Nematic (STN) display, the twist angle is chosen between 180° to 270° depending on the LC mixture and

the desired steepness of the electro-optic curve (Figure 2.3). To obtain twists greater than 90° requires that optically active dopants known as chirals be added to the nematic liquid crystal. The amount of chiral in the chiral nematic mixture is determined by both the desired twist and the thickness of the cell and it is usually about 1.0% by weight for typical materials.

While the TN and the STN displays are both twisted nematic structures with the directors anchored on the boundaries, the STN does not operate in exactly the same way that the TN operates. In the TN mode, polarizers are placed either parallel or perpendicular to the directors at the surface, This configuration excites only one normal mode so that either the ordinary or extraordinary rays traverse the cell. The pitch of the STN is 2-3 times smaller than the pitch of the TN so the STN is not even close to obeying the Mauguin condition(Chapter 4). This means that the propagating modes in an STN are elliptically polarized. The polarizers in an STN display must be placed in directions off-axis with respect to the director at the surfaces of the cell to optimally excite the two normal modes and achieve satisfactory contrast through their interference. The ellipticity of the normal modes are related to the pitch and the wavelength of the light. When transmitted through a layer with twist angle ϕ, linearly polarized light becomes elliptically polarized with ellipticity ε given by[22]

$$\varepsilon = \tan\left[\frac{1}{2}\sin^{-1}\left(\frac{2u}{1+u}\sin^2[\phi(1+u^2)^{1/2}]\right)\right] \qquad (2.2)$$

where $u = \pi\Delta nd/\phi\lambda$.

For a TN display, we take $\phi = 90°$, $\Delta nd = 550$ nm and $\lambda = 550$ nm which gives an ellipticity of $\varepsilon_{TN} = 0.088$ a very low degree of ellipticity. For an STN display, we take $\phi = 240°$, $\Delta nd = 1100$, and $\lambda = 550$ nm which gives $\varepsilon_{STN} = 0.24$ which is considerably

higher. Because of the elliptical polarization in an STN, the polarizer angles are chosen so that the transmission has a minimum at approximately 550 nm. This leads to the highest photopic contrast. True black and white operation can only be achieved by external compensation of the elliptically polarized light by retarders or the Double STN method (see Chapter 5).

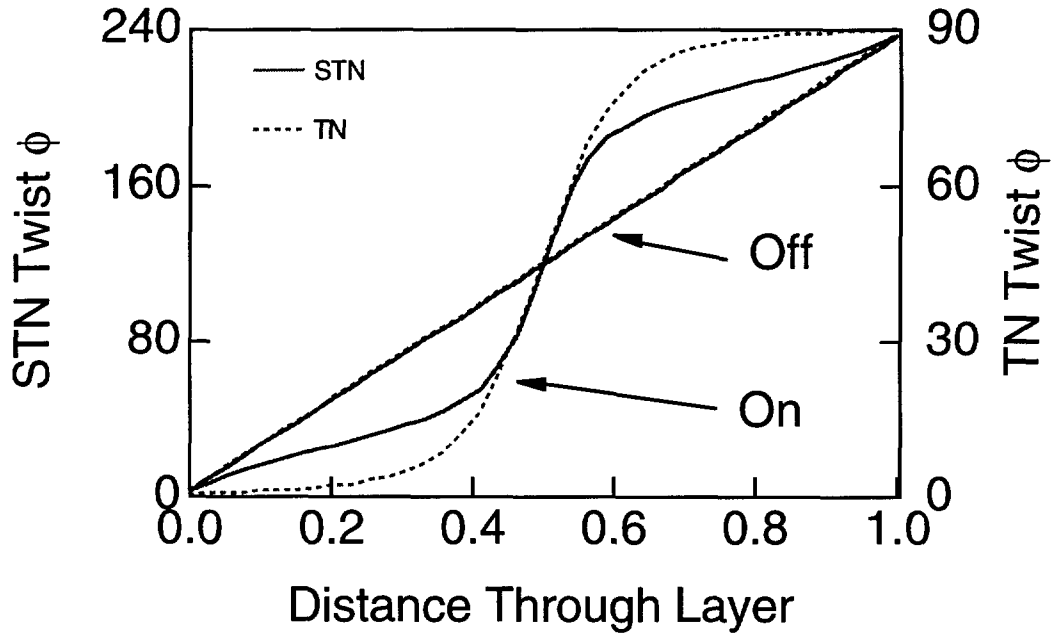

Figure 2.7 The twist of TN and STN cells as a function of distance through the layer for the select and non-select states.

For proper operation, STN displays require that the director have a pretilt of 4° - 10° at the surfaces of the cell[5]. If the pretilt is too low, the liquid crystal molecules can form an in-plane striped texture which scatters light and makes the cell impossible to multiplex[23]. The normal configuration of the director in a twisted nematic device is known as the Freedericksz configuration. In this configuration, the director only changes its orientation perpendicular to the LC layer. The striped distortion is caused by the presence of an energetically favorable configuration in which the director changes its

orientation in a direction parallel to the LC layer as well as perpendicular to it. There are several device and material parameters that influence the formation of the striped texture, but only a few of these stabilize the Freedericksz configuration without reducing the steepness of the electro-optic curve[5].

Increasing the twist of a nematic device is not the only way to influence the electro-optic performance of the display. Studies show that there are several device and material parameters that affect the steepness and shape of the electro-optic curve [5]. The steepness of the electro-optic curve is related to the steepness of the electro-distortional curve which is a measure of the midlayer tilt as a function of voltage. The electro-distortional curve is influenced by twist angle, pretilt angle, d/p (cell gap thickness to pitch) ratio, elastic constant ratios and the dielectric anisotropy.

3 Color In Liquid Crystal Displays

There are several methods that may be used to obtain a full color liquid crystal display. Each method may be placed into one of three broad categories, temporal, spatial, and coincident [24]. These categories refer to the manner in which the light is received by the observer and the way in which it is perceived. There are also two broad categories that describe the type of color mixing that occurs in the display itself, additive and subtractive. Table 3.1 shows a few of the most popular types of liquid crystal displays and the color mixing categories in which they belong. Notebook computer displays use additive color mixing in which the three additive primaries, red, green, and blue are combined in parallel with varying intensities to obtain the desired color via spatial observer mixing. The LCD uses spatial separation of the primaries into red, green and blue color triads much as in a color shadow mask CRT. The triad must be small enough that the eyes perceives it as coming from one source, in effect adding the primaries to form a single color. Another form of color mixing is subtractive, really multiplicitive, color mixing in which the three subtractive primaries, cyan, yellow and magenta, which are complements of the additive primaries, are combined in optical series to obtain the desired hues. Subtractive color is inherently coincident, as light from the display pixel has already been combined by spectral multiplication, the same process as used in color film development. Figures 3.1 and 3.2 show a comparison of additive and subtractive color technologies.

Table 3.1 Color mixing in different types of displays.

Display Type	Display Mixing	Observer Mixing
TSTN	Subtractive	Coincident
Color Stripe AMLCD	Additive	Spatial
Dichroic Mirror	Additive	Coincident
Color Shutter	Additive	Temporal

The visual electromagnetic spectrum covers the wavelength range from roughly 380 nm -780 nm. For a broad band source, the additive primaries are each one third of the spectrum. The convention that blue light covers the range from 380 nm -500 nm, green light 500 nm -600 nm, and red light from 600 nm- 780 nm will be used in this discussion. The subtractive primaries are the colors that result when one of the additive primary colors is removed from a balanced white light source. A magenta filter absorbs (or reflects) green light while passing blue and red light relatively unattenuated. Cyan similarly passes green and blue light while blocking red light. Yellow light is the result of removing blue light from white light. When these three subtractive filters are placed in series, the optical spectra are multiplied, each filter removes one portion of the spectrum rendering black. Two of the filters in series will give one of the additive primaries. Figure 3.3 shows the subtractive and additive primaries and their relation to one another. From this figure we see that mathematically speaking:

$$\text{Cyan} = \text{Blue} + \text{Green} = 1 - \text{Red}$$
$$\text{Yellow} = \text{Green} + \text{Red} = 1 - \text{Blue}$$
$$\text{Magenta} = \text{Blue} + \text{Red} = 1 - \text{Green}$$

where unity represents white light.

It should be emphasized that for the subtractive color system to work properly, each cell must effectively eliminate one third of the spectrum. A yellow cell must not only appear yellow but it must in fact extinguish a substantial portion of the blue light. In other words, the color coordinate of the subtractive primary is not nearly as important as the actual transmission spectrum.

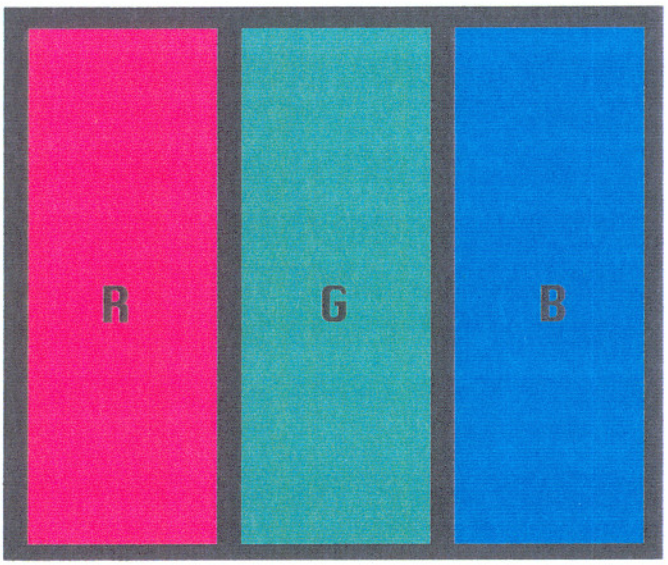

Figure 3.1 Additive color mixing, shown in the spatially separated mode. To show cyan, magenta, yellow or white, two or more subpixels must be addressed simultaneously.

There are three unique ways to make a three layer subtractive color stack, the permutations only depend on which subtractive primary, cyan, yellow or magenta is placed in the center of the stack, since it is immaterial which direction the light propagates through the stack. As will be presented in Chapter 5, there are very important reasons why only one of these permutations is used in the design of subtractive color STN LCD displays.

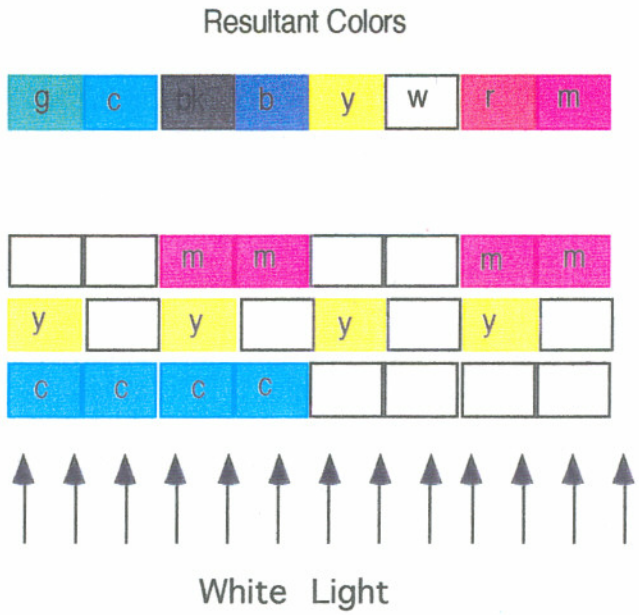

Figure 3.2 Subtractive color mixing, which is always coincident. Showing three layers, each with eight pixels, stacked on top of one another. No subpixels are necessary since each stack of pixels can show any color.

3.1 Measuring Color

Throughout this dissertation, colors will be specified by their coordinates on the 1931 CIE chromaticity diagram [25] shown in Figure 3.3. Any color that the 1931 CIE standard observer can perceive is uniquely represented by a point on this diagram as well as a brightness figure which corresponds to a third coordinate, Y, perpendicular to the x-y chromaticity plane. Colors located near the boarder of the diagram are considered saturated, while colors in the interior are washed out pastels. Changes in hue are measured by movement along the outside border. Any color can be located on this diagram either by direct measurement using a colorimeter or by measuring the spectral power distribution of the radiation. Most color measurements that were obtained for this investigation were done so using the spectral distribution method. There are other, more recent color space diagrams such as the 1976 CIE - UCS Chromaticity diagram[26] which

are better at representing color differences, but these diagrams and conventions have not been widely used and so will not be used here.

Spectral measurements were made using a Model 704 SpectraScan by Photo Research. This type of spectraphotometer uses an array of over 300 photodetectors along with a diffraction grating to measure the photometric intensity in 2nm increments over the range 380nm to 780nm. Transmission measurements of LCDs and color filters can be quickly made using the computer interface software which automatically divides the measured sample spectra by the previously measured source spectra.

Once the transmission spectrum T(λ) has been determined, the chromaticity coordinates x, y, brightness Y as well as photopic transmission T can be computed for any given source spectrum S(λ) by use of the equations below[25].

$$x = \frac{1}{Q}\int S(\lambda)\bar{x}(\lambda)T(\lambda)d\lambda \qquad (3.1)$$

$$y = \frac{1}{Q}\int S(\lambda)\bar{y}(\lambda)T(\lambda)d\lambda \qquad (3.2)$$

$$Y = \int S(\lambda)\bar{y}(\lambda)T(\lambda)d\lambda \qquad (3.3)$$

$$T = \frac{\int S(\lambda)\bar{y}(\lambda)T(\lambda)d\lambda}{\int S(\lambda)\bar{y}(\lambda)d\lambda} \qquad (3.4)$$

where Q is given by

$$Q = \int S(\lambda)\bar{x}(\lambda)T(\lambda)d\lambda + \int S(\lambda)\bar{y}(\lambda)T(\lambda)d\lambda + \int S(\lambda)\bar{z}(\lambda)T(\lambda)d\lambda \qquad (3.5)$$

and $\bar{x}(\lambda)$, $\bar{y}(\lambda)$and $\bar{z}(\lambda)$are the tristimulus values tabulated by the CIE in 1931. The integrals are over the visible wavelength range 380nm to 780nm. The integral can be computed numerically or, as is typically done, by conversion to a summation. Radiation below 400nm and greater than 700nm does very little to influence the chromaticity or brightness of a color and therefore the sum may in fact be taken from 400nm to 700nm if

necessary. Some direct color measurements were taken with the model CS-100 Chroma Meter by Minolta. This device returns color data directly, giving x, y, and Y values.

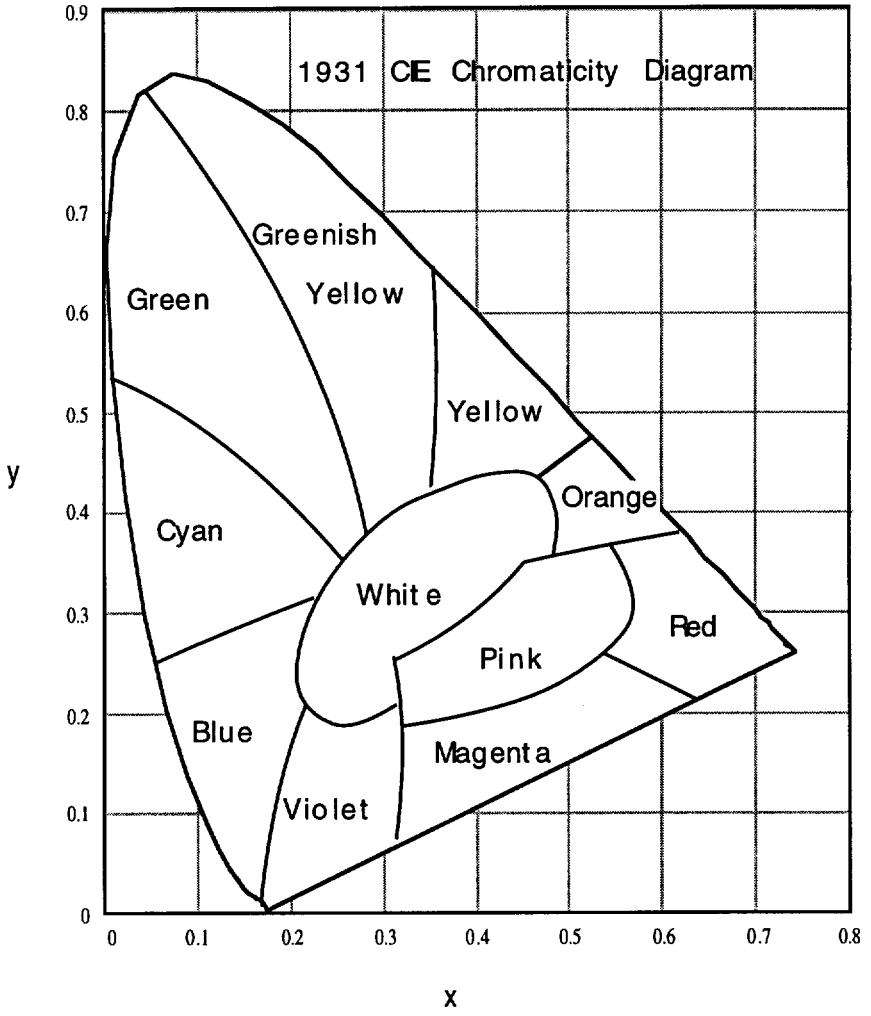

Figure 3.3 1931 CIE Chromaticity Diagram showing the location of various colors[25]

Assuming a broad band, white light source, any color besides white must have a transmission of less than 100% since at least some portion of the incident illumination must have been absorbed (or reflected) in order for the display to appear colored. The

highest luminous transmission possible for any given color has been determined by MacAdam and is shown in Figure 3.4. The luminous transmission of a display should be as close as possible to the maximum for any color.

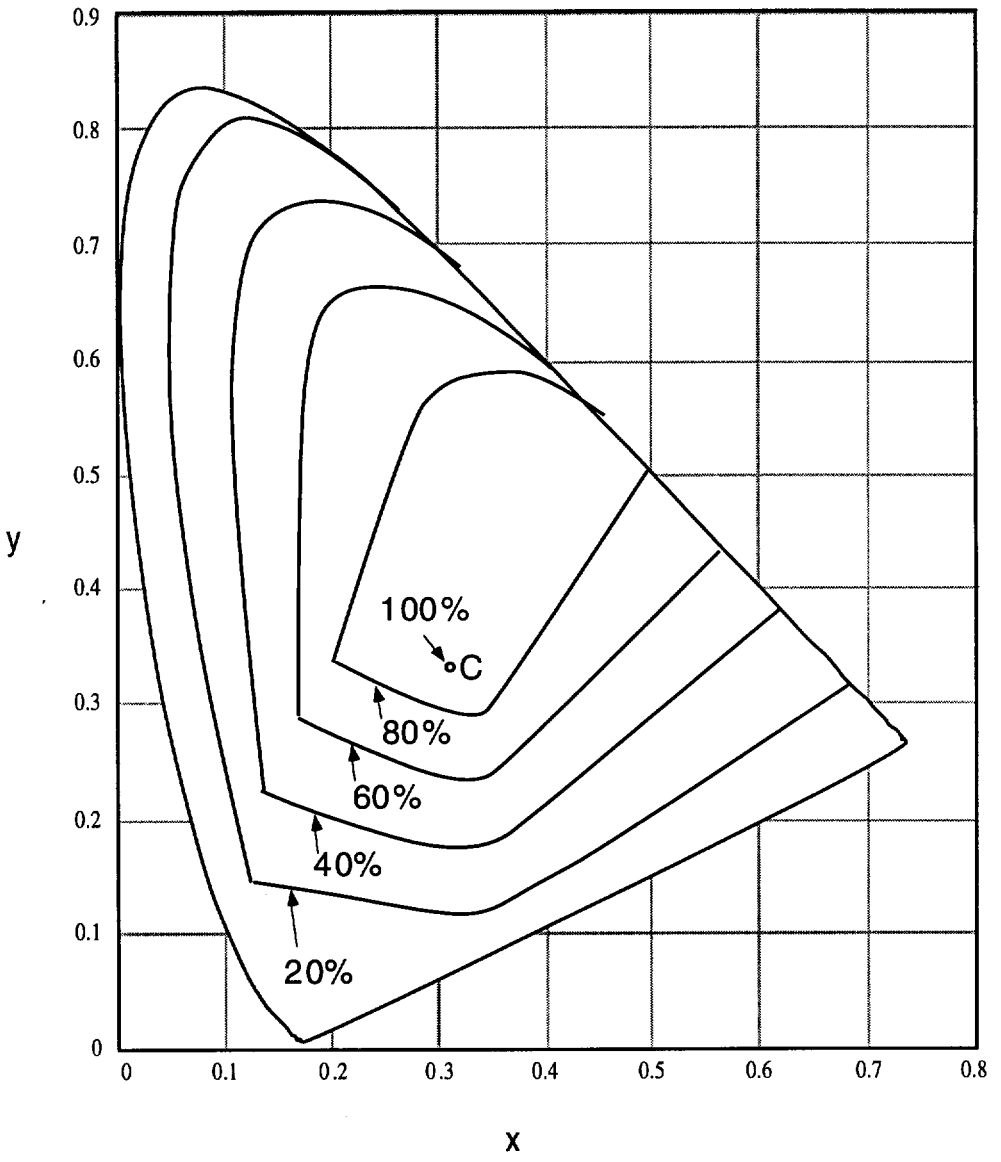

Figure 3.4 Showing the maximum transmission possible for a given color coordinate assuming light source C as designated by the CIE[25].

3.2 Subtractive color modeling in LCDs

Subtractive color liquid crystal displays can be thought of as an electronic transparency with each cell in the stack representing the presence or absence of one subtractive dye. Each layer in the stack modulates the intensity of its complementary additive color. In the normally black mode, the select state of a cyan cell, should appear uniformly colorless, while the nonselect state should block the transmission of red light, making the pixel appear cyan. Yellow cells should likewise block blue light while magenta cells should be able to block the transmission of green light.

There are many different types of displays that can be used to design a color stack composed of three subtractive color units. Guest-host LCDs are an obvious choice. A guest-host display is an LCD which has both alignment layers parallel to each other so that there is no twist in the structure. An external polarizer is aligned with its transmission axis parallel to the liquid crystal. An added dichroic dye is aligned by the liquid crystal material in much the same way that added dichroic dyes are aligned by stretched polyvinyl alcohol (PVA) to form polarizers. When the pixel is off, the dye absorbs light like a color filter would. When the pixel is on, the dye aligns with the electric field and the pixel becomes colorless. Because there is no twist in the structure, the electro-optic curve is even shallower than that of a TN cell. This shallowness of the EO curve is further exacerbated by the fact that the guest-host effect is a volume effect which means that large voltages are required to sufficiently decrease the thickness of the boundary transition layers and turn the cell fully on. The shallow EO curve precludes its use in high information content passive addressed displays. The guest-host could be used in an active matrix, but the high voltages required make this expensive and impractical considering the need for three cells.

The next two most likely candidates for subtractive color passive addressed displays are the TN or STN cell but again the TN cell has the same disadvantage as the

guest-host cell, low contrast in a high information content passive matrix. This leaves us with the STN which can be produced relatively cheaply so that three cells without color filters are approximately the same cost as a single color filter STN. Our study will focus on the theoretical and practical limits in terms of color, brightness and contrast for subtractive color using STNs.

The next question is how to generate the subtractive color switching capabilities in an STN cell. There are two ways to get color in an STN. The first and most obvious way is to use the natural birefringence color that the STNs exhibit when placed between neutral polarizers[5,27]. As described in the previous chapter, the STN effect excites both the ordinary and extraordinary normal modes and these modes interfere causing a coloration when combined with an output polarizer. By choosing the liquid crystal and device parameters properly, it is possible to produce a fairly broad gamut of colors. Color selective dichroic polarizers which, when combined with the LCD's ability to rotate light, can also be used to produce color in an LCD[8,9,28]. Since color can be produced in an STN in two ways, we must look at the limitations and requirements of each of these methods.

3.2.1 Cholesteric Polarizers

Cholesteric color selective polarizers are being developed which can circularly polarize light over a selected waveband. For use with STN, these must be converted to linear polarizers with a quarter waveplate. Cholesteric polarizers have several advantages over their linear counterparts. First, the minimum wavelength of the absorption band can be easily tuned. Secondly, because they are interference polarizers rather than dye polarizers, the edges are very steep which gives good separation of primaries. The main disadvantage to using these types of polarizers is that they do not have good contrast.

Cholesteric polarizers usually leak between 2% and 5% when crossed. This leakage would result in a maximum contrast of 10:1 which is very poor.

One solution to this problem is to combine the cholesteric with a very weak linear color selective polarizer. The combination of the polarizers result in a single polarizer which has respectable contrast as well as better separation of the primaries as compared to the linear color selective polarizers alone. Fig 3.8 shows the transmission of a cyan dichroic color selective polarizer combined with a converted cyan cholesteric polarizer.

Although this may seem like the best possible solution for TSTN, the demand for cholesteric polarizers is not high enough to merit extensive development by chemical companies.

3.2.2 Color Selective Polarizers

Color selective polarizers are dichroic dye polarizers which have been designed so that, unlike neutral polarizers, the dyes do not absorb the entire optical spectrum. For instance a cyan color selective polarizer absorbs red light when its transmission is crossed with linearly polarized light and passes all light equally when parallel to the linearly polarized light. As long as the LCD rotates the vibration axis of linearly polarized light 90° in one of its states, the performance of the color polarizer becomes the determining factor in the limit of the display system. For this reason it is important that we consider the theoretical limits of dichroic color selective polarizers as well as the status of the currently available polarizers. To fully understand these limits, we must remove the effect of the LCD on the performance of the display. The theoretical limitations and current state of the art are investigated under certain conditions. First, it is assumed that the source used in each model is a continuous black body type source with a color temperature of 6500° K. Secondly, to remove the influence of the LCD, each LCD is

assumed to be a perfect 90° rotator of light in one state and perfectly transparent in the other state. Aperture ratios of each cell are assumed to be 100%.

To fully specify the behavior of a polarizer, the transmission spectra of the polarizer must be taken for orthogonal polarizations. Polarizers are measured with the spectraphotometer as follows. A neutral polarizer is placed in front of a tungsten halogen light source to give linearly polarized light. On top of this is placed a single sheet of clear glass to simulate the reflection losses of the sample. The "source" is measured and the clear glass is removed. The polarizer which is to be measured is then placed with its transmission axis first parallel and then perpendicular to the linearly polarized light and the transmission spectra are measured yielding $T_{\parallel}(\lambda)$ and $T_{\perp}(\lambda)$. These two spectra completely specify the behavior of the measured polarizer.

Crossing color selective polarizers only blocks light in the portions of the spectrum that both polarizers analyze. Hence a red polarizer crossed with a yellow polarizer will appear reddish yellow since the only part of the spectrum that they both analyze is blue. When using color selective polarizers, it is important to understand the proper way to multiply the transmission spectra of each polarizer to in order to get the desired result. Since input light is unpolarized, we must average the results we would obtain from the two orthogonal situations. For instance, if we cross a cyan polarizer with a green polarizer the resulting transmission spectrum for an unpolarized light source is given by

$$T(\lambda) = \frac{C_{\perp}(\lambda) \cdot G_{\parallel}(\lambda) + C_{\parallel}(\lambda) \cdot G_{\perp}(\lambda)}{2} \qquad (3.6)$$

where $C_{\perp}(\lambda)$ is the transmission spectra of the cyan polarizer in when crossed with polarized light, $C_{\parallel}(\lambda)$ is the transmission spectra when parallel with polarized light and similarly for $G_{\perp}(\lambda)$ and $G_{\parallel}(\lambda)$.

As discussed in the introduction, there are three distinct ways to make a subtractive color stack. When using color polarizers exclusively, each different configuration requires a different set of color selective polarizers. We need to determine the types of color selective polarizers required in any one of the three configurations. Lets look at the first configuration, with magenta at the top, yellow in the middle, and cyan at the bottom. We know we must start with a magenta polarizer on top, since we need to analyze green but nothing else yet. The next polarizer controls both a magenta cell and a yellow cell so both green and blue must be analyzed, this means we need a red polarizer. The next polarizer is part of both the yellow cell and the cyan cell so red and blue need to be analyzed, we need a green polarizer. Finally, the last polarizer needs to be cyan since it only controls a cyan cell. As shown in Figure 3.5 in this and the other two configurations, we have two subtractive primary color polarizers on the inside and two additive primary color polarizers on the outside.

First, block-type dichroic dyes are modeled to get an understanding of the theoretical limits of the technology. Block-type dyes are dyes that have infinitely steep edges on the absorbtion bands. Non-overlaping block-type dyes give the maximum possible transmission. Next, the color gamut of the best currently available dichroic polarizers is shown. Current color selective polarizers define the limits of what may be the best performance that can reasonably be achieved.

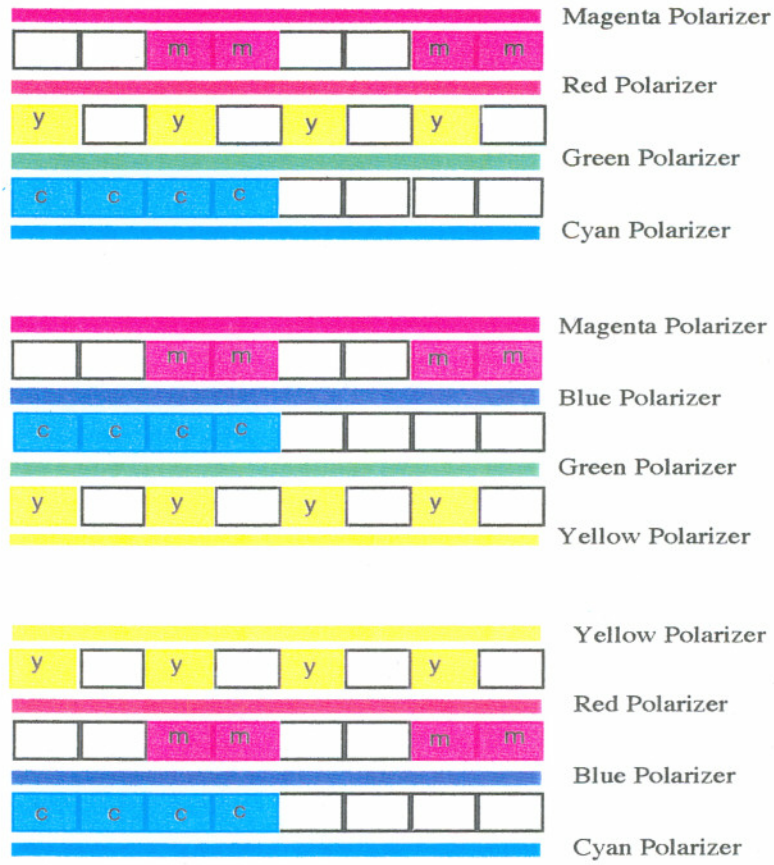

Figure 3.5 The three different ways in which a subtractive color display can be made with color selective polarizers. The resultant colors for each case will appear the same as in Figure 3.2.

3.2.2.1 *Block-type Dichroic Polarizers:*

A block-type filter is one in which the band pass edges of the filter are infinitely steep. A subtractive primary block-type filter blocks one third of the visible spectrum in a single band while an additive primary block-type filter passes one third of the visible spectrum in a single band. It can be shown that the color gamut of a combination in series of perfect subtractive primary block-type filters with no overlap, is identical to the combination of the complementary additive filters when combined in parallel[29]. One result of this is that the CIE coordinates of the combination of the subtractive block-type

filters form a perfect triangle just as do additive color filters. Additive three color systems always have a triangular color gamut when plotted on the 1931 CIE chromaticity diagram. This is because the spectra are being added together and the diagram is designed to be geometrical in nature. The color coordinate of the resultant must lie on the line joining the two original colors. In a subtractive system, the spectra are multiplied. Any overlap in the subtractive color filters results in a CIE gamut that is bowed outward at the subtractive color positions. Because block-type dyes have no overlap, they behave just like additive systems in the way in which colors are added. One important difference is that the maximum transmission for a subtractive color system made with perfect subtractive dichroic polarizers is 50% while an additive color stripe system using perfect polarizers and perfect block-type color filters can only pass 16.66% of the incident light as stated in the introduction. It can also be shown that the maximum saturation for any hue is always formed from filters in which the spectral transmittance have only values of one or zero, and that the spectrum has at most two transitions between zero and unity[30].

We see that theoretically, with perfect LCDs and block-type dichroic dyes the subtractive system is three times more transmissive. The area of the color gamut in a block dye arrangement is fixed. Depending on the choice of cutoffs though, the color triangle may be shifted so that either red, green or blue become more or less saturated.

Figure 3.6 shows the color gamuts of three different block-type dye configurations. Block dye configuration 1 has a yellow dye with perfect cut at 500 nm, magenta dye cut at 500 nm and 600 nm and cyan dye with cut at 600nm. Block dye configuration 2 has yellow cut at 500 nm, magenta cuts at 500 nm and 590 nm, and cyan cut at 590 nm. Block dye configuration 3 has cuts at 500 nm and 580 nm. This block-type dichroic polarizer can be considered the limit of any subtractive display since there is not any overlap in the absorption spectra. Perfect spectral colors are undesirable since each

subtractive color must block one third of the spectrum and should pass as much of the remaining spectrum as possible so as to have the highest possible transmission. We can see from this experiment, in Figure 3.6 that the color gamuts of the non-overlapping block dye configurations are approximately constant in area. In other words, for a given source the only advantage that can be made in modifying the cut points of the block dye configurations is in rotating the triangular color gamut. No improvement can be made in expanding the overall area of the color gamut while maintaining the same color saturation levels.

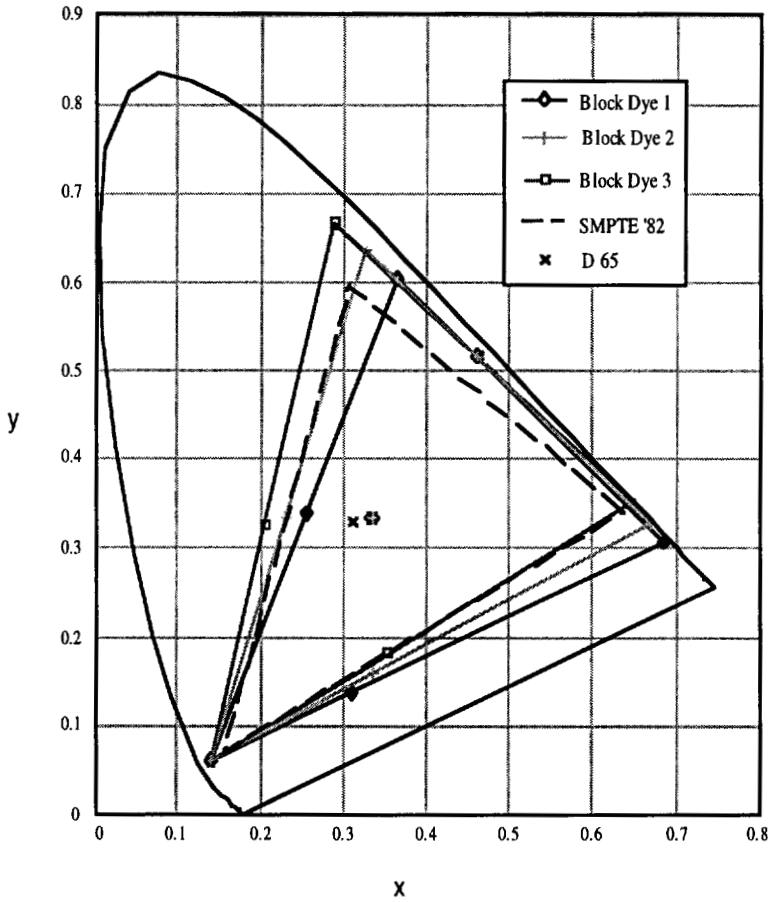

Figure 3.6 Color gamuts of three different block dye configurations. The SMPTE 1982 color primaries are shown for reference.

3.2.2.2 *Current Color Polarizers*

As shown in the previous section the performance of subtractive color LCD displays is very much dependent on the types of colored polarizers available. Currently the technology is hampered by a lack of high quality colored polarizers. The best set of currently used polarizers have several shortcomings. Figure 3.7 and Figure 3.8 show the transmission spectra of the cyan and magenta polarizers that are currently used in most TSTN products[21]. The cyan polarizers tend to have very poor green edges. The cyan polarizer is intended to modulate only the red portion of the spectrum, but in fact substantial modulation of the green will occur as well. The magenta polarizers have an excellent red edge but suffers from severe modulation of blue. Additive primary color selective polarizers have the worst performance, especially green which requires at least two different dyes to absorb the red and blue. The result is significant overlap resulting in very poor edges with reduced transmission in the green portion of the spectrum.

If we measure the best set of currently available polarizers for each configuration we would have an idea of the maximum possible contrast and transmission that can be expected from each configuration with current polarizer technology. A study was done which measured the transmission, contrast and gamuts of our best set of currently available polarizers for each of the above configurations. Table 3.3 shows the polarizers used in the study.

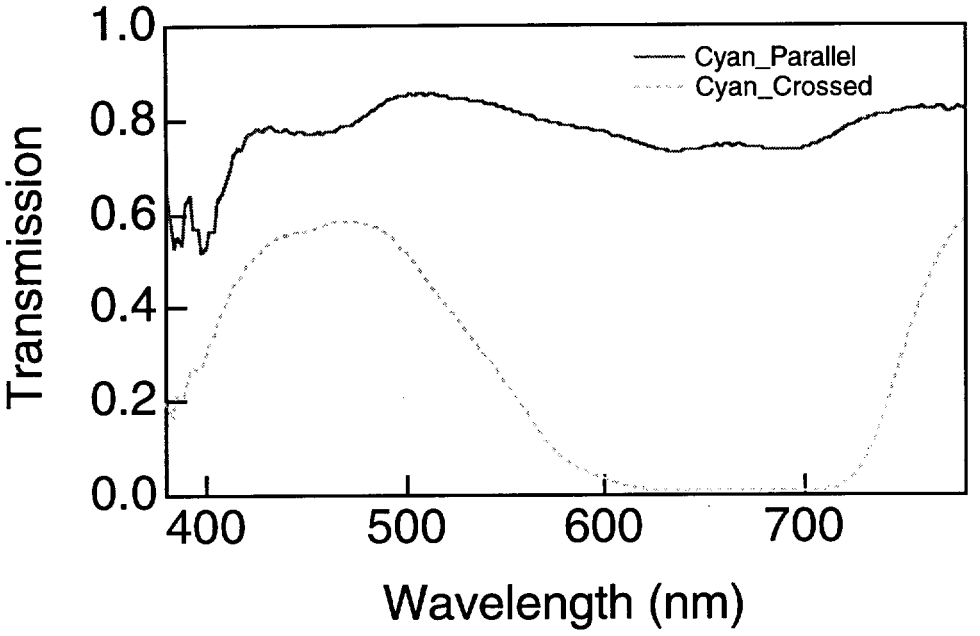

Figure 3.7 The transmission spectra of the best currently available cyan polarizer with pass axis both parallel and crossed to linearly polarized light.

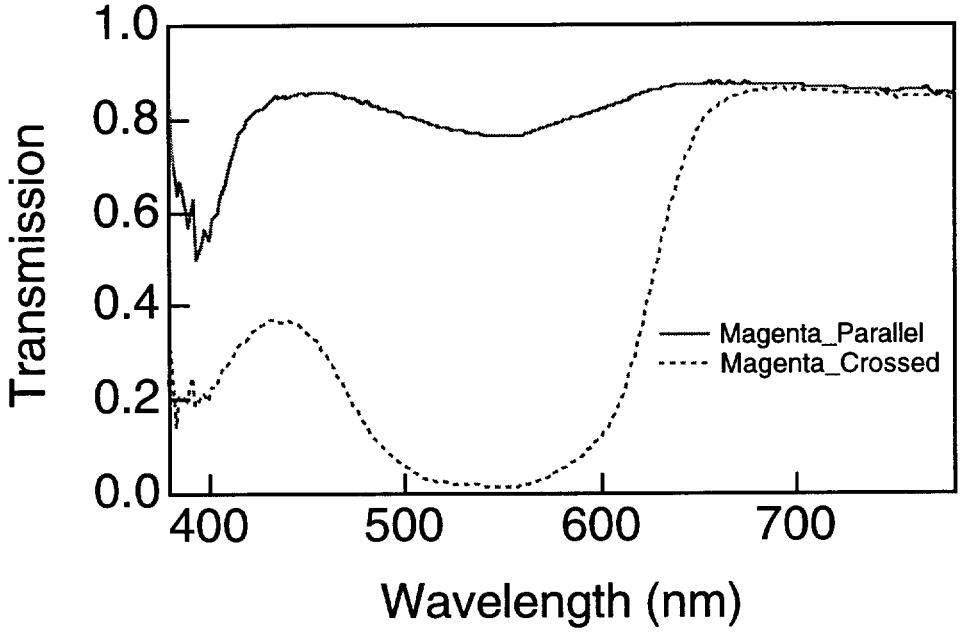

Figure 3.8 The transmission spectra of the best currently available magenta polarizer with pass axis both parallel and crossed to linearly polarized light.

Table 3.2 Best set of color polarizers used in the measurements

Polarizer Color	Best Available
Cyan	Sanritz CC2B
Yellow	Polatechno Y4
Magenta	Polatechno V36-18245-T
Red	Polatechno VC2-R01-18SL
Green	Polatechno G-18245T
Blue	Sanritz CC2B(Cyan) + SSC2S(Violet)
Neutral	Polatechno SKN-18245T

Table 3.3 shows the contrast and transmission that has been measured for each of the three configurations of Figure 3.5 as well as a configuration using birefringence color for the center yellow cell (Section 3.2.3) using the polarizers in Table 3.2 . The polarizers were measured as follows. The polarizers were all laminated on to glass slides. An unpolarized source was measured with four transparent slides to remove the loss due to surface reflections. The transmission of the light was then measured with a polarization insensitve spectro-photometer in each of the eight possible distinctive orientations of the polarizers assuming just two orientations per polarizer. Since the orientation of the first polarizer is not important, the next three polarizers can take one of two values, either crossed or parallel to the first polarizer. This yields eight orientations and eight colors, including black and white, from which the transmission and contrast can be obtained. These values would indicate the theoretical maximum since it assumes that the LCD itself is a perfect rotator of polarized light. For measuring the standard configuration which uses birefringence color, the central yellow cell was measured both in the select and non-

select state with the other two polarizer having two possible orientations again yielding eight distinctive colors.

Table 3.3 Measured transmission and contrast of the four configurations using best available polarizers, and assuming perfect LCD performance.

Configuration	Transmission	Contrast
MRGC	19.69	90:1
MBGY	18.42	108:1
YRBC	17.17	151:1
Standard TSTN (CNNM)	21.53	156:1

The only configuration besides the standard TSTN that does not have an objectionable greenish color in the black state is CGRM but that also has the lowest contrast and suffers from a very poorly saturated yellow and blue primaries.

3.2.3 Birefringence Color

The birefringence coloration of an STN may also be used to produce colors. It is possible to create a wide range of colors by placing an LCD cell between two neutral polarizers which can be oriented in any direction with respect to the surface director orientations, but subtractive color requires that each cell is able to switch between a colorless state and a state in which one additive color is extinguished. When polarizers are oriented at $\pm$ 45° to the director orientations there will be equal excitement of both normal modes and destructive interference will take place in at least one wavelength. Figure 3.9 shows these birefringent colors produced between neutral polarizers oriented as above for a variety of different values of Δnd. When an STN cell is turned fully on, the effective

retardation (Δnd) of the cell is typically 60% of the non-select effective retardation. The figure shows that all three subtractive colors can be produced with birefringence alone but only the yellow can be switched to a colorless state. The select and nonselect transmission spectra of a typical yellow cell is shown in Figure 3.10

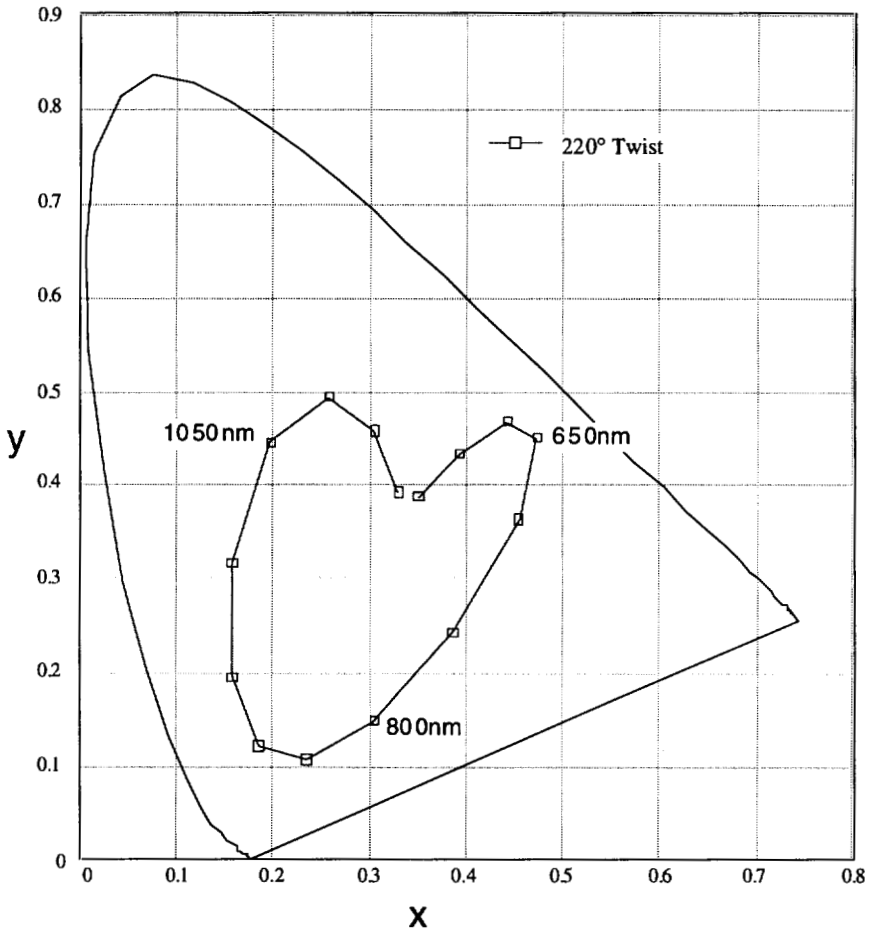

Figure 3.9 The color gamut obtainable from the typical range of birefringence values 500nm ≤ Δnd ≤ 1200nm for a 220° twist STN with the polarizers crossed at ± 45° to surface directors.

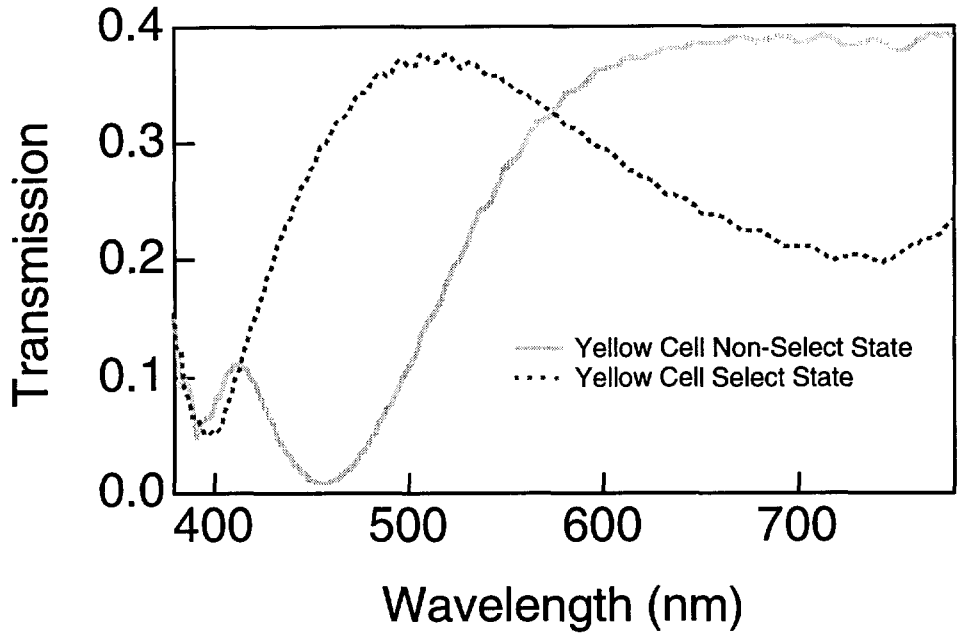

Figure 3.10 Example of the select and non-select transmission spectra for a yellow cell operating with pure birefringence color.

3.2.4 "Standard" TSTN Using Birefringence Color

Because of the poor characteristics of additive color selective polarizers as used in subtractive mode, with respect to contrast, another configuration was developed. In this configuration, which became the standard used in all commercially available TSTN displays, the center cell was operated on purely birefringent color so that the two polarizers in the center of the stack could be neutral[9]. Having neutral polarizers in the middle allowed the color selective polarizers on the outside of the stack to be analyzed more completely, resulting in higher contrast as well as a less colored black state. Only one solution was found for which birefringent color could be used for the center cell, and this was with the yellow cell in the center and the red and green polarizers replaced with neutral polarizers. The center cell switches naturally between yellow in the non-select

state and white in the select state when placed between two neutral polarizers which are oriented at ± 45° to the rub directions.

Configurations 2 and 3 in Figure 3.5 would only have one cell in common with the standard TSTN. One advantage of these configurations is that very good yellow color selective polarizers have been developed recently. The red, blue and green color selective polarizers are not nearly as good as the cyan, yellow and magenta polarizers because more than one absorption peak is required to produce these colors. In fact, the only blue polarizer that we could use was made from laminating a cyan polarizer to a magenta polarizer. Doing this produces a polarizer with poor transmission characteristics.

In principle, it should not matter in which order the cells are placed since each cell should operate independently from the others. If the bands that each cell controlled do not overlap, this would be true. In reality this is not in general true since a cyan cell which should only modulate red, modulates to some extent both green and blue. Likewise yellow cells do not only modulate blue, and magenta cells do not only modulate green. Secondly, the cell in the middle shares polarizers with the two cells on the outside and the order which the cells are stacked determines which types of color selective polarizers can be used.

3.3 Current State of Additive & Subtractive Color Systems

This section looks at the current state of additive and subtractive displays. Specifically, how does each method compare in terms of contrast, transmission and color gamut in theoretical calculations based on both optimized and currently available polarizer and filter dyes. We also need to look at the extent to which these limits have been realized in commercially available display systems and look at trends for the future.

3.3.1 Additive Systems

3.3.1.1 Color Stripe LCD Displays

By far the most popular type of color liquid crystal display uses color filters in a striped arrangement[1]. Each pixel is separated into three sub pixels one each for red, green and blue. While this is the perfect way to emulate an emissive display like the color CRT, which also uses a sub pixel arrangement, it is not very efficient in its use of light. An average of two thirds of the light is absorbed at each sub pixel due to the color filters. This means that since half of the light is already absorbed by the first polarizer, the maximum theoretical transmission through the system is just 0.33 times 0.50 or 16.66%. This high theoretical transmission can only be attained with perfect operation of the LCD, a 100% aperture ratio and no losses from surface reflections. When more reasonable values are used for LCD efficiency and aperture ratio, the typical transmission drops to between 4 and 6%.

In additive LCD systems, the contrast is limited only by the contrast of the neutral polarizers. Modern polarizers, even high transmission polarizers, have typical polarizing efficiencies of greater than 99.7% and contrast ratios of 300:1 or greater. The TN effect can be very efficient at rotating the polarization of the light so it is not unusual to find AMLCDs with contrast ratios of 200:1 or better. The color gamut of a color stripe LCD is dependent on the choice of color filters. Many LCD manufacturers consciously desaturate the colors of the filters so that they can achieve higher transmission figures. Desaturuation of the color filters leads to very small color gamuts and especially an inability to display saturated cyans, magentas and yellows.

Another way to improve transmission figures is by tuning the backlight or lamp so that it has peaks in its output at the same wavelengths that the color filters transmit the most. When this is done by carefully choosing phosphors or arc sizes in lamps, the

results can be higher transmission as well as improved luminous efficiency. However, when arc lamps that have peaks in the interband region of the filters are used, the effective transmission of the LCD can be as much as 20% less than the same LCD when used with a broad band tungsten-halogen lamp.

3.3.1.2 *Dichroic Mirror/ Beam Spliter Systems*

In dichroic mirror systems, typically three small active matrix LCDs are used so that light is not absorbed in color filters[31]. The light is separated into three colors by using dichroic mirrors that efficiently reflect one additive color while passing the other two. Separated light is then sent through the monochrome LCDs and then the light is recombined with a combiner prism, see Figure 3.11. These systems can have very wide color gamuts because of the ability to make almost perfect notch type color filters using a thin film deposition process. These systems also do not need sub pixels since the light is split up before it is passed through three different LCDs and then combined to form one image. This is what we referred to as a coincident additive color system.

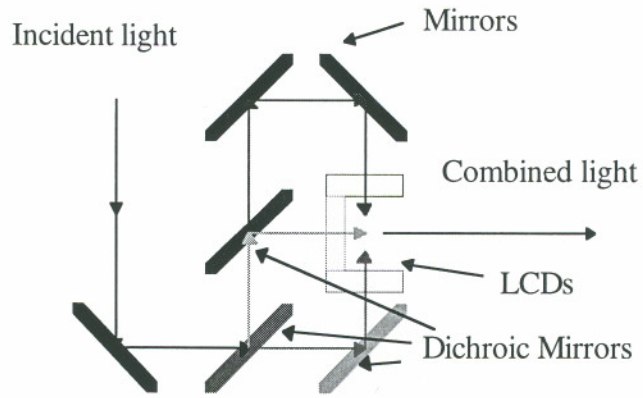

Figure 3.11 Schematic drawing of a dichroic mirror LCD projector.

Another system has been reported recently that uses three dichroic mirrors to reflect red, green, and blue light at different angles towards a single color filter AMLCD so that they may be focused into their respective sub pixels using a lenticular lens array [32]. This system should theoretically have all of the advantages of additive systems, a wide color gamut, and should not suffer from the loss of light incurred in other additive systems.

3.3.2 Subtractive Color Systems

3.3.2.1 TSTN with two colored polarizers and two neutral polarizers

This design is currently the only type of subtractive color display in production [28]. It has three cells with each controlling one additive band. The magenta cell is made with a neutral and magenta polarizer and controls the green portion of the spectrum. When the cell is in the non-select state, there is a transmission minimum in the visible spectrum at about 540nm while in the select state the cell appears clear with a uniform transmission of about 25-30%. The cyan cell uses one neutral polarizer and one cyan polarizer to control the red portion of the spectrum. In the non-select state there is a minimum in the optical spectrum at about 620nm while the select state also appears clear with uniform transmission in of 25-30%. The yellow cell controls the blue portion of the spectrum, it is designed to use birefringence color exclusively and therefore is sandwiched between the two neutral polarizers that the two other cells use. The non-select state appears yellow with a minimum at approximately 470nm while the select state again is clear with uniform transmission over the entire spectrum.

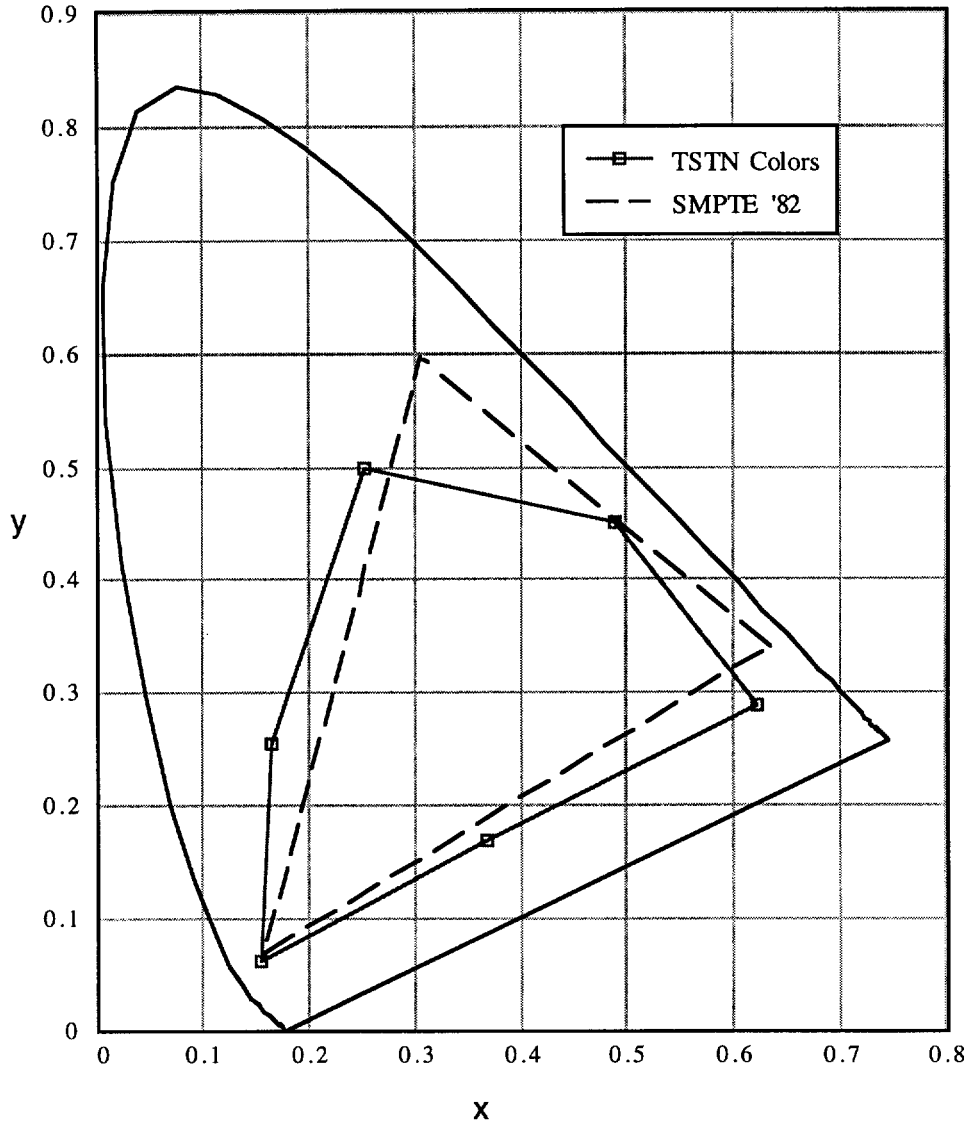

Figure 3.12 Color gamut of TSTN with cyan and magenta polarizers on ideal rotators and a yellow cell operating in the birefringence mode. The 1982 SMPTE color primaries are shown for reference.

The limits of this type of display are of course very much dependent on the types of color polarizers that are available. We have examined several magenta and cyan polarizers and settled on V36-18245T by Polatechno for our magenta polarizer and CC2B by Sanritz for our cyan as stated in Table 3.2. Given these two color selective polarizers as well as a high transmittance neutral polarizer, the limit of these colors is really only

dependent on the ability of the LC to rotate light in the given wavelengths by 90°. In this type of display, the yellow cell relies on birefringence to switch the blue therefore this cell must not rotate light at all wavelengths by 90°. The other two cells on the other hand can rotate every wavelength by 90° since the colored polarizer selectively blocks only the desired band. We can assume then that the best we can do is to have a single yellow cell operating in the birefringence mode with perfect rotators for the other two cells. This type of situation is easily simulated and as described in Section 3.2.2.2, this was done. The colors, transmission, and contrast when measured represent the limits of this configuration. The results of this simulation are shown in Figure 3.12

3.3.2.2 *TSTN with all color polarizers*

This configuration is a superset of the previously described configuration. There are several different combinations of colored polarizers that will work in this type of configuration. Since each layer controls only one color, the polarizers on the top and bottom of the stack only need to analyze one band. The polarizers that fall between two cells must analyze two bands. Hence we can have all combinations of additive and subtractive primary color polarizers such that there are two subtractive primary color polarizers on the outside of the stack and two additive primary color polarizers on the inside of the stack. This gives us three distinct configurations distinguished by which primary is controlled in the center of the stack. As shown in section 3.2.2, Table 3.3, the color-polarizer-only configurations do not perform as well as the TSTN configuration that uses neutral polarizers and birefringence color for the yellow cell. This is mainly because of the lack of good red, green and blue color selective polarizers. Figure 3.13 shows the color gamut of an all color polarizer TSTN using configuration CGRM from Table 3.4. Note the very poor yellow and blue primaries.

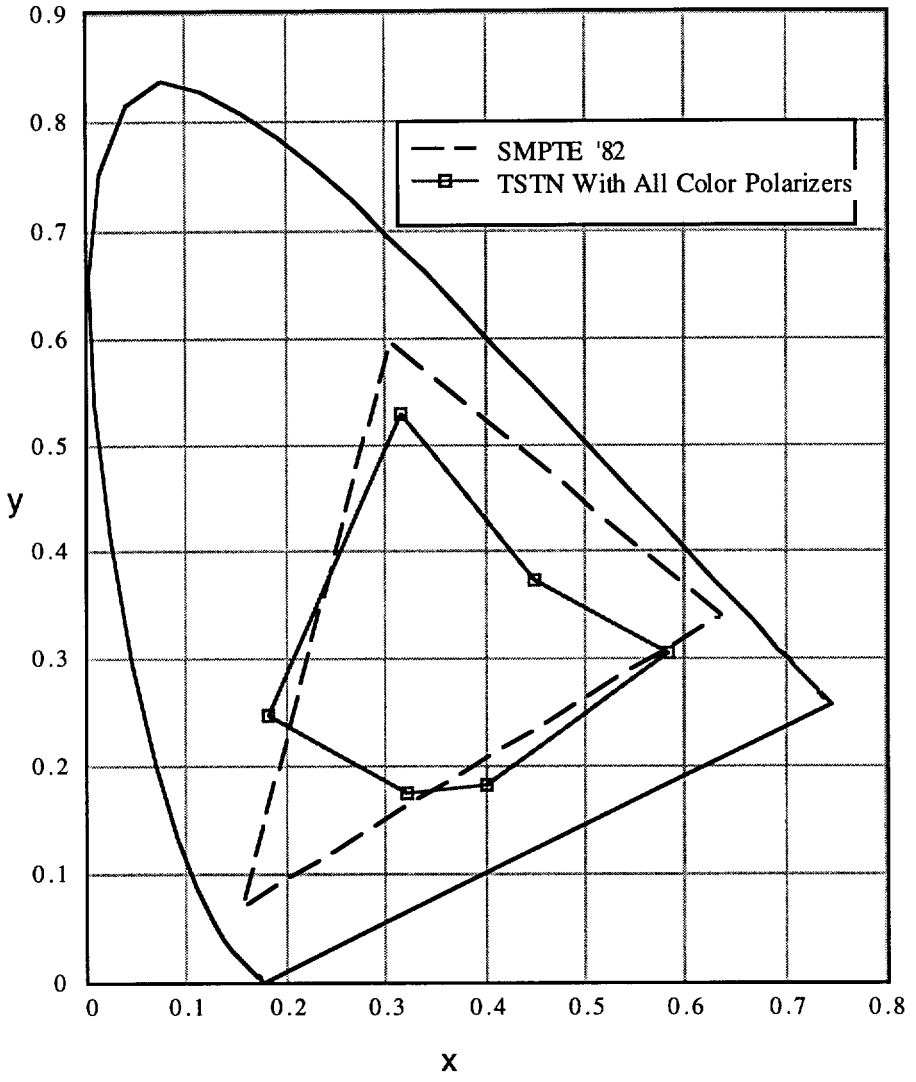

Figure 3.13 The color gamut of a TSTN using only color polarizers and assuming that the LCDs are ideal rotators. The SMPTE specified color primaries are shown for reference.

3.4 Conclusion

Experience with the four color printing process shows that subtractive color is capable of very high quality color reproduction. In color displays the advantage with subtractive color is mainly in the ability for higher transmission values as compared to traditional color stripe additive color LCDs. Although the trend is towards using the thin film dichroic mirror three paths systems that are very efficient for projection, this is not

possible for a thin desktop display or notebook computer display. If color polarizer technology develops to the extent that the red, green and blue polarizers become more like block dyes, the possibility of using subtractive color with an Active Matrix TN display may become possible. For now, subtractive color should be limited to traditional TSTN displays which incorporate a yellow cell which uses pure birefringent color.

4 MODELING OF TWISTED NEMATIC LCDS

Because of the immense number of variables involved in optimizing an STN or TSTN display, numerically modeling the electro-optic performance is essential. Modeling the optical behavior of an LCD allows one to modify several variables simultaneously and predict the performance of the cell to a good degree of certainty. Historically, the optical behavior of twisted nematic and cholesteric liquid crystals have been modeled in two ways. One method, generally referred to as the 4x4 matrix method involves first a determination of the exact director configuration of the LCD for every applied voltage using elastic continuum theory [33]. The director configuration depends on the applied voltage, the geometrical design of the cell, and the material properties of the liquid crystal itself. Next the optical properties of that particular configuration are determined by solving Maxwell's equations[34,35]. This approach requires computing a new director configuration for each voltage and carrying out the 4x4 matrix calculations at each voltage. While giving nearly exact solutions, this approach is computationally intensive and slow.

Instead of solving Maxwell's equations, we could also use Jones matrices to describe the optical properties of the slabs[36]. The Jones calculus is a method that approximately solves Maxwell's equations in planar media for uniform director configurations and normal incidence. This method essentially treats each optical element in a light train as a 2x2 matrix and the light is described by a 2 dimensional vector defined by the electric field. The liquid crystal structure is approximated by a series of birefringent layers which have uniform tilt and twist. One must still compute the director

configuration, but now the Jones matrix represents a small slab of the liquid crystal structure. The transmission of the full structure is obtained by multiplying the Jones matrices of the entire structure together. One disadvantage to the Jones matrices is that they do not keep track of surface reflection losses. This is not a very serious flaw since it can be experimentally removed by including another surface in the reference source when measuring transmission. The Jones method should only be used for normally incident light, but this is fine for the purposes of this investigation since projection LCD displays collimate the light within a few degrees before it enters the LCD.

In 1985 a single simplified Jones matrix was derived by Scheffer and Nehring and independently by Raynes which could describe a uniformly twisted and tilted birefringent layer by only a few variables, the average birefringence, the thickness, the total twist and the direction of the input director[37,38]. With this method, the director configuration is implicitly assumed and therefore modeling of the STN can be done rapidly simply by adjusting a few parameters.

Although the single Jones method has been widely used to model STNs, its use was restricted to the non-select state which is approximately uniformly twisted and tilted. The Jones method requires, in principle that the liquid crystal director have uniform tilt and twist distributions throughout the layer. It has been shown through elastic constant modeling that in the driven state, the tilt of the liquid crystal director is not a constant throughout the layer and the twist distribution is not uniform [39]. This means that, in principle, the select state of an STN layer can not be described by a single Jones matrix but rather needs to be divided up into a series of mini-layers where the tilt and twist are approximately constant. Through modeling, it will be shown that, in fact, a single simplified Jones matrix can be used to describe the select state of an STN throughout the good portion of its useful operating range. Different voltage levels on the

LCD can be modeled simply by changing the effective birefringence in the Jones matrix calculations

Software was developed to numerically model the transmission of light through a twisted nematic structure. In order that the user can carry out the model interactively, the model is designed to use the Jones method exclusively in an attempt to conserve computational time. In modeling the behavior of the cell in the driven state, no attempt is made to define the actual tilt or twist or even define an average twist or tilt, instead a more phenomenological approach is taken. Cells are measured under certain conditions and fitted to a transmission curve derived from a numerical calculation. The LCD, at any given voltage, can then be attributed to the same parameters as the Jones parameters of the fitted curve. In other words, we can derive a Jones matrix which is phenomenologically correct just by fitting the Jones parameters to a measured curve. This makes modeling of the LCD a mere matter of characterizing, at each voltage, the three Jones parameters; the total twist ϕ, the effective retardation, Δnd which takes tilt in to account, and δ, the dispersion of the birefringence.

4.1 Jones Calculus Treatment

The Jones Calculus is a matrix treatment of polarized light which makes it possible to determine the effects on a beam of light when a series of optical elements are introduced into its path [36]. Invented in 1940-41 by R. Clark Jones, the Jones Calculus treats incident light by a 2 dimensional electric field vector, and any non-scattering, non-depolarizing optical element, such as a partial polarizer, retarder, or rotator by a 2x2 matrix. The effect of the optical element on the incident light is computed by a multiplication of the vector by the matrix. If depolarizing elements are used the Mueller 4x4 matrices must be used since Jones matrices have no way of dealing with partial

polarization[40]. Aside from depolarization, the Mueller matrices offer no benefit over the use of the Jones matrices and are in fact much more complicated to setup[40].

4.1.1 The Jones Vector

The Jones Vector for an electromagnetic wave is a represented by a 2 dimensional vector that consists of the amplitudes and phases for the x and y components of the electric field associated with the wave. For example, horizontally polarized and right-circularly polarized light have the full Jones vectors

$$\begin{bmatrix} \mathbf{E}_x \\ \mathbf{E}_y \end{bmatrix} = \begin{bmatrix} \mathbf{A}_x e^{i\varepsilon_x} \\ \mathbf{0} \end{bmatrix} \text{ and } \begin{bmatrix} \mathbf{E}_x \\ \mathbf{E}_y \end{bmatrix} = \begin{bmatrix} \mathbf{A}_x e^{i\varepsilon_x} \\ \mathbf{A}_x e^{i(\varepsilon_x + \pi/2)} \end{bmatrix} \tag{4.1}$$

These have a simplified form as well, which does not preserve the phase information about the wave but which makes them easier to manipulate. These simplified and normalized forms are given by

$$\begin{bmatrix} \mathbf{E}_x \\ \mathbf{E}_y \end{bmatrix} = \begin{bmatrix} \mathbf{1} \\ \mathbf{0} \end{bmatrix} \text{ and } \begin{bmatrix} \mathbf{E}_x \\ \mathbf{E}_y \end{bmatrix} = \begin{bmatrix} \frac{-\mathbf{i}}{\sqrt{2}} \\ \frac{\mathbf{1}}{\sqrt{2}} \end{bmatrix} \tag{4.2}$$

for the same types of polarized light as above. The intensity of the light is computed by the standard electromagnetic calculation below

$$\mathbf{I} = \mathbf{E}_x \mathbf{E}_x^* + \mathbf{E}_y \mathbf{E}_y^* \tag{4.3}$$

where the * represents the complex conjugate.

4.1.2 The Jones Matrix

Optical elements can be described in the Jones calculus as 2x2 matrices. The effect of the optical element is obtained by multiplying on the left the light vector by the optical element matrix. The product is then a vector representation of the polarization state of the resultant light. Just as the Jones vectors have full and normalized forms, so do the Jones matrices. The full and normalized Jones matrices of an ideal homogeneous linear polarizer with transmission axis horizontally oriented are

$$J(0) = \begin{bmatrix} \mathbf{e}^{-\frac{2i\pi nd}{\lambda}} & 0 \\ 0 & 0 \end{bmatrix} \quad \text{and} \quad J = \begin{bmatrix} 1 & 0 \\ 0 & 0 \end{bmatrix} \tag{4.4}$$

where n is the refractive index, d is the thickness of the film and λ is the wavelength of the light. For an orientation of the polarizer at the angle θ, we apply a unitary transformation of the horizontal polarizer Jones matrix by applying a rotation matrix $S(\theta)$ to the right side of the Jones matrix and the counter-rotation $S(-\theta)$ to the left side as shown below.

$$J(\theta) = S(-\theta)J(0)S(\theta)\begin{bmatrix} \cos(\theta) & \sin(\theta) \\ -\sin(\theta) & \cos(\theta) \end{bmatrix}\begin{bmatrix} 1 & 0 \\ 0 & 0 \end{bmatrix}\begin{bmatrix} \cos(\theta) & -\sin(\theta) \\ \sin(\theta) & \cos(\theta) \end{bmatrix} \tag{4.5}$$

If θ is equal to $\pi/2$ then the rotation will result in a vertically oriented polarizer and the Jones matrix becomes :

$$J(\pi/2) = \begin{bmatrix} 0 & 0 \\ 0 & 1 \end{bmatrix} \tag{4.6}$$

Non ideal polarizers have the Jones form

$$J(0) = \begin{bmatrix} p_{\parallel} & 0 \\ 0 & p_{\perp} \end{bmatrix} \tag{4.7}$$

where

$$p_{\parallel} = \sqrt{k_{\parallel}} \qquad \text{and} \qquad p_{\perp} = \sqrt{k_{\perp}} \tag{4.8}$$

and $k_{||}$ and $k_{\perp}$ are the respective transmittances of the polarizer when parallel and perpendicular to a reference neutral polarizer.

The full and normalized Jones matrices for a retarder with retardation δ oriented at an angle 0° with respect to a polarizer transmission axis is

$$J(0,\delta) = \begin{bmatrix} e^{i\delta/2} & 0 \\ 0 & e^{-i\delta/2} \end{bmatrix} \tag{4.9}$$

this matrix can also be modified for any orientation by use of the unitary rotation described earlier.

It can be shown that for light of a given wavelength, an optical system consisting of any number of retarders, partial polarizers, and rotators, is optically equivalent to a system containing four elements, two retarders, one polarizer, and one rotator[36]. This is an important idea since it will allow us to replace complicated systems by equivalent, and much simpler systems. Twisted nematic liquid crystals, which can be considered as a stack of an infinite number of infinitesimally small birefringent slabs each rotated with respect to one another, represent a complicated optical structure that can be greatly simplified with an equivalent representation.

4.2 Optical Behavior of Supertwist Nematic LCDs

The first insight into the way in which twisted birefringent structures behaved optically was obtained by Mauguin in 1911 in his study of cholesteric molecules [41] and described further by De Vries in 1951[42]. Mauguin described the rotation of polarized light by a liquid crystal which had been placed between two substrates which were subsequently twisted by some angle ϕ. Mauguin's theory relied on an approximation by which the pitch of the liquid crystal was much larger than the wavelength of the incident light. This is known as the Mauguin condition[41] (pp. 16, 20) and is formally written as

$$\frac{\Delta nd}{\lambda} >> \frac{\phi}{\pi} \qquad (4.10)$$

where Δnd is the effective retardation of the LC layer, λ is the wavelength of the light and ϕ is the total twist of the layer.

A typical TN cell has the following device parameters $\Delta n = 0.08$, d = 6mm, $\phi = 90°$ and $\lambda = 550$nm. For these parameters, the TN cell gets marginally close to satisfying the Mauguin condition with :

$$\frac{\Delta nd}{\lambda} \approx 0.87 \quad and \quad \frac{\phi}{\pi} \approx 0.5 \qquad (4.11)$$

Although a TN cell is only somewhat close to obeying the Mauguin condition, in practical applications, these cells are able to operate in that mode because although the normal modes are somewhat elliptical, the minor axis of one mode can exactly cancel the

major axis of the other mode. Typical values for an STN in the non-select state are as follows $\Delta n = 0.15$, $d = 6.0\mu m$, $\phi = 240°$, and again λ is taken to be 550nm. The STN cell is even further from the Mauguin condition since we have

$$\frac{\Delta nd}{\lambda} \approx 1.6 \quad \text{and} \quad \frac{\phi}{\pi} \approx 1.33 \tag{4.12}$$

Because of the fact that STN devices do not satisfy the approximating conditions above, behavior is less easily understood and therefore optimization is more difficult. A complete model which does not rely on approximations is presented below.

Consider a typical STN with a total twist of 240° and a pretilt of 5°. In the non-select state, the twist is fairly uniform and the tilt of the LC layers is only slightly dependent on the distance through the cell. We can approximate the director configuration as a distribution of constant tilt and uniform twist. In the select state, on the other hand, the tilt is much higher, 50-80°, in the center of the cell than at the surfaces. The twist of the select state is also mostly in the center of the cell since the director at the surfaces is tightly bound to the alignment layer.

4.2.1 The Jones Matrix for Non-Select State

As can be seen from Figure 2.7, the non-select state has almost perfectly uniform twist throughout the LCD, and the tilt is more or less constant throughout the layer. With a director configuration that varies uniformly through the cell it is fairly simple to describe its effect on light by a single Jones matrix with only a few basic parameters.

The Jones matrix for an LCD was developed in 1985 by Scheffer and Nehring[37] and independently by Raynes and Tough[38] to describe the optical behavior of a TN or STN cell in the relaxed state. This treatment was also later expanded to include other

more specific cases [43,44]. Consider light incident on the cell normal to the surface. We can view the cell as a collection of m birefringent layers each of whose principle axes is rotated by an angle γ with respect to the previous layer. The effective birefringence of the layer is just the normal birefringence of the liquid crystal Δn times $\cos^2(\bar{\theta})$ where $\bar{\theta}$ is the average tilt of the director in that layer. Since each layer is just a simple retarder, the Jones matrix for a birefringent layer with effective retardation Δnd and fast axis oriented at angle $m\gamma$ is given by Equations 4.5 and 4.9 and is shown below

$$J_m = \begin{bmatrix} \cos^2(m\gamma) + e^{-i\pi\Delta nd^*/\lambda}\sin^2(m\gamma) & \cos(m\gamma)\sin(m\gamma)\left[1 - e^{-i\pi\Delta nd^*/\lambda}\right] \\ -\cos(m\gamma)\sin(m\gamma)\left[1 - e^{+i\pi\Delta nd^*/\lambda}\right] & \cos^2(m\gamma) + e^{+i\pi\Delta nd^*/\lambda}\sin^2(m\gamma) \end{bmatrix} \quad (4.13)$$

By taking the limit $m \to \infty$, and $m\gamma \to \varphi$ the total twist across the liquid crystal cell, we obtain the unitary Jones matrix for a twisted structure as shown below[45,38]

$$J_\infty(\phi, \Delta nd, \delta) = \begin{bmatrix} a & b \\ -b^* & a^* \end{bmatrix} \quad (4.14)$$

where a and b are given in the expressions below and the * represents complex conjugation.

$$a = \cos(\phi)\cos(\pi\Gamma) + \frac{\phi}{\pi}\frac{\sin(\phi)\sin(\pi\Gamma)}{\Gamma} - i\frac{\Delta nd}{\lambda}\frac{\cos(\phi)\sin(p\Gamma)}{\Gamma} \quad (4.15)$$

$$b = \sin(\phi)\cos(\pi\Gamma) + \frac{\phi}{\pi}\frac{\cos(\phi)\sin(\pi\Gamma)}{\Gamma} - i\frac{\Delta nd}{\lambda}\frac{\sin(\phi)\sin(p\Gamma)}{\Gamma} \quad (4.16)$$

Here ϕ is the total twist of the LCD, Δn is the birefringence, d is the thickness of the cell, λ is the wavelength of the light, and Γ is given by

$$\Gamma = \sqrt{\left(\frac{\Delta nd}{\lambda}\right)^2 + \left(\frac{\phi}{\pi}\right)^2} \qquad (4.17)$$

The effective retardation with dispersion taken into account, $\Delta nd = \Delta nd(\lambda)$ is the retardation of the liquid crystal at the wavelength λ. The effective birefringence can be computed assuming a simple Cauchy model for the dispersion of Δn, i.e. [46].

$$\Delta n = A + \frac{B}{\lambda^2} \qquad (4.18)$$

where A and B can be related to a dispersion factor δ which is defined by:

$$\delta = \frac{\Delta n(435.9nm)}{\Delta n(667.8nm)} \qquad (4.19)$$

Since most retarders are specified by retardation at or near 550nm it is convenient to transform the above Cauchy equation (4.18) to one in which the two free parameters are the birefringence at 550nm and the dispersion factor δ. Under these circumstances, Equation (4.18) becomes [21]:

$$\Delta nd\ (\lambda) = \Delta nd(550nm)\frac{\left[1+(\delta-1)\frac{\left[\left(\frac{667.8}{\lambda}\right)^2-1\right]}{\left[\left(\frac{667.8}{435.9}\right)^2-1\right]}\right]}{\left[1+(\delta-1)\frac{\left[\left(\frac{667.8}{550}\right)^2-1\right]}{\left[\left(\frac{667.8}{435.9}\right)^2-1\right]}\right]} \qquad (4.20)$$

A typical liquid crystal has a dispersion factor δ given by the approximation δ = 1+ Δn [21]. This means that for most highly birefringent liquid crystals, δ ranges from 1.05 to 1.25.

The transmission of light through the LCD can be computed from the equation shown below.

$$T = \frac{(E_{xf}E_{xf}^{*}+E_{yf}E_{yf}^{*})}{(E_{x0}E_{x0}^{*}+E_{y0}E_{y0}^{*})} \qquad (4.21)$$

where E_{x0} and E_{y0} are x and y components of the incident electric field and

$$\left(E_{xf}E_{yf}\right) = J\begin{pmatrix}E_{x0}\\E_{y0}\end{pmatrix} \qquad (4.22)$$

where J is the Jones matrix for the LCD. Since J is a unitary matrix, unpolarized incident light will emerge unpolarized with the same intensity, and the transmission will be 100% for all wavelengths, except for any loss due to surface reflections. Unpolarized light is treated by averaging the contributions from the two orthogonal components of plain polarized states. In other words, we take the contributions from both horizontally and vertically polarized light and average the results. It is equally valid although

computationally more difficult to average the contribution from left and right circularly polarized light.

When the LCD is placed between two ideal polarizers, a simplified expression for the transmission is obtained[38].

$$T = \frac{1}{4}\left[1 + \left\{\cos^2 \pi\Gamma - \left(\frac{\phi}{\pi}\right)^2 \frac{\sin^2 \pi\Gamma}{\Gamma^2}\right\}\cos 2(\beta - \gamma) + \left(\frac{\Delta nd}{\lambda}\right)^2 \frac{\sin^2 \pi\Gamma}{\Gamma^2}\cos 2(\beta + \gamma) + \left(\frac{\phi}{\pi}\right)^2 \frac{\sin 2\pi\Gamma}{\Gamma}\sin 2(\beta - \gamma)\right] \quad (4.23)$$

where β is the angle that the polarizer makes with respect to the input director orientation and γ is the angle that the analyzer makes with respect to the output director orientation, and ϕ and Γ are as they were defined previously.

This expression can be simplified further under certain conditions. One special condition that is of importance in STNs is the case where the input and output polarizers make angles of +45° and -45° with the input and output director angles respectively. This condition is referred to as the 45° crossed polarizer condition. In this special case the transmission reduces to a sine squared function in Γ.

$$T = \frac{1}{2}\sin^2\left(\pi\sqrt{\left(\frac{\Delta nd}{\lambda}\right)^2 + \left(\frac{\varphi}{\pi}\right)^2}\right) \quad (4.24)$$

Figure 4.1 shows Equation (4.24) plotted against $\Delta nd/\lambda$ for several different LCD twist angles.

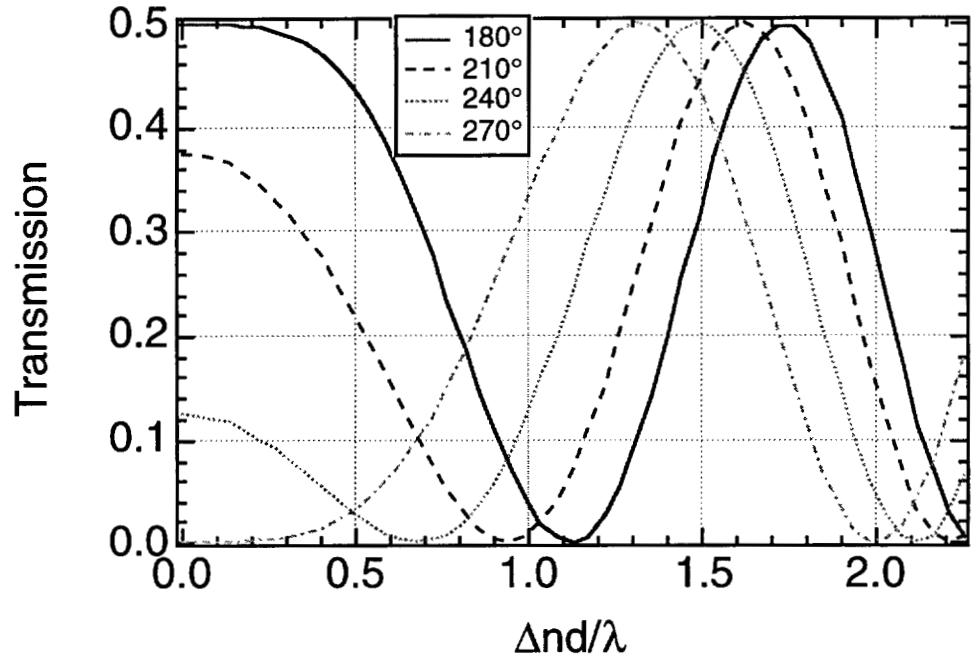

Figure 4.1 Showing the behavior of the transmission versus the product Δnd/λ for several different twists and 45° crossed polarizer orientation.

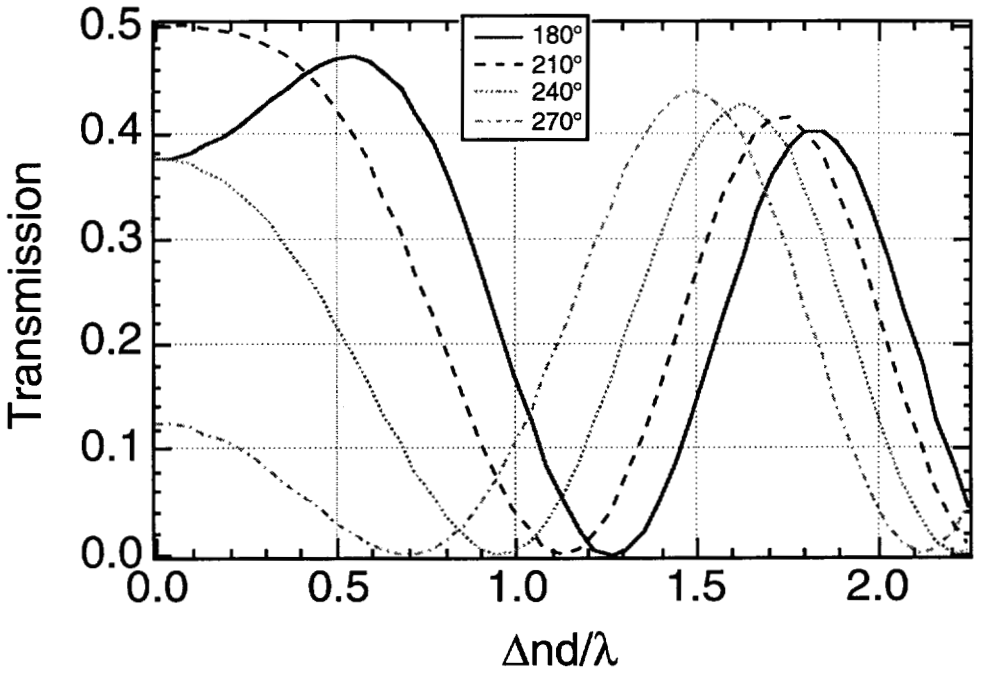

Figure 4.2 Showing the behavior of the transmission versus the product Δnd/λ for several different twists and β = 60°, γ = 30° polarizer orientation.

For polarizers oriented both at +45° or -45° to their respective director orientations, i.e. rotate one polarizer 90° from the previous case, the transmission will take the form of the complementary cosine square function in Γ. When polarizers are placed at angles other than 45° such that $\beta + \gamma = 0°$ or 90° the transmission is a modulated sinusoidal function in Γ. In this case transmission will never be as high as 50% for any wavelength. Figure 4.2 shows Equation (4.23) plotted against $\Delta nd/\lambda$ with $\beta = 60°$ and $\gamma = 30°$ for several different LCD twist angles.

The standard optical setup that was used to determine the Jones parameters of the device is as follows. Assuming that the rubbing directions are known, neutral polarizers are placed at ±45° to the rub directions so that if the light followed the twist, these polarizers would be appear to be crossed. The transmission spectra is then measured and fitted to a Jones Matrix that when placed in an identical setup has a sufficiently close transmission spectra.

This expression simplifies under certain conditions, for example, when the Mauguin condition is satisfied i.e. $\Delta nd/\lambda >> \phi/\pi$. For that case the Jones matrix becomes the equivalent of a retarder with fast axis parallel or perpendicular to the front rubbing direction, and retardation Δnd followed by a perfect rotation by an angle ϕ.

4.2.2 Jones Matrix for the Select State

The derivation of the Jones matrix for the STN was based on the assumption that the LCD consisted of a series of thin birefringent layers uniformly twisted over the entire thickness of the device. This is not the case for the select state of an STN where the distribution of the twist and tilt are not at all uniform. If one were to try to construct a similar matrix for the select state of an STN by multiplying successively the individual

matrices of the layers as prescribed by the director distribution, it would not be possible to do in a closed form. The traditional way to model the select state is to use the 4x4 method, but as explained earlier, this is not a desirable option since one would need to calculate the director configuration for each voltage level. One central point of this dissertation is that it is not necessary to resort to either approach because it is always possible to identify a Jones matrix whose modeled transmission matches the transmission of a select state. It will be shown that the transmission of a cell in the select state can in fact be modeled by a Jones matrix that is identical to that of the non-select state aside from the difference in the product Δnd and the dispersion δ.

In order to verify the assertion above that the simplified Jones method can be used to model any practical LCD device, a thorough simulation of an LCD transmission spectra was done with a complete elastic constant model and Jones matrix modeling on 50 layers. For this simulation, the device parameters such as twist, elastic constants, dielectric constants, optical anisotropy, and cell thickness are used to compute the twist and tilt distributions and the reduced voltage required for any given midlayer tilt angle. These tilt and twist distributions are then used to calculate the spectral transmission of the LCD for any given polarizer orientations. Although this method is computationally intensive, it is widely regarded the best method for LCD modeling.

The spectral data from this complete model can be compared with the Jones model for a similar device and the effective birefringence of the device can be inferred. Figure 4.3 is a series of transmission curves which were calculated using the complete elastic model and using the complete Jones model as well as the corresponding transmission curves calculated using the simplified Jones model. The elastic model can calculate the tilt and twist distribution given a midlayer tilt angle. From this data, the complete Jones calculations can be done to produce the transmission curves. Table 4.1 shows the device parameters for the complete Jones model which are required and

corresponding simplified Jones device parameters for the modeling of an LCD which has a midlayer tilt angle of 50°.

Table 4.1 The parameters required to calculate the transmission of an STN LCD in both the complete Jones model and the simplified Jones model. Transmission spectra for the parameters shown are compared in Figure 4.3.

Parameter	Elastic constant modeling/ Full Jones Model	Simplified Jones Model
k_{33}/k_{11}	1.5	-
k_{22}/k_{11}	0.6	-
$\Delta\varepsilon/\varepsilon_{\perp}$	2.5	-
ϕ	-240°	-240°
d/p	-0.666	-
Pretilt angle input side	5°	-
Pretilt angle output side	5°	-
ne	1.7	-
no	1.5	-
d(μ)	6.0	-
β	45°	45°
α	-45°	-45°
Midlayer tilt angle	50°	-
δ	1.00	1.00
Δnd(nm) effective	-	705

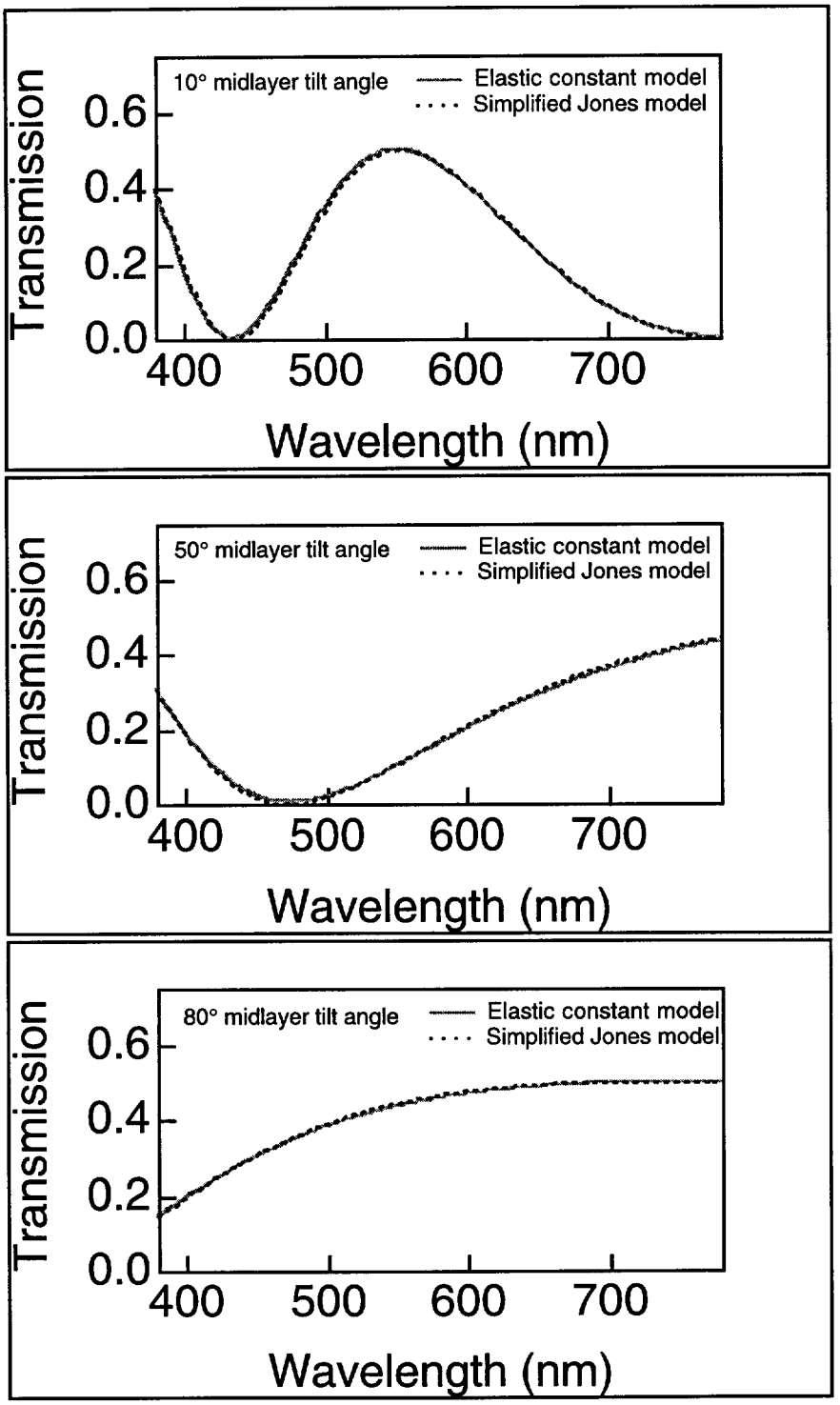

Figure 4.3 The transmission spectra calculated from both the complete elastic calculation with the compete Jones model (solid lines) and the simplified Jones model (dashed lines).

For all midlayer tilt angles from 0° to 60°, the transmission spectra derived from the complete model was able to be modeled by the simplified model only varying the effective birefringence. For higher midlayer tilts, the simplified model required a modification of the dispersion factor along with the effective birefringence but still the model was quite capable of duplicating the transmission spectra. The multiplex ratio of passive addressed devices limit the voltage range, therefore, the midlayer tilt is also limited. Even for a simple VGA device, the voltage selection ratio of 1.066 means that the midlayer tilt of the select state is at most 55°. What this means is that while modeling passively addressed devices, there is not any loss of precision when using the simplified Jones model.

Figure 4.5 shows the modeled and measured transmission spectra of a cyan-type cell in both the select and non-select states. The parameters used in the simplified Jones matrix are given in table 4.2. The measurements were done with two neutral polarizers oriented at ±45° crossed. So as to account for surface reflections, the source was initially measured with the LCD sandwiched between two pieces of uncoated soda-lime glass. The glass pieces were then replaced with the neutral polarizers and then the cell was remeasured. There is a considerable amount of noise at the shorter wavelengths due to the fact that the source lamp that we used was a tungsten halogen lamp which has a characteristic blackbody profile with a color temperature of approximately 3000K. Since there is much more red light than blue light, the computed transmission is noisier in the blue. Aside from the noise and surface reflections, the spectra match very well and at least as well as can be obtained from the full Jones model with elastic constant modeling.

Table 4.2 Parameters used in modeling the transmission spectra from Figure 4.4.

Jones Parameter	**Non-select**	**Select**
Twist (ϕ)	-230°	-230°
Retardation (Δ**nd**)	1025	750
Dispersion (δ)	1.23	1.28
Polarizer Orientation (β)	45°	45°
Analyzer Orientation (α)	-45°	-45°

The most instructive way to view the behavior of an STN is by looking at the behavior of the transmission versus voltage as the product Δnd is varied since this is what happens in the operation of the cell as the pixels are driven to different states. Figure 4.3 shows the behavior of the product Δnd vs. voltage for a cell which was designed to be the magenta cell in a TSTN stack. Since this is designed for a dual scan VGA device i.e. one that operates as two separate 240 x 640 devices, the multiplexing for a VGA screen is 240:1 and the selection ratio is 1.067. The idea is to keep the select voltage 1.067 times the non-select voltage, and position the voltages on the steepest part of the curve to get the greatest effect. This defines the select and non-select Δnd for this device and efforts to optimize the display should be based on the values of Δnd which this defines. In Figure 4.5, the non-select Δnd is 790nm and the select Δnd is 515nm. These values can be input directly into the Jones matrices along with the dispersion, twist, polarizer orientations, and compensation values for optimization.

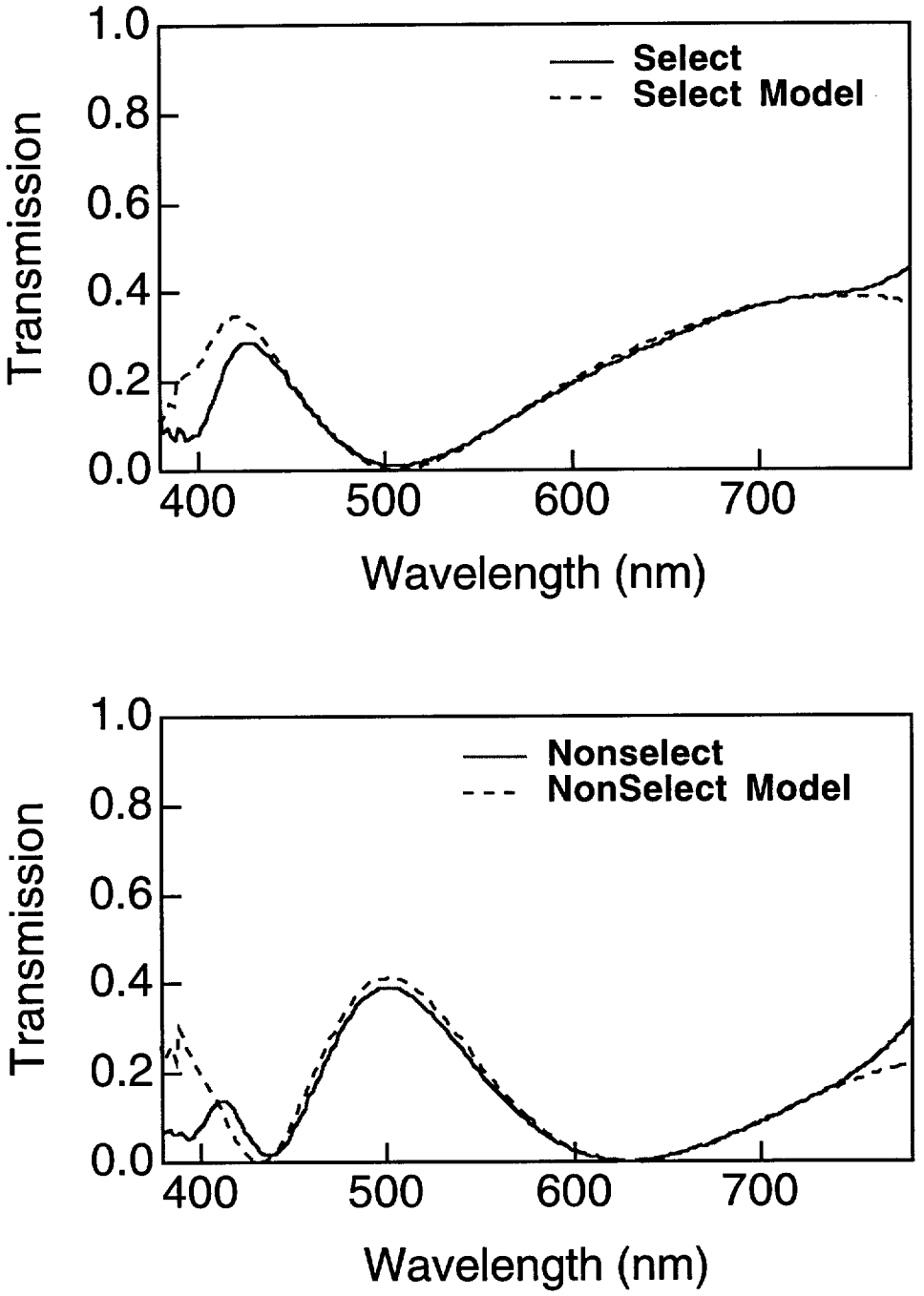

Figure 4.4 Comparison of the modeled transmission of an STN and the actual measured transmission for both the select and non-select states.

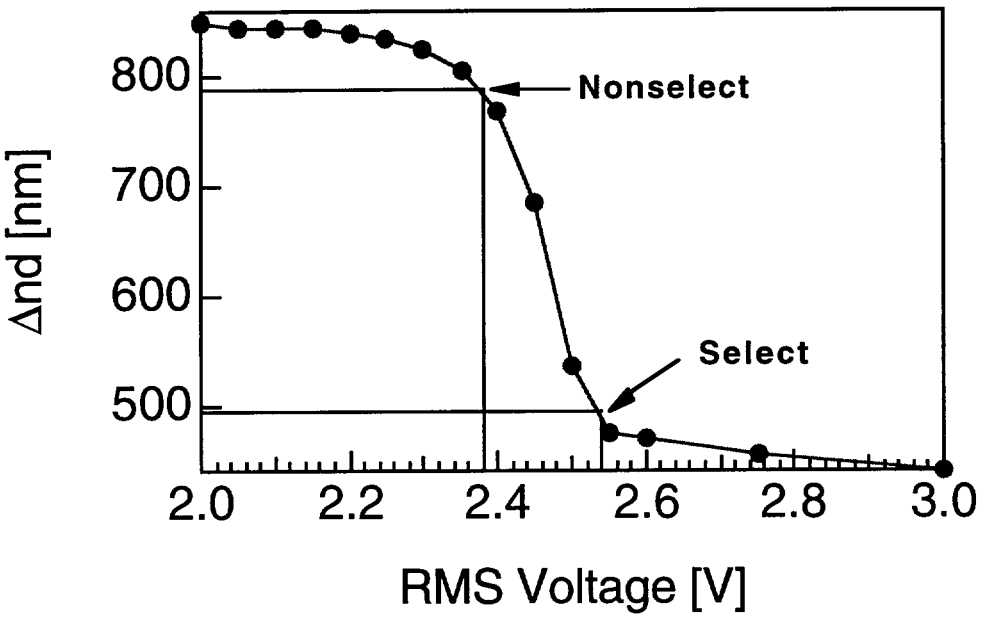

Figure 4.5 Δnd vs. voltage for an STN used as a magenta cell in a TSTN

Once the Jones matrix of the cell is determined for each voltage by means of fitting a curve to the data points as described above, optimization of the cell can be undertaken by modeling alone. The values and angles of the compensation layer can be adjusted on the computer interactively without the need to make a physical mock-up until a satisfactory configuration has been identified.

4.3 Software Implementation & Graphical User Interface

Because of the simplified nature of the Jones Matrix representation, it is possible to calculate the optical transmission of normally incident light "on the fly". An implementation of this type of interactive mode calculation requires a graphical user interface with controls for each variable. The modeling software was developed for a

Macintosh environment to take advantage of the elegant graphical user interface that is provided by its operating system. The code was written in FORTRAN and compiled using the Mactran Plus compiler by DCM Data Products Corporation. Two separate applications were developed, one application was used simply for optimizing a single cell, while another was developed to simulate an entire TSTN stack. A complete code listing for the single cell model is included in Appendix 1.

Features of the single cell program include transmission and contrast plots as a function of wavelength for both the select and non-select states as well as photopic transmission and contrast averaged over the entire spectrum. The program also calculates and plots the CIE coordinates of the resultant light from each state in the 1931 standard chromaticity diagram. The user can also choose to include in the modeling as many as two retardation films, see Figure 4.6.

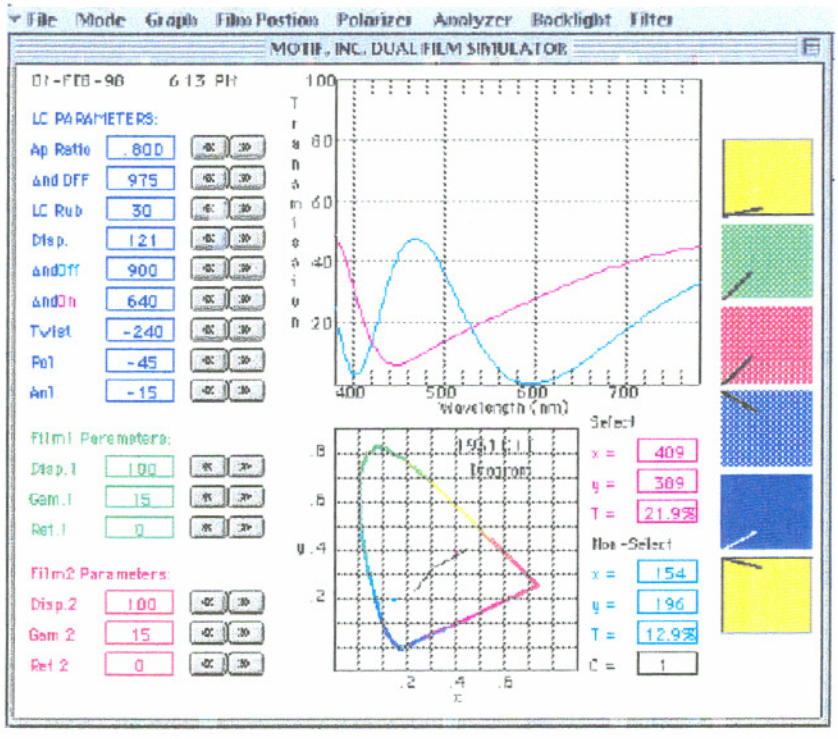

Figure 4.6 The graphical user interface of the single cell STN modeling program.

The full TSTN model allows modeling of the transmission of three cells in optical series with as many as four polarizers and four retardation films, see Figure 4.7. The positions of each element in the optical series can not be changed. Polarizers are specified by setting them to ideal, or by loading a file which contains the transmission of the polarizer when parallel and crossed with an ideal polarizer. The only parameter of the polarizer that can be adjusted on the fly is the angle with respect to the input director of the LC. As with the single cell model, the retardation films are specified by their birefringence, dispersion, and the angle of the slow axis with respect to the input director of the LC. An option to select or import illumination source spectral data has also been included which can be used to compute the chromaticity and calculate the transmission and contrast.

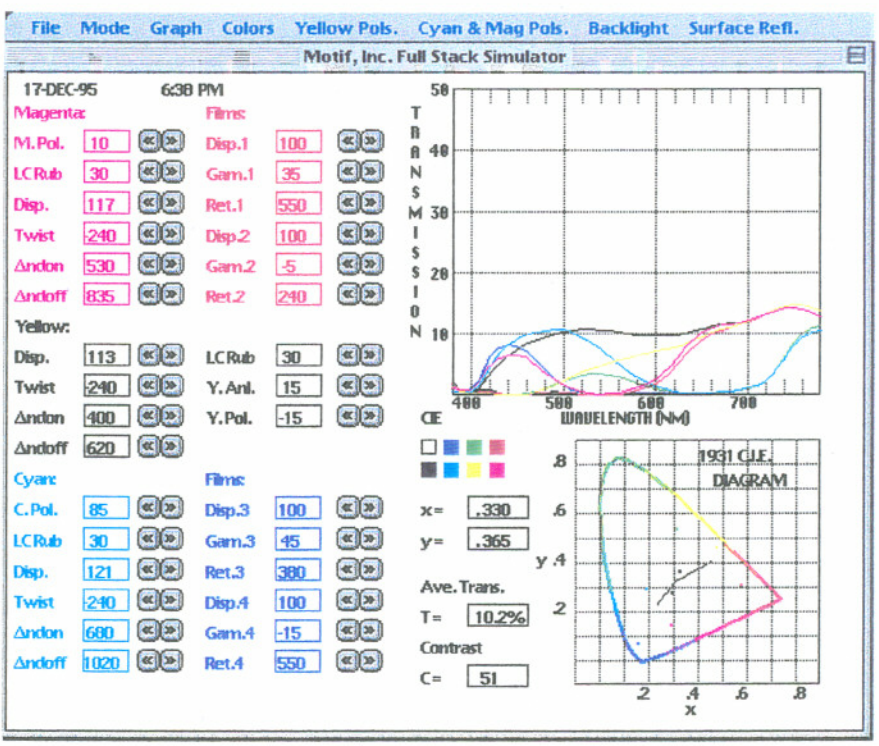

Figure 4.7 The graphical user interface of the TSTN modeling program.

4.4 Conclusions

At this point, we can make the approximation that the only variables that changes as a function of voltage is the product Δnd and the dispersion. This is not necessarily true because the change in the tilt and twist distributions which cause first order changes in the birefringence can also have second order effects. This is made especially clear if we consider that the Jones matrix for the nonselect state was derived in Equation 4.14 based on uniform tilt and twist distributions. The select state of an STN on the other hand, does not have uniform tilt and twist distributions and therefore the derivation is not valid. The direct comparisons of the Jones model with the complete model of the select state which calculates the distributions does a full Jones calculation on as many as 100 layers shows that the Jones model is effective even for very strong electric fields and very high midlayer tilt angles. We know that the Jones method agrees with the measured values almost perfectly in the non-select state and the select state and intermediate states on the can be approximated by a Jones matrix as long as we do not lose sight of the fact that the Δnd used in the Jones model must be fitted from the real transmission curves. What makes the Jones method is superior is that it is computationally much more simple which allows for interactive calculations

5 COMPENSATION AND OPTIMIZATION OF TRIPLE SUPERTWIST NEMATIC LCDS

It has already been shown that TSTN is a viable choice for cheap, full color, high resolution flat panel or projection displays. There are many possible uses for this type of display and it is therefore extremely important that the technology be tailored to meet the needs of the many different uses. Tailoring or tuning a TSTN display is a very complicated process that is as much art as it is science. The issues that need to be addressed in tuning a TSTN stack are listed below:

1. Resolution: The higher the resolution, the steeper the electro-optic curve needs to be to handle the high selection ratio. Steep EO curves usually mean that temperature effects are more pronounced and uniformity is harder to maintain. The trends in the marketplace are for higher and higher resolution, which will only make the design and optimization process more difficult.
2. Switching Speed: Passively addressed STN LCDs should have a long switching time so that transmission is not decreased during the time that the pixels are not addressed between frame updates. Cells used in active addressing mode with shorter frame times should have very fast response times to allow for video rates and better contrast[47]. The switching speed of the LCD is affected by the cell gap and the operating temperature of the device, higher temperatures and smaller cell gaps mean faster response times for the liquid crystal.
3. Operating Temperature: The cells need to be designed for the intended operation temperature. All pertinent measurements should be taken at normal operating

conditions for the intended application. Most projection applications will see operating temperatures on the LCD of 40°-50°C.

4. Contrast Ratio/ Transmission: Many applications stress the brightness of the display over the contrast ratio of the display but there may be applications for low ambient light that stress contrast over brightness. There is usually a tradeoff between these two quantities in the tuning of a TSTN display.
5. Color Gamut/ Color Temperature: The chromaticity of the white point is determined by the relative efficiencies of the three panels as well as the color temperature of the illumination source.
6. Size of Display/ Aperture Ratio: The aperture ratio, which is the ratio of the transmissive or active area of the display to the opaque area of the display, is greatly influenced by the size of the LCD panel and the resolution of the display. The design rules in the processing of the LCD panels also influence the aperture ratio since advanced processing, using very fine masks can limit the amount of the display that is not active. A high aperture ratio is very desirable both for its benefits in transmission but also for its benefits in contrast. If the zero voltage state of the LCD is not close to the non-select state of the LCD, the gaps between the pixels will not be black leading to poor contrast. If the aperture ratio is poor, this situation must be avoided or a chrome mask can be used over the inactive area to completely prevent light from passing through.
7. Cell Geometry Requirements: Some adjustments in design geometries can sometimes be implemented to make use of existing tooling or to keep production cost down by designing more than one cell with the same geometries

There are two distinct reasons for undertaking an optimization procedure. First many current designs have fallen outside of the ever changing specifications. This is especially true for STN displays which are competing for the display dollar against a far

superior, although more expensive, AMLCD. In these instances the focus is on improving the transmission, contrast and color gamut by merely rotating the polarizers and retarder on an existing display. These optimizations are extremely cheap to implement, but do not usually result in marked improvements. The second reason for using an optimization process is to port an existing TSTN design to a new system with the best possible tuning for the intended application. This process may involve the introduction of new LCD materials and entirely different masks and processes, as a result, this type of optimization is easy to implement as it is truly a new design, but it is always easier to optimize when there are as many variables as possible available and the results can be dramatic.

Each cell in a subtractive color stack needs to be "tuned" so that it will extinguish as broad a spectral band as possible. Because of the interdependence of cells on each other, care must be taken to insure that the extinguished bands properly overlap so that the black state does not leak any light, especially in the bands in which the eye is most sensitive. The ability to properly tune a cell is very much determined by application for which the cell is designed. In general it is always harder to design a TSTN stack for high multiplexing. High multiplexing display designs offer several challenges. First is the trouble finding LC material with steep electro-optic characteristics. Second is dealing with the low aperture ratios that are usually associated with cells that have high pixel counts. Third, because it is not easy finding LC materials with steep EO curves, the highly multiplexed cells tend to have larger twists which are less efficient at rotating light. Finally, steep EO curves make dealing with cell nonuniformities more difficult since small changes in voltage can lead to large optical differences.

There are many things that need to be considered when tuning a cell. If the aperture ratio of the cell is low, i.e. the interpixel gaps are big compared with the pixel, and there is not a black matrix employed, it is important to ensure that the zero voltage

state of the device is not too different from the non- select state. This ensures that the gaps will be fairly dark if the cells are aligned properly. One mistake commonly made in some designs is that the colors, and therefore the black state are optimized at zero volts rather than at the non-select voltage which is usually a slightly different Δnd value. This leads to poor contrast if the aperture ratio is high but may be necessary if the gaps, which are at zero volts, comprise a good portion of the display.

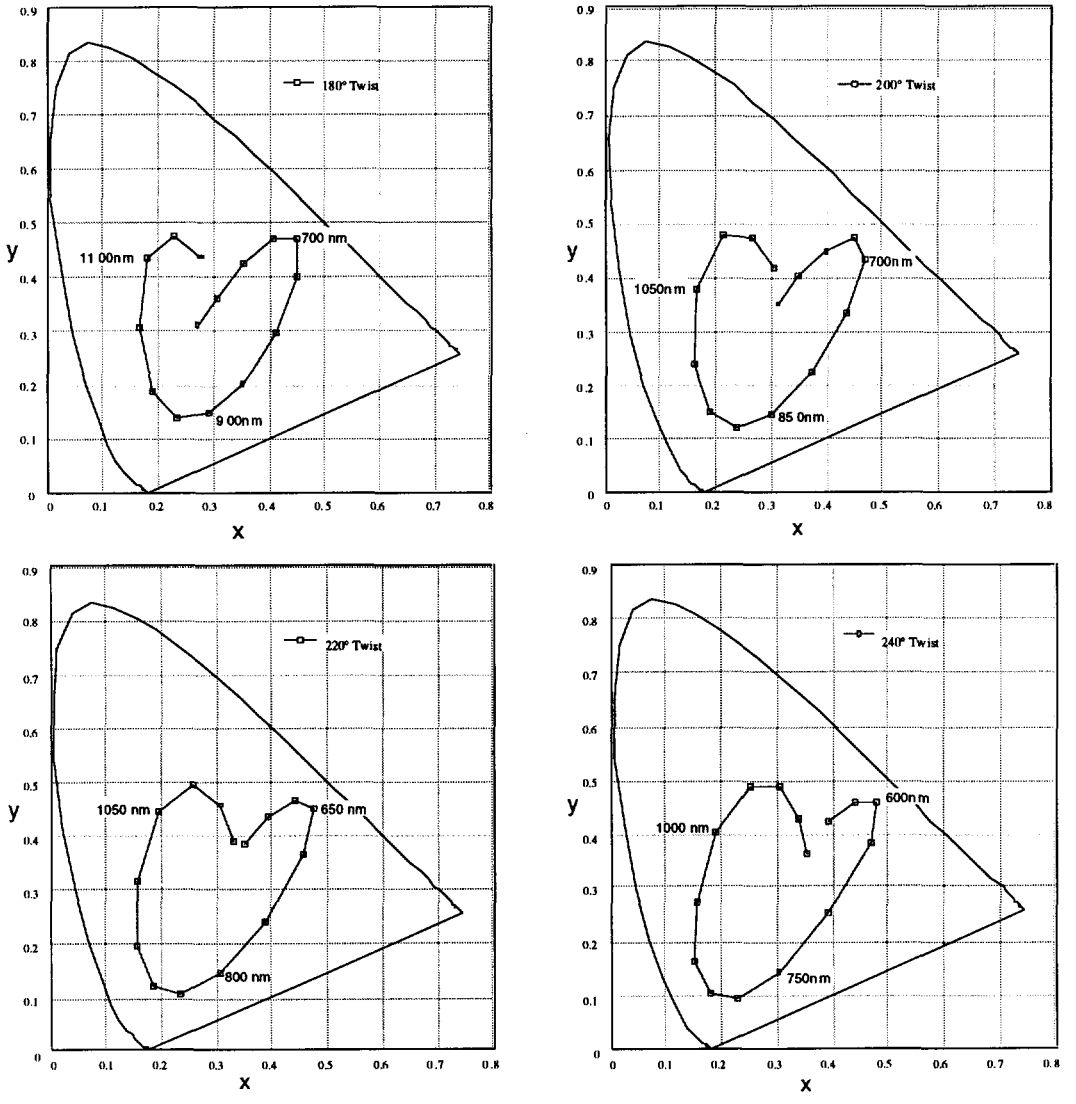

Figure 5.1 The color gamuts obtainable with pure birefringence color for various twist cells over the range Δnd = 500nm to Δnd = 1200nm.

Since each cell requires different optimization, we will examine each type of cell separately, but we can make a few observations regarding the colors that STN birefringence is able to produce [48,49]. Extensive modeling was done to simulate the behavior of an LCD. Figure 5.1 shows the colors on the CIE chart produced when STNs of different twists are placed between two neutral polarizers under the standard condition, i.e. ±45° with respect to the directors on each surface, and the product Δnd is varied over the range 500 nm to 1200 nm. From these charts, we see that yellow corresponds to between 650-750nm, cyan corresponds to 950-1050nm and Magenta corresponds to 800-900nm depending on the twist. These values are good starting points in the design of each cell since the ability to obtain the desired color is already demonstrated.

5.1 Uncompensated TSTN Display

In this section, the process of obtaining the parameters of an uncompensated TSTN stack will be described. Later on in the chapter the method of fine tuning the stack with external compensation layers to achieve much better performance will be described. Before obtaining the parameters of an uncompensated TSTN, the application of the LCD needs to be defined. In this case, the following general features will be assumed since they correspond to a typical VGA TSTN application.

Resolution: 640 x 480 Dual Scan: 240:1 selection ratio

Cell Gap: 6 μm

Threshold voltage: 1.5 - 2.5 rms volts

5.1.1 Yellow

The yellow cell is unique for the standard TSTN because only the birefringence color of the cell is used and no color polarizers are employed. To get a yellow birefringence color we want only one oscillation in the transmission spectrum with a minimum at about 470-480nm. Depending on the twist of the cell, this usually means a Δnd of approximately 730nm. Since this cell is tuned with birefringence color only, it is important to choose an LC material that matches the electro-optic requirements for a twist between 210-220° since this is the range of twists that give the best edge on the green without passing too much blue or reducing the transmission of red light in the select state.

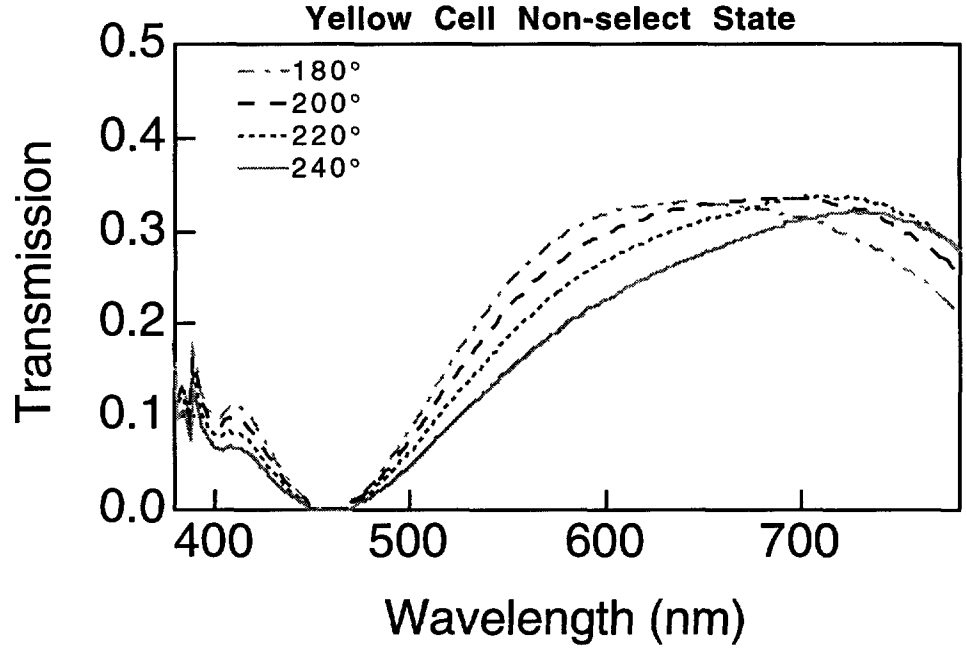

Figure 5.2 Transmission of a yellow cell in the non-select state for various twists. The lower the twist, the steeper the green edge.

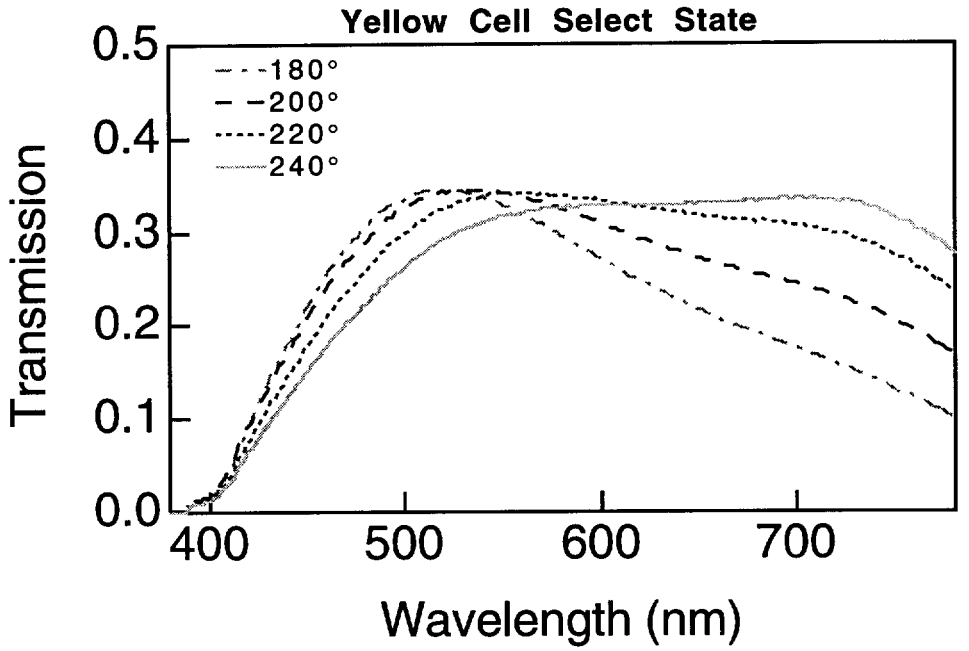

Figure 5.3 Transmission of a yellow cell in the select state for various twists. The lower the twist, the poorer the transmission of red light.

Cells designed with a minimum at 470-480nm will pass some blue light but it is important to remember that we are interested in a cell which when combined with the other two cells is able to yield a reasonable looking black state. Therefore it is preferable to pass too much blue rather than too much green. For this reason, the yellow cell usually has a slightly pink look to it although the resulting yellow color of the display stack is quite saturated.

The yellow cell is the first cell that should be designed since the other cells in the stack are designed around it. Once the yellow cell is designed, the polarizer orientations of the neutral polarizers in the cyan and magenta cells is determined. For aesthetic reasons and for viewing angle considerations, the yellow cell is typically designed with the rub directions on the top and bottom substrates symmetric about the horizontal axis of the cell as shown in Figure 5.4

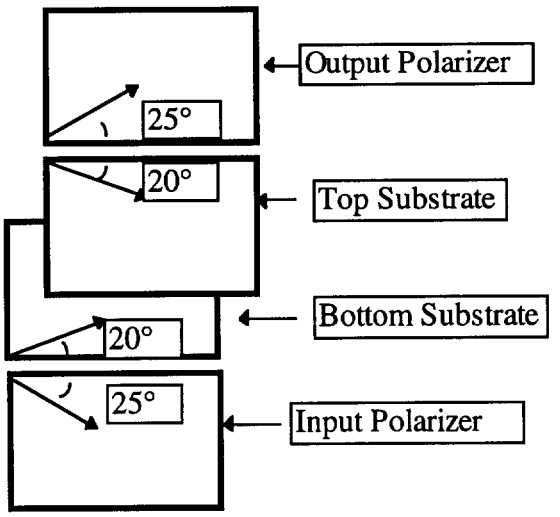

Figure 5.4 Orientations of the rubbing directions and polarizer pass axes for a left handed 220° twist yellow TSTN cell.

The twist of the cell and polarizer configurations have already been chosen so that now we need to choose a liquid crystal material for this cell. Since we would like the non-select state of the LCD to have a Δnd of 730 nm, and the cell gap of the LCD is 6 μm, we need a material with a Δn in the relaxed state about 10% greater than 0.730 μm / 6 μm = 0.1216 or about 0.1338. Our displays also require threshold voltages between 1.8 and 3.0 Volts because of the display drivers being used. The electro-optic performance of each of the candidates needs to be measured before the best material can be determined. The measurement of electro-optic performance is done as follows. Cells are prepared in a manner which simulates the device conditions when placed in a full TSTN stack. For the yellow cell, this is done by placing polarizers on the cell as shown Figure 5.4 at +/- 45° to the rub directions and then putting a blue filter over the cell to simulate the cyan and magenta cells in the off state. A uniformly increasing voltage is applied across a backlit LCD and the brightness is measured by a Newport optical power meter. Signals from both the optical power meter and the voltage source are sent to an analog curve tracer.

The steepness of the electro-optic curve is, as earlier stated, dependent on both the material as well as the twist of the device. Since we determined that the best twist for a yellow cell was between 210° and 230° we need to measure the electro-optic curve of each material for several twists in that range. Since this device is intended for use in a VGA display in a dual scan mode, the number of addressed rows is 240 so the selection ratio of 240:1 means that the device should have, $V_{on} = 1.066\ V_{off}$. As stated in chapter 2, the steepness of the electro-optic curve ζ is the ratio V_{90}/V_{10}. When looking for the right material, the typical rule of thumb is that $2(1-\zeta) = (1-V_{on}/V_{off})$ hence for this display, we need devices for which $\zeta \approx 1.033$. Figure 5.5 shows the modeled transmssion spectra of the yellow cell in the select and non-select states.

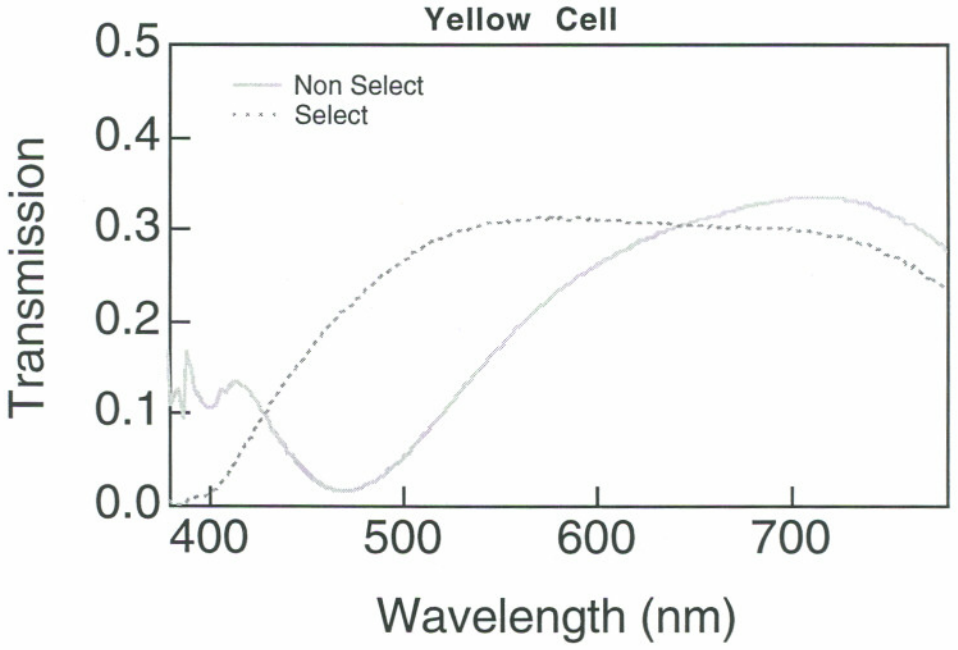

Figure 5.5 Modeled transmission spectra for the select and non-select states of a 220° twist yellow cell with orientations as in Figure 5.4.

5.1.2 Cyan

Again looking at the available color gamut of an LCD for various twists and birefringence values between 500 nm and 1200 nm, we see that the uncompensated cyan cell requires a much higher Δnd product than the yellow cell. The color of an STN only becomes cyanish at high Δnd values between 1050 nm and 1200 nm as seen in Figure 5.1. This fact causes problems in the tuning of devices that have very small cell gaps ($\leq$ 4.5 μm). Since the highest available Δn for LC material is 0.21, a 4.5 μm device would only yield a Δnd product of 950 nm which is not high enough to design a cyan tuning using the most intuitive design process. In this case though, with a 6 μm cell gap, a highly birefringent nematic will be more than sufficient to obtain the desired value for Δnd. A careful analysis of the available LC materials leads to the selection of ZLI 5049-000 for the cyan material[50]. This material requires a twist of approximately 230° to achieve the proper electro-optic curve steepness[50]. Since the orientation of the output polarizer is determined by the yellow cell (input polarizer of the yellow cell), and its twist is -230°, the geometry of the cell is also determined and is shown below. For this material the birefringence of the select state is 1050 nm while the birefringence of the non-select state is 680 nm.

Figure 5.7 shows the modeled transmission of the uncompensated cyan cell. The uncompensated cyan cell suffers from poor transmission in the select state as well as poor extinction of red light in the non-select state. It is also quite obvious that the cyan cell does not modulate red light alone since the transmission of blue and green light are reduced in going from the non-select to the select.

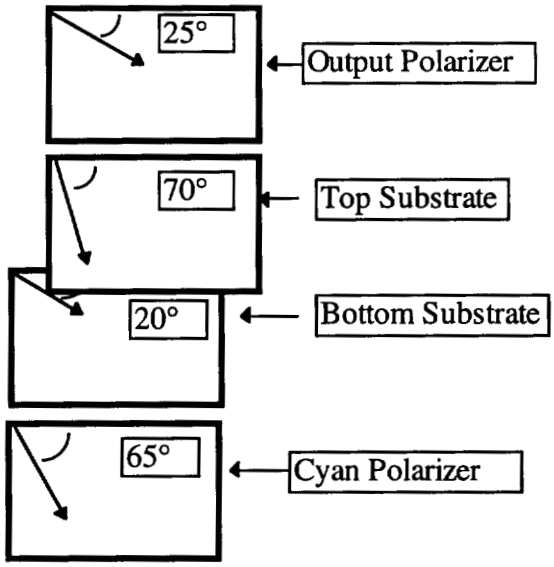

Figure 5.6 Orientation of the polarizers and rubbing directions of the LCD for the cyan layer in an uncompensated TSTN display.

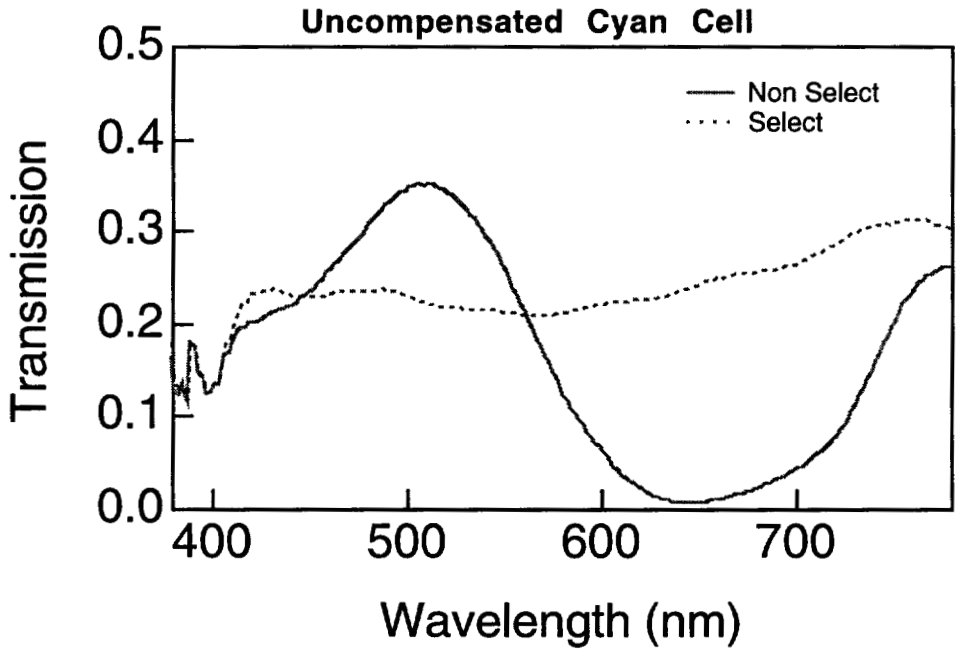

Figure 5.7 Modeled transmission spectra of the select and non-select states of a 230° twist uncompensated cyan cell with polarizer orientations as in Figure 5.6

5.1.3 Magenta

For the magenta cell, Figure 5.1 shows that the desired birefringence of the nonselect state should be approximately Δnd = 850 nm. A cell with this nonselect birefringence will typically have a select state birefringence of 580 nm given the multiplex ratio. Although the material used in the cyan cell is more birefringent than necessary, it still is able to switch nicely between 850 nm and 580 nm at the 240:1 selection ratio. Unfortunately, even with the magenta polarizer, the select state is usually not transmissive enough in the blue to yield a really nice white state. The orientation of the input polarizer is determined from the yellow cell below (output polarizer of the yellow cell) and the twist is 230° so again the geometry of the cell is determined and is shown in Figure 5.8.

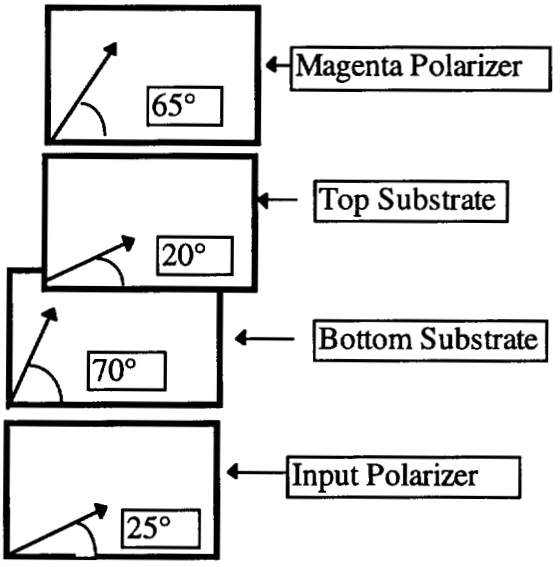

Figure 5.8 Orientation of the polarizers and rubbing directions of the LCD for the magenta layer in an uncompensated TSTN display

Figure 5.9 shows the modeled transmission of the uncompensated magenta cell. Similar to the uncompensated cyan cell, the uncompensated magenta cell also suffers from poor

transmission in the select state and poor extinction of green in the non-select state. The uncompensated magenta cell also does not modulate green light alone since the blue light is reduced in going from the non-select state to the select state.

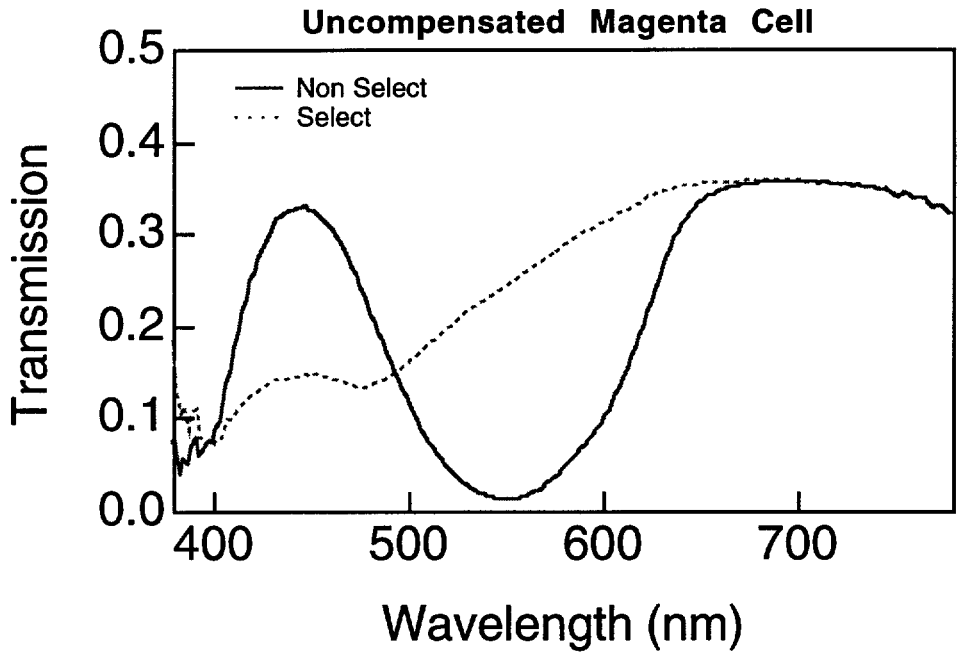

Figure 5.9 Modeled transmission spectra for the select and non-select states of an uncompensated magenta cell with polarizer orientations as in Figure 5.8

5.1.4 Result of uncompensated cyan, magenta and yellow cells

The modeled transmission spectra of the uncompensated TSTN is shown in Figure 5.10. It can be seen that for this design, the contrast is fairly poor, with severe light leakage in the black state especially at the transition wavelengths. The transmission and color temperature of the display is also poor since the white state lets very little green and blue light through as compared to the red light.

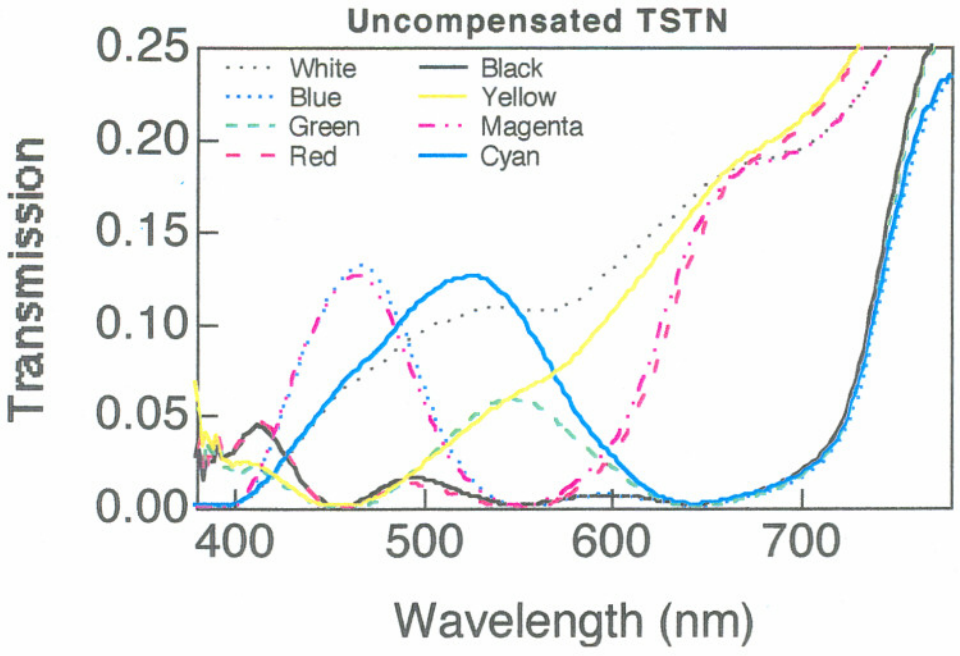

Figure 5.10 Modeled transmission spectra of the uncompensated TSTN display described in this chapter. The eight colors here are all the possible combinations of the three cells in the select and non-select states as in Figure 3.2

5.2 Compensation Using Double STN "DSTN" Method

Since STN displays are not inherently black and white, it was understood early on that commercially acceptable contrast could only be achieved though external compensation[5,51]. The first successful compensation of the STN was the DSTN or Double STN [52]. This structure consists of a normal STN cell, monochrome or color stripe, patterned in the standard matrix, with a separate unpatterned and undriven STN. The undriven STN or compensator, is a mirror image of the driven STN. The twist of the compensator is the same magnitude except that it is of the opposite handedness and with the director at the surfaces oriented at 90° to the orientation of the driven cell. The combination of the two cells are mutually compensating in the undriven state since whatever one STN layer does, the other layer undoes. When placed between crossed polarizers, the non-select state appears dark. The driven state is not compensated so the

select state appears light. Figure 5.11 shows a schematic representation of the principle of DSTN.

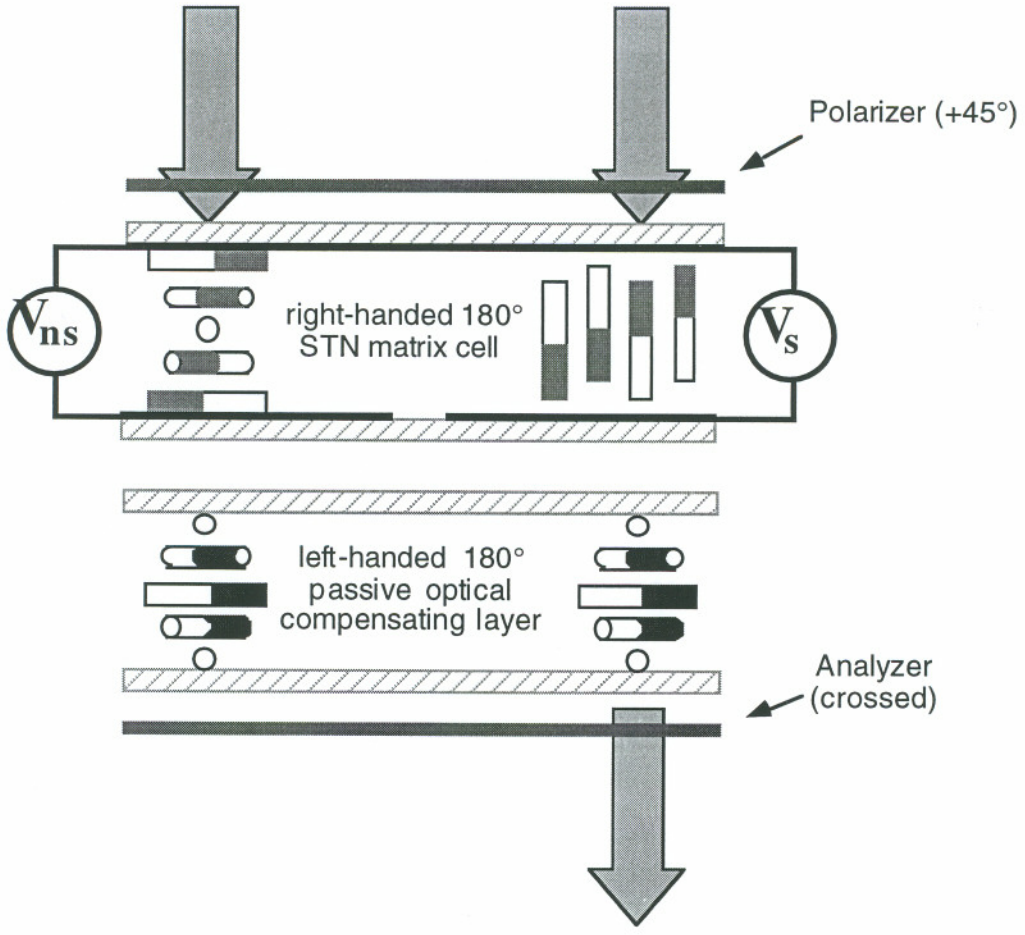

Figure 5.11 Schematic Representation of a DSTN for 180° twist cell.

DSTN displays were quite popular for a few years but the excess weight and increased thickness were real drawback for laptop and notebook computer displays. Then it was realized that the same effect could be obtained if the passive STN were replaced with several sheets of retardation film configured to mimic the passive STN structure [51]. Many of the lessons that were learned in the compensation of STN cells for black and white operation are readily adaptable to compensation techniques used for subtractive color TSTN design.

5.3 Compensation Techniques for TSTN

The original uncompensated TSTN design was a big breakthrough in that it was one of the first avenues for projection displays to reach the desired qualities of brightness and color [9]. Even with its success, there were a few problems, the first problem was that the cyan and magenta cells did not switch monotonically from cyan to white or magenta to white without changing their hue. The role of the cyan cell is to control only the red light transmission while leaving the transmission of the blue and green light unaffected. The reason that this was not happening is that the spectral minimum of the LCD were just sliding in wavelength as the voltage changed. This, along with the sloping edges of the polarizers meant that the amount of green light had the possibility of decreasing even as the voltage increased. Similar problems existed for the magenta cell. A second and related problem was that the transmission minima of the LCDs were not broad enough to overlap properly and create a good, dark, neutral black state. It turns out that there is one solution which can be used to alleviate both of these problems.

There are several manufacturers which can supply either stretched Polyvinyl Alcohol (PVA) or Polycarbonate (PC) retardation film in a variety of retardation values. The proper use of this type of retardation film for compensation of the LCD displays has a dramatic effect on the performance of the display. In this section, the methods for application of either PVA or PC retardation film to an individual TSTN panel in order to achieve better contrast and monotonic grayshade control will be discussed.

A simple retarder with a retardation of δ does not change the phase of the polarized light that has the same wavelength as the retardation value[40] since it is just a full waveplate for that wavelength. In other words a 650 nm retarder has no effect on the phase of 650 nm light as it is in effect, a full wave plate. A 650 nm retarder on the other hand does have an effect on the phase of light at any wavelength besides 650 nm. What this means is that with a retarder placed between the LCD and polarizer, we can alter the

transmission of an LCD at some wavelengths while keeping the transmission characteristics of the LCD at other wavelengths unchanged. The goal of compensation is to improve the contrast of the nonselect state and enhance the transmission of the select state. The retarders that are used correspond with the wavelength of light that is being extinguished in the non-select state. As an example, lets look at the transmission of the uncompensated cyan cell described in the previous section (Figure 5.7), and compare it to the transmission of the same cell which has been compensated with a 650 nm PVA retarder placed between the LCD and the cyan polarizer. Figure 5.12 shows the modeled transmission spectra of a compensated cyan cell. There is obvious improvement both in the broadness of the minima between 600 and 700 nm in the non-select state as well as improved transmission of the select state. As an added benefit of this compensation, the intermediate states do a much better job in modulating the transmission of red light only.

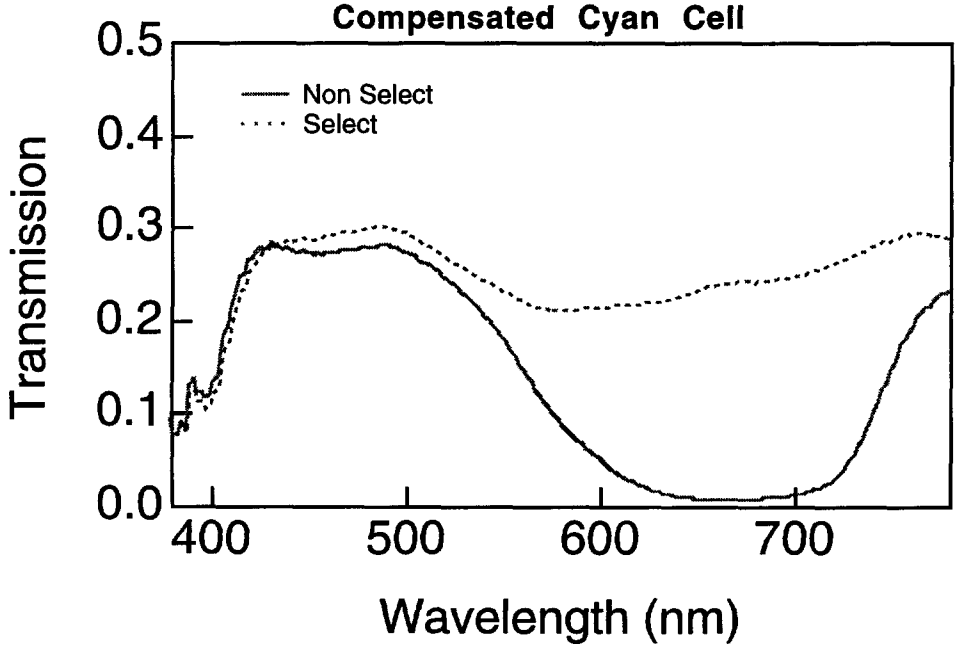

Figure 5.12 Modeled transmission spectra of the select and non-select states of a 230° twist cyan cell compensated with 650nm PVA and with polarizer orientations as in Figure 5.6. As compared to Figure 5.7, this compensated cell shows improvement in both transmission of the select state as well as extinction of the red band in the non-select state.

If we apply the same technique to the magenta cell, we would assume that we needed a 550 nm retarder placed between the magenta polarizer and the magenta LCD. Because of availability, a more convenient value to use is 570 nm PVA. Figure 5.13 shows the modeled transmission of a compensated magenta cell. Again, when compared with Figure 5.9, there is obvious improvement in both the select and non-select states as well as the intermediate states which now only modulate green light.

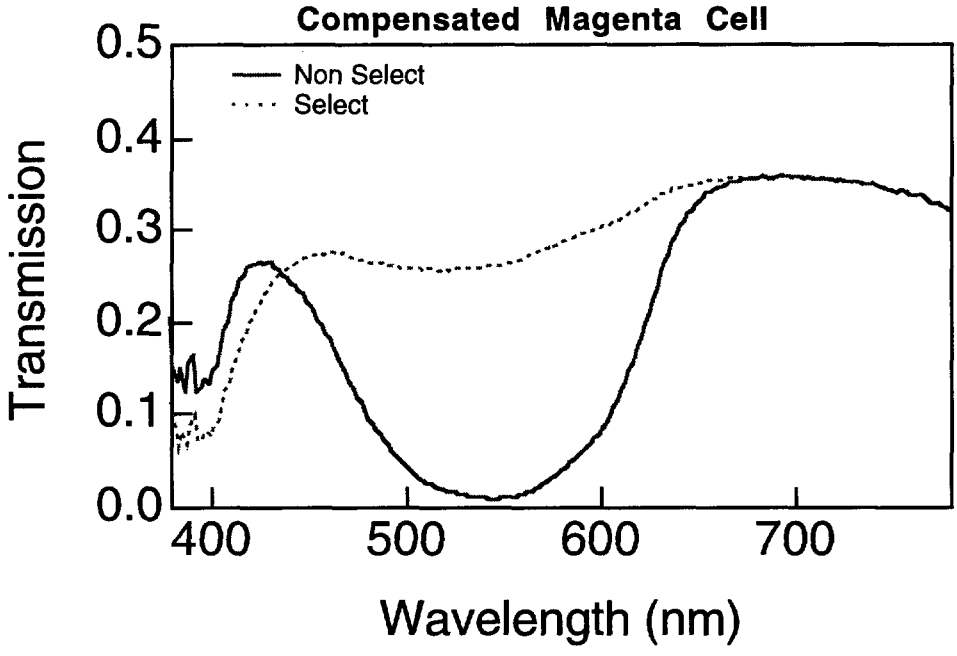

Figure 5.13 Modeled transmission spectra for the select and non-select states of a 230° twist magenta cell compensated with 570nm PVA and with polarizer orientations as in Figure 5.8. As compared to

Figure 5.9.

While the results of the compensation of the individual cells may not be dramatic looking, the results on the entire display are very impressive. While the transmission of the uncompensated TSTN is only 11.4% and the contrast only 22:1, the compensated

TSTN is over 14% transmissive and has a contrast ratio of 49:1. Aside from these two improvements, the color gamut of the compensated TSTN also is slightly wider and shows better saturation of primaries see Figure 5.15.

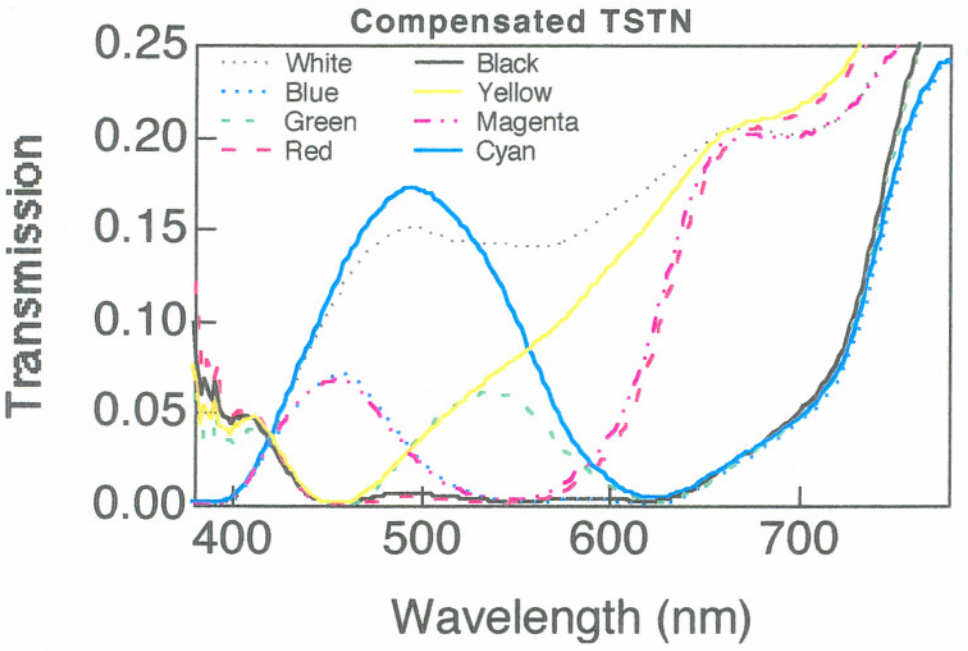

Figure 5.14 Modeled transmission spectra of the compensated TSTN display discussed in this chapter. As compared to Figure 5.10, the compensated display has much better transmission, a better color gamut and more than double the contrast ratio.

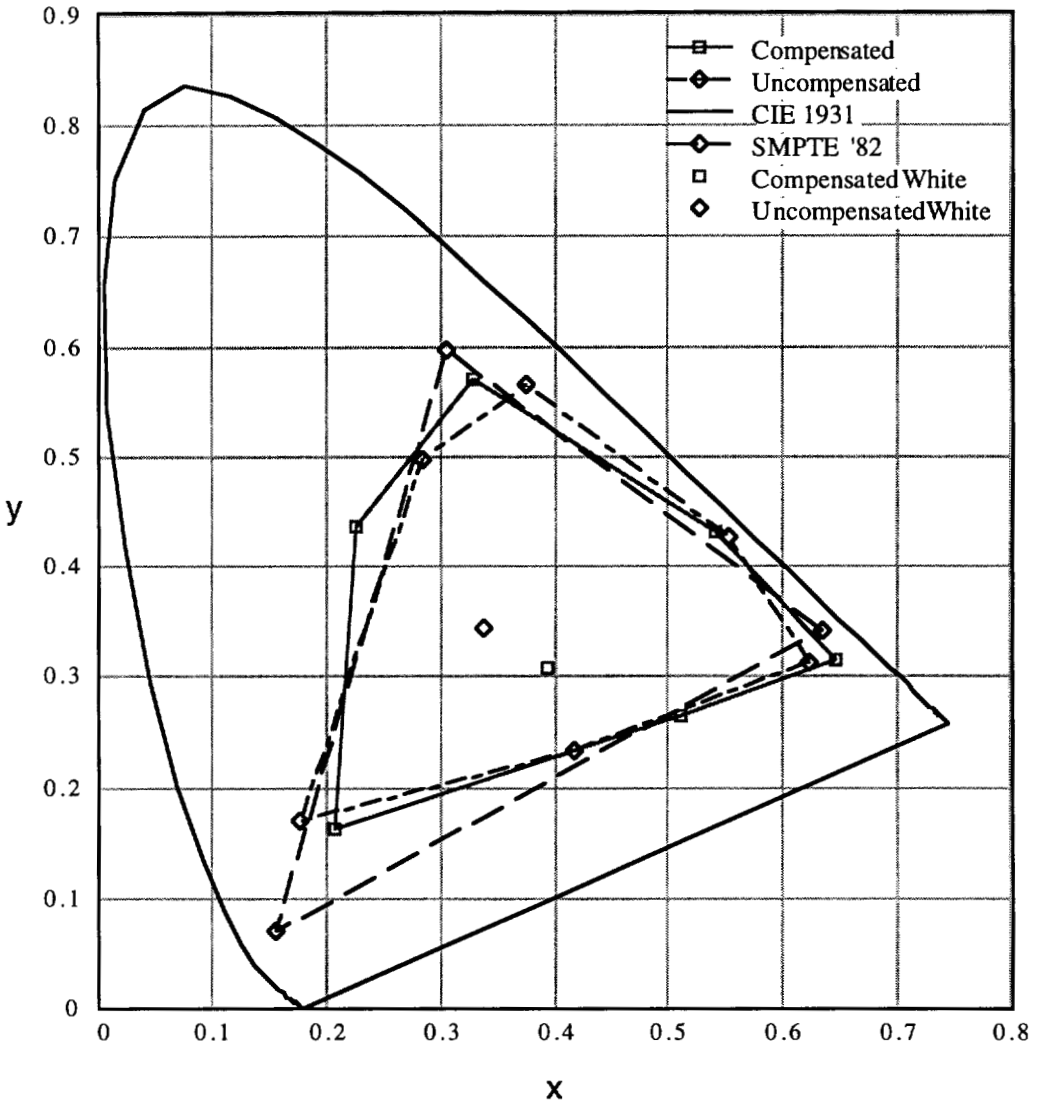

Figure 5.15 Comparison of the color gamuts of an uncompensated TSTN display with a compensated TSTN display.

5.4 Fine Tuning

The previous section described the process of compensating a TSTN with a first order method. In this section, a process will be described which takes that method one step further in an attempt to get even better results. This process relies heavily on the interactive mode of the modeling software that was developed during this investigation.

The interactive mode allows one to step through many values of retardation, retarder angle, and polarizer angles in rapid succession while getting immediate feedback about the design.

The process may begin with the first order design shown in the previous section and then, using the software, make small changes to the retarder value until a local maxima is found in the design. Then one might make small adjustments to the retarder angle followed by adjustments in the polarizer angle (cyan or magenta polarizer only). The process may then be repeated. In this manner, the original design may evolve into a completely new design. Typically the improvements at this stage are small but it is an important procedure in any case.

Another technique that is useful to try is using a retarder with a value double the full waveplate value. This again will leave the transmission minima unaffected but will do very different things to the rest of the transmission than the original full waveplate. For instance, one might use a 1050 nm or 1100 nm retarder for the magenta cell. This has been done for some designs and can work quite well.

Finally, one might use two retarders to compensate each cell. This gives two more degrees of freedom and is just as easy to model using the interactive software. Designs of this type has been designed based on modeling, but the costs associated with the addition of two more PVA films is not justified by the improvements.

5.5 Practical Examples

This section consists of four examples of TSTN tuning using the approach described in the previous sections. Each one of these examples is slightly different in their intended use and so the design requirements are also very different.

5.5.1 Example 1 : TSTN with each cell having the same geometrical design

Manufacturing LCD cells is a very complicated process which needs to be precisely controlled. In a factory such as the one at Motif, the control of that process is much harder to maintain if there are several different types of substrates that need to be processed. In this example, we considered the benefits of each cell in the stack being identical except for the liquid crystal material. This means that each cell would have the same total twist and rub directions which makes the production process far simpler since every cell goes through an identical production process until the point at which they are filled with liquid crystal. This enhances process control and would hopefully result in higher yields and better uniformity. This also has important benefits for the company that purchases the cells since prices are lower in larger volumes.

The design concept is based on the assumption that, by inserting additional retarders (acting as half wave plates) into the standard TSTN configurations, we could both rotate the plane of polarization emerging from the neutral polarizers, but also gain improved "tuning" with the extra degrees of freedom. A half waveplate can rotate the plane of polarization of linearly polarized light by twice the angle between the fast axis of the retarder and the plane of polarization of the light.

This stack, being designed for VGA resolution, required a large enough twist for steep electro-optic curves while not too steep to compromise the performance of the yellow cell with regard to the green edge steepness. Based on the analysis of the previous sections and keeping in mind Figure 5.1 as well as the availability of LC material, 235° twist was found to offer the best compromise in the quality of color versus the steepness of the electro-optic curves for all three cells.

Beginning again with the yellow cell, we see that the 235° twist results in the following configuration for symmetrically rubbed surfaces:

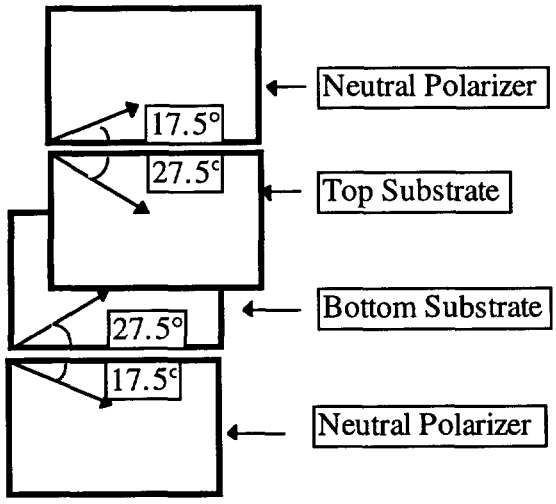

Figure 5.16 Configuration of 235° yellow cell used in TSTN stack

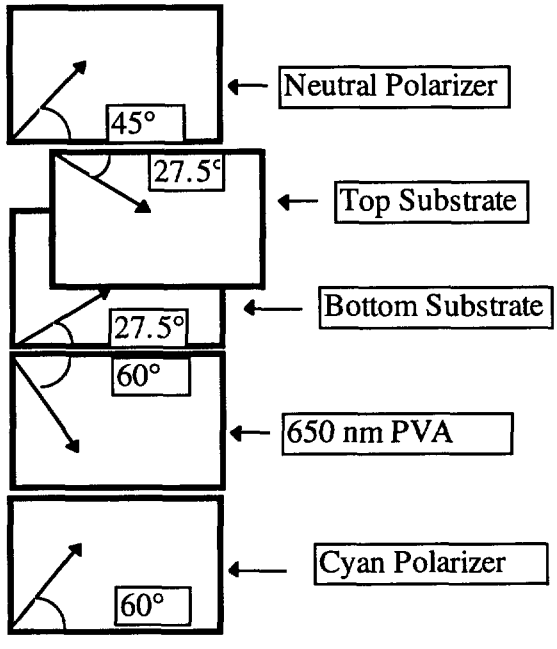

Figure 5.17 Configuration of cyan tuning if the cyan cell is rubbed the same as the yellow cell above in Figure 5.16.

Since the goal is to have the same geometry for all the cells, the cyan and magenta cell configuration can be now independently designed using the same geometry as the yellow cell. Using a 235° twist symmetrically rubbed cyan cell, a good tuning can be found with the following configuration.

The neutral polarizer is not in the proper orientation to allow the cyan design to append to the yellow design, but we can employ the use of a "half wave plate" to rotate the plane of polarization of the light. For instance, in order to use an existing TSTN design, the plane of polarization needs to be rotated in order that it coincides with the plane of polarization that the light would have had if the next cell in the system used its own polarizer. For the cyan cell above, a 330 nm retarder placed between the LCD and the neutral polarizer and oriented at will rotate the plane of polarization of the 660 nm red light by the required 62.5° when the PVA is oriented such that the fast axis is at about 31.25° from the pass axis of the neutral polarizer.

Similarly the magenta cell can be designed in the same way with a 240 nm retarder acting as a half-wave plate for the 550 nm green light. A system such as the one described has been modeled and the results of the model are shown in Figure 5.18. The transmission of the design is 14.7% without the surface reflections taken into account which would reduce it to 11.0%. The contrast of the design is 69:1. The original intent of the design was to take three cells of identical construction and build a TSTN were fulfilled without either improving or reducing the performance as compared with standard TSTN designs. Although the 240 nm retarder is not exactly half wave of 550 nm green light, it is just this sort of exception that we should expect to see if the extra PVA film is used as an additional degree of freedom in the optimization process.

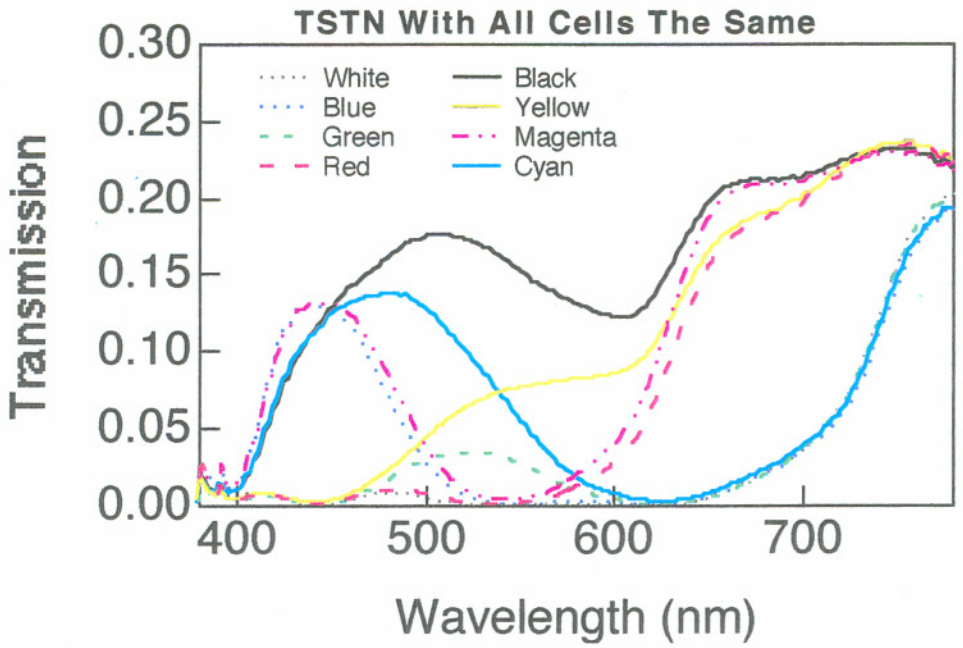

Figure 5.18 Modeled transmission spectra of a TSTN with all of the cells having the same geometry. Surface reflections are not taken into account

5.5.2 Example 2: TSTN design for "Datawall" application

A TSTN stack was developed for use in a modular display in which there may be a matrix of 20 x 15 (300 total) 10 inch diagonal display units each multiplexed with a duty ratio of 32:1. The matrix of display modules would yield a large area 175 inch diagonal VGA resolution display. This type of display would be particularly attractive for retail settings and commercial advertising in the same manner as the JumboTron types of displays made from "single pixel CRTs". An arrangement such as this also gives a lower cost alternative for lower resolution 1/4 VGA display which are approximately 88 inches in diagonal but only require a matrix of 10x7 or 70 total display modules. Although this may seem like an expensive display solution, the cost per square inch of display is quite competitive and offers several advantages.

A duty ratio of 32:1 corresponds to a selection ratio of 1.196. This high selection ratio gave us the freedom to lower the twist angles of the cells. We manufactured cells

filled with the standard yellow material and cyan/magenta material at several different twists to determine the proper twist angle for the 32:1 duty ratio. Both the yellow and the cyan/magenta material were found to have the proper EO slopes when the twists were about 170°. For symmetry reasons and also because of manufacturing ease, we chose to make the cells all at 180° instead to see how good we could get. Making the cells all 180° twist and applying the general rule that the polarizers be placed at crossed 45° makes the design similar to the one described in Section 5.5.1 except that there is no need for half-wave plates. Figure 5.19 below shows the modeled transmission of the "Datawall" while Figure 5.20 shows the measured transmission spectra. The two transmission plots show remarkable similarity verifying the theory and the value of the modeling software.

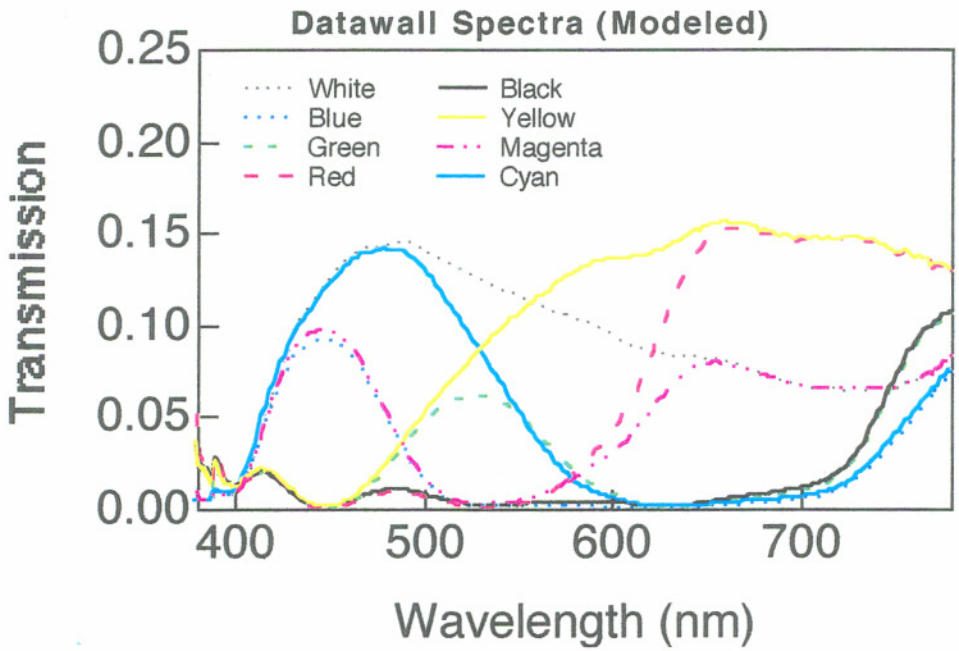

Figure 5.19 Modeled transmission spectra of the low resolution "Datawall" TSTN display.

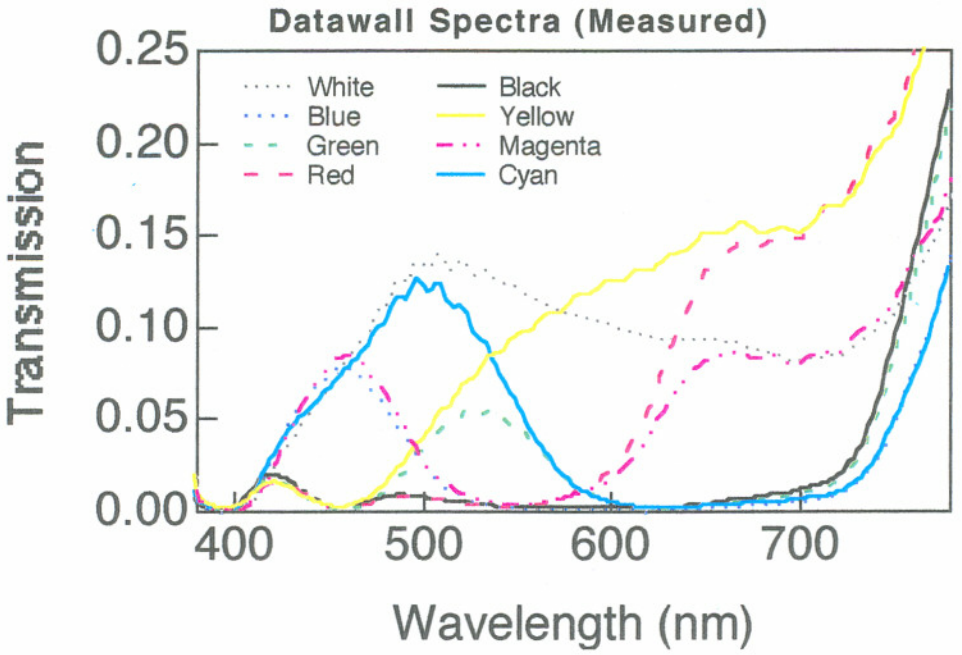

Figure 5.20 Measured transmission spectra of the low resolution "Datawall" TSTN display.

5.5.3 Example 3: "Pearl" Design For Active Addressing

A small (2 inch by 2 inch) TSTN display, code named "Pearl", was also being developed to be used in a projection application and also using Motif's proprietary addressing scheme called Active Addressing. This LCD drive scheme was developed to allow passive matrix displays to run at video rates. The Pearl cells, requiring video rates had much smaller cell gaps of 4.5 μm as opposed to 6.0 μm. This small cell gap means that the maximum birefringence Δnd available is only 950 nm as opposed to 1200 nm. This placed especially hard burden on the cyan cell design. Figure 5.21 shows the modeled "Pearl" transmission spectra and Figure 5.22 shows the measured spectra.

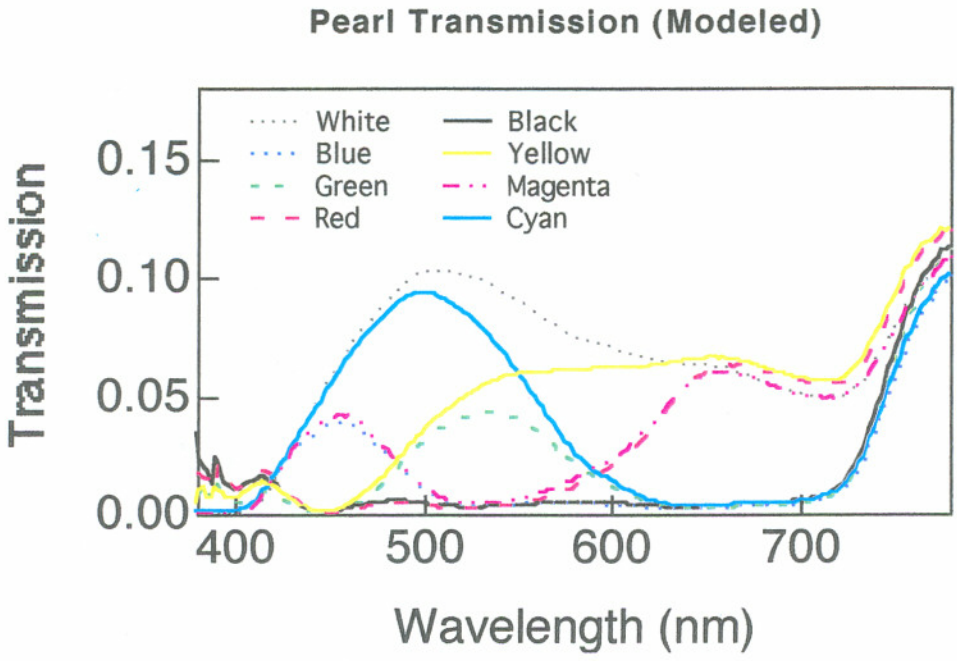

Figure 5.21 Modeled transmission spectra of the Active Addressed "Pearl" TSTN display. Surface reflections and aperture ratio are not taken into account.

The discrepancy in the overall transmission 9.8% modeled vs. 5.9% measured can be accounted for because of the fact that the small "Pearl" cells had a fairly low aperture ratio of only about 65% as opposed to the "Datawall" which had an aperture ratio of nearly 95%. If taken into account durring the modeling procedure, the modeled transmission would have been closer to 6.2% which is only 5% higher than the measured value.

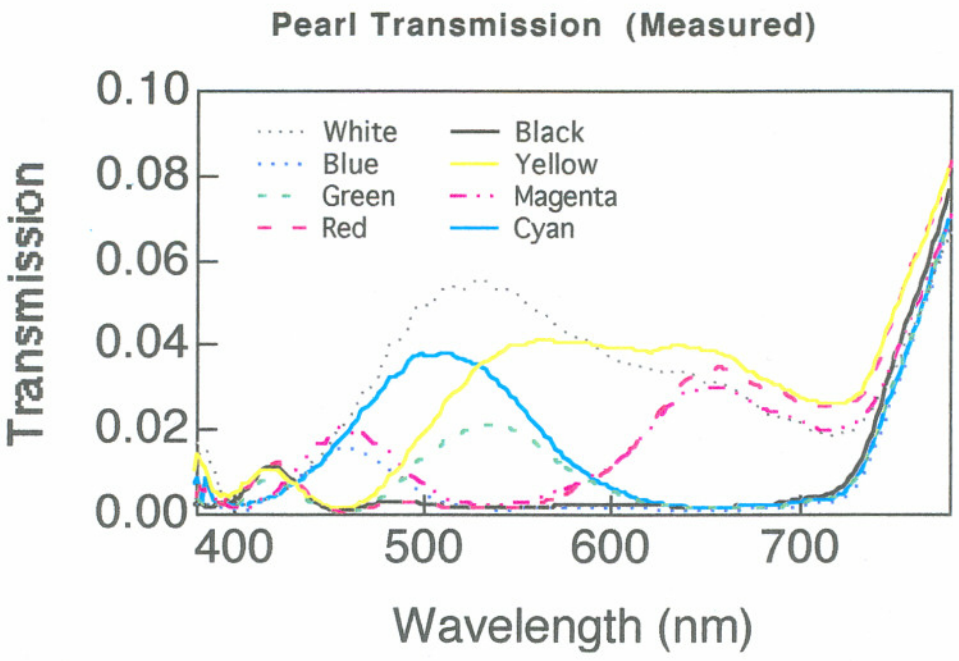

Figure 5.22 Measured transmission spectra of the Active Addressed "Pearl" TSTN display.

5.5.4 Example 4: Improved Design for XGA Projection Panel

As a last example, there existed a design code named "Osprey" using TSTN in a very high resolution XGA projection panel intended for use with an overhead projector. Because of the high resolution, the selection ratio for these displays was particularly low leading to poor performance since the design for this display had been simply ported from a low resolution version with the main difference being a slight increase in twist to allow for the lower selection ratio. The performance deficiency was mainly in the lack of contrast which was due to the fact that the yellow cell was designed in favor of transmission over contrast. The modeling showed quite clearly that the yellow mixture had too low a Δnd so that the yellow state never blocked enough blue light to provide a good black state. This also lead to desaturated reds and cyanish green colors.

The Δnd of the original mixture was only Δnd = 535 nm in the nonselect state giving a minimum at approximately 410 nm. The STN modeling program showed that this tuning required a higher Δnd of nearly 600 nm in the nonselect state for really good contrast which would have a transmission minimum at 460 nm. Since the selection ratio was so low though, this would have lead to undesirable loss in the white state since the mixture would not have been able to turn on far enough. A Δnd of 580 in the nonselect with a minimum at 440nm would be able to provide reasonable contrast and yet not compromise the transmission of the white state.

Measured transmission spectra of the original "Osprey" design as well as the new and improved design are shown below. The contrast of the improved design increased by over a factor of two from just under 10:1 to over 25:1. Aside from the contrast the display remained fundamentally the same.

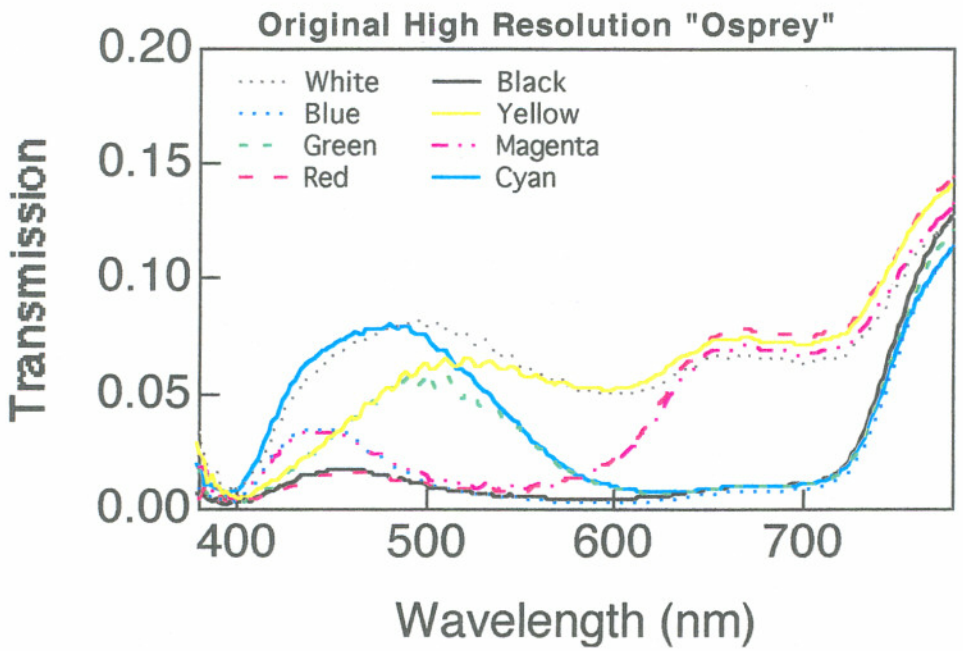

Figure 5.23 Measured transmission spectra of the high resolution "Osprey" TSTN display with the original yellow cell.

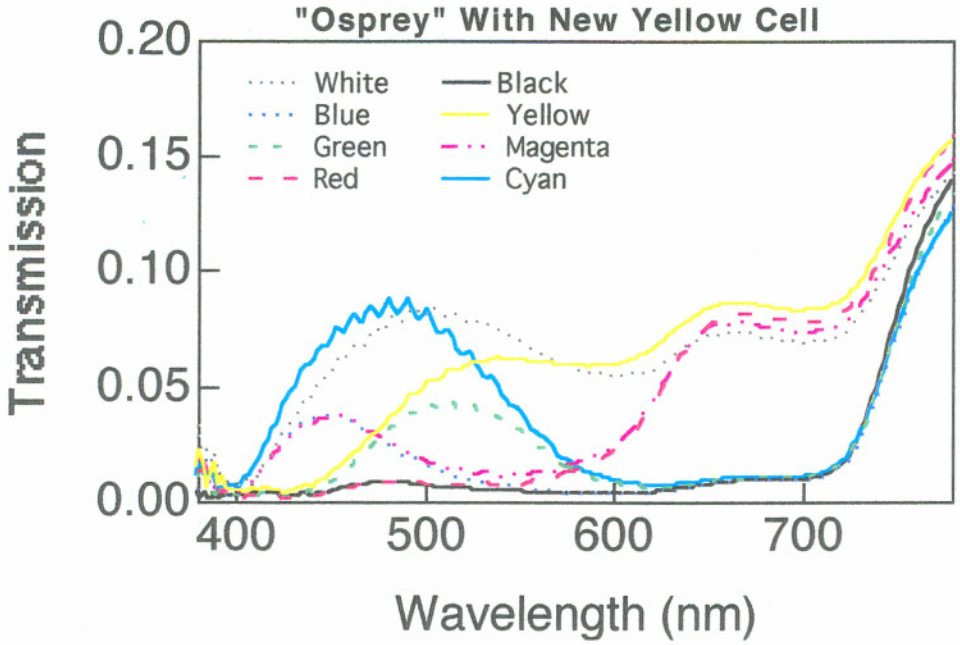

Figure 5.24 Measured transmission spectra of the high resolution "Osprey" TSTN display with a new and improved yellow cell.

5.6 Conclusion

TSTN performance can be improved with tuning procedure which makes use of interactive modeling software. The examples show quite well the ability of the modeling software to predict the performance of the design. Without modeling software to simulate the design performance, the shear number of variables as well as the time consuming prototyping would prohibit the rapid introduction of new designs as well as decrease the quality of designs.

6 TEMPERATURE COMPENSATION OF STNS

One of the biggest problems with the subtractive color TSTN design is the adverse effect that temperature gradients in the cell have on the appearance of the display. This becomes especially critical in a projection system where temperatures are apt to be high and cooling is nonuniform. The operating voltage of the STN display is highly dependent on the operating temperature. In color filter STN system, temperature differences across the display result in a difference in contrast or transmission from one part of the display to another. In a subtractive TSTN color system, on the other hand, temperature gradients can also cause differences in color from one part of the display to another. This is because each cell in a subtractive color stack can have different temperature profiles. For these reasons, it is especially important to try to compensate the electro-optic behavior of the displays in the TSTN stack to make them as temperature insensitive as possible. Many displays offer electronic control of the brightness and contrast which is fairly effective in correcting for the increase in temperature that the display undergoes as it reaches operating temperature. However, these controls are unable to compensate for temperature variations across the cells and are also a nuisance to use if the display is slow to stabilize. A better approach is *in-situ* temperature compensation which addresses these problems by making the device inherently more stable.

6.1 Analytical Background

The most important device parameter to compensate for temperature is the threshold voltage. The threshold voltage of a mixture is dependent on several parameters,

the elastic constants, the d/p ratio, the dielectric anisotropy, and the birefringence, each of which is temperature dependent. The threshold voltage, V_{th} of a non-twisted nematic layer with zero pretilt, for example, is given by[16]:

$$V_{th} = \pi \sqrt{\frac{k_{11}}{\varepsilon_0 \Delta\varepsilon}} \qquad (6.1)$$

where k_{11} is the splay elastic constant, $\Delta\varepsilon$ is the dielectric anisotropy and ε_0 is the permitivity of free space (8.85×10^{-12} F/m). The threshold voltage will typically decrease as the temperature is increased. This is because $k_{11} \propto S^2$ and $\Delta\varepsilon \propto S$ so $V_{th} \propto \sqrt{S}$, where S is the order parameter of the liquid crystal[16]. The order parameter, of course decreases as the temperature increase until at the clearing point of the liquid crystal, it abruptly becomes equal to zero.

The threshold voltage V_{th} of a twisted chiral nematic layer is approximately given by [53]:

$$V_{th} \approx V_{th}^0 \sqrt{1 + \{[\frac{k_{33}}{k_{11}} - 2\frac{k_{22}}{k_{11}}]\frac{\phi}{\pi} + 4\frac{k_{22}}{k_{11}}\frac{d}{p}\}\frac{\phi}{\pi}} \qquad (6.2)$$

where V_{th}^0 is the threshold voltage of the non-twisted nematic layer with zero pretilt, d is the thickness of the liquid crystal layer, p is the pitch, ϕ is the twist angle of the cell, and k_{11}, k_{22} and k_{33} are the splay, twist and bend elastic constants, respectively.

There is little that can be done to alter the inherent temperature dependence of the birefringence and elastic constants [54]. However, the d/p parameter offers a unique opportunity to compensate for changes in the other parameters. One can compensate the temperature dependence of the threshold voltage by carefully designing the temperature

dependence of the pitch of the chiral nematic mixture. As seen from Equation 6.2, the natural tendency for the threshold voltage V_{th} to decrease with temperature can be counteracted by having the pitch of the chiral mixture also decrease with temperature. All known chiral dopants, however, cause the pitch to increase with temperature, further exacerbating the problem. The desired temperature dependence can be obtained by combining a chiral dopant of the opposite handedness to the nematic mixture and adjusting both doping concentrations so that the pitch of the mixture decreases as the temperature of the mixture is increased[54,55]

The temperature dependence of the pitch can be formally written as a power series in temperature[55]:

$$\frac{1}{pc} = A + BT + CT^2 + ... \qquad (6.3)$$

where p is the pitch in μm, c is the concentration of the chiral dopant in weight%, A, B and C are material constants that must be determined experimentally, and T is the temperature in ° Celsius. The material constant A is the helical twisting power (HPT) of the dopant in μm·weight %. This coefficient as well as B and C are generally dependent on the host nematic mixture as well as the dopant and must therefore be determined for each mixture. When two chiral dopants are combined, and keeping only the terms linear in T, the pitch Equation 6.3 becomes[55]:

$$\frac{1}{p} = (c_+A_+ + c\_A\_) + (c_+B_+ + c\_B\_)T \qquad (6.4)$$

where the index + refers to the right handed chiral dopant and - refers to the left handed dopant. The object is to choose materials and concentrations such the coefficient ($c_+B_+ + c_-B_-$) has a small positive value.

An issue that one should consider before attempting to engineer the temperature dependence of the pitch is that a decrease in the pitch can cause the onset of the two dimensional striped texture that occurs when the material leaves the Freedericksz configuration [5]. Care should be taken to ensure that the onset of stripes does not occur over the range of temperatures that the display is to be operated. This problem can also be avoided by increasing the pretilt of the mixture slightly.

6.2 Experimental Procedure

The temperature dependence of the pitch for a right handed chiral dopant 3786 and a left handed chiral dopant 9209F in the nematic mixture ZLI 4620 was measured. The measurements were taken by using a plano-convex lens, (radius of curvature R = 51.68 mm) which had been coated with a polyimide alignment layer on the curved surface and rubbed, This lens was placed on a rubbed planar substrate with the LC mixture in between. Assuming that the rub directions are parallel, the director, being firmly anchored at each boundary, will twist in multiples of 180° leaving boundaries between consecutive integer multiples as shown in Figure 6.1. The diameter D_n of consecutive 180° disclinations were measured and scaled according to the lens combination on the microscope. The pitch p of the liquid crystal is computed as follows. According to the Pythagorean theorem we have:

$$(R - H_n)^2 + \left(\frac{D_n}{2}\right)^2 = R^2$$

which, since $H_n^2 \ll D_n^2 \ll R^2$ gives to first order.

$$D_n^{\,2} = 8RH_n.$$

But since the distance H_n of the n^{th} disclination is equal to np/2, we have

$D_n^2 = 4Rnp$.

A plot of D_n^2 vs. n yields a slope of 4Rp from which the pitch is easily computed.

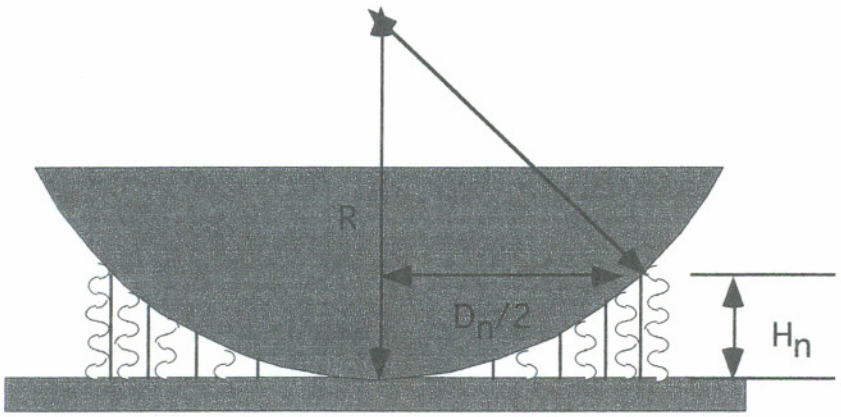

Figure 6.1 Plano convex lens on glass substrate. Dark rings (straight lines) are seen at disclinations between regions of consecutive 180° twists.

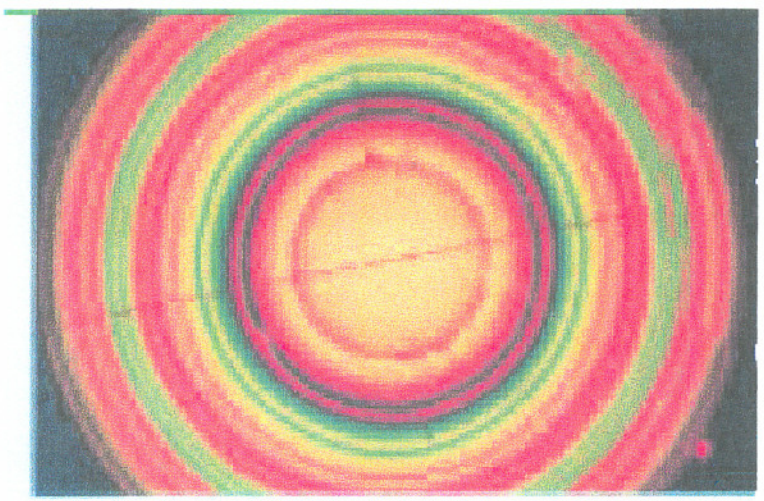

Figure 6.2 Picture of a non-twisted nematic between a slide and a lens with polarizers adjusted for best contrast between disclinations.

Pictures were taken with a Jenalab polarizing microscope attached to a computer controlled heat chuck so that precise temperature dependence can be obtained. For each mixture, measurements were made every 5° C over the range of temperatures from 20°C - 75°C. Figure 6.1 shows one of the pictures used to obtain a pitch measurement.

Table 6.1 HTP coefficients of LC mixtures

LC Mixture	A (μm • weight %) $x10^{-2}$	B (μm • weight %/°C) x 10^{-5}
4620 1.04% 9209F	-8.606	2.122
4620 1.21% 3786	14.254	-30.647

Since both left handed and right handed chirals are combined in the nematic LC to compensate, this procedure is done on both of these dopants in the nematic at the uncompensated doping levels. The temperature coefficients for each dopant were obtained by a linear interpolation of the temperature dependence of the mixtures. Figure 6.4 shows the temperature dependence of the pitch for both the left handed and right handed chirals in ZLI 4620. Also plotted in the figure are the linear interpolations that were used to define the HTP coefficients in Table 6.1.

Once the HTP coefficients are known, we are left to solve a simple system of two equations and two unknowns. The desired temperature dependence of the pitch is estimated, and the concentrations of the dopants in the compensated mixture are computed. LCDs are made with the new mixture and the temperature dependence is measured. The temperature dependence may need to be estimated again for either a stronger or weaker compensation effect.

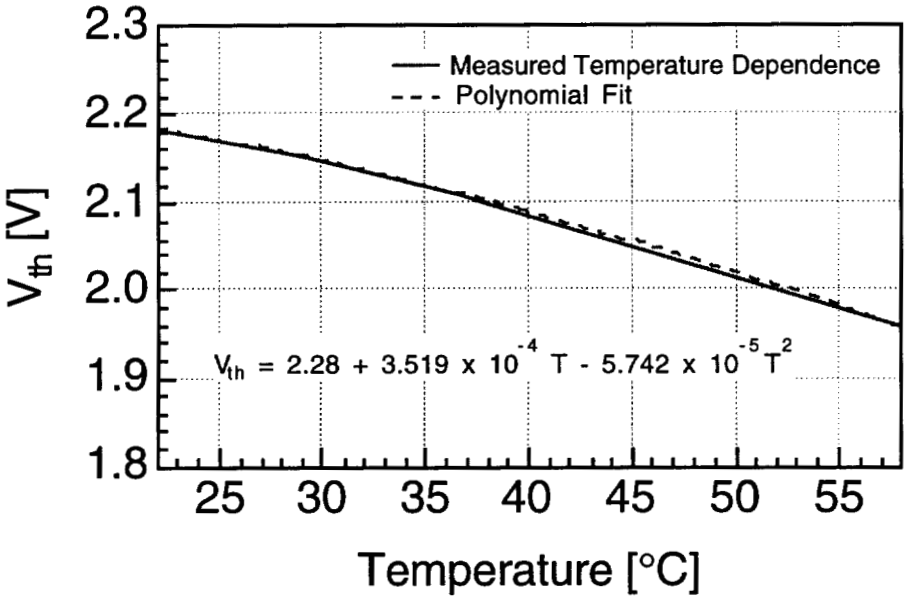

Figure 6.3 Temperature dependence of the threshold voltage V_{th} in the mixture ZLI 4620 1.04 % 9209F. The solid line is the measured dependence and the dashed line is an interpolation.

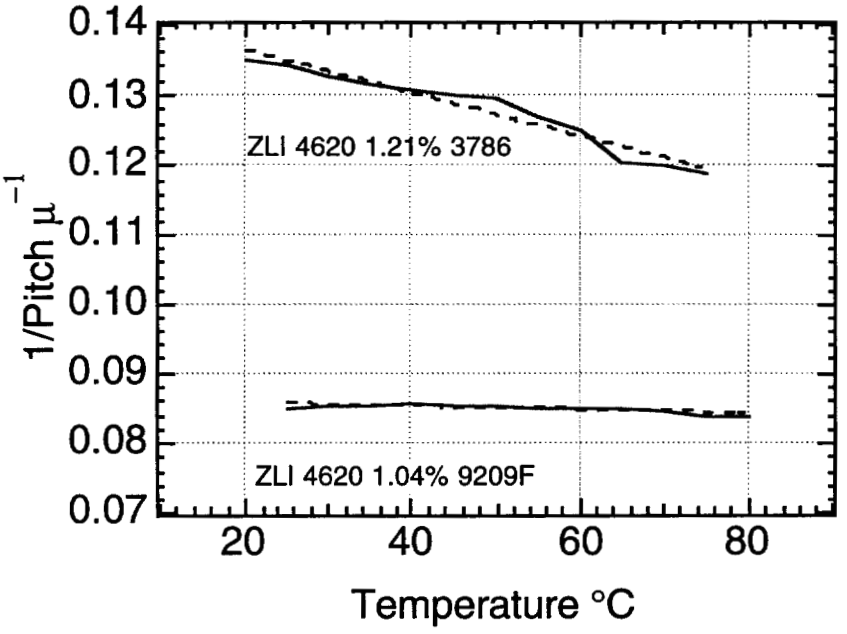

Figure 6.4 Showing the variation of pitch with temperature for two different chiral dopants in ZLI 4620. The solid lines are measured and the dashed lines are interpolations.

6.3 Results

The chiral nematic mixture that we were trying to temperature compensate was used for the yellow cell in a TSTN stack. The cell had a twist of 230° and was filled with ZLI 4620; 1.04% 9209F a left handed chiral dopant. This mixture was one of the least sensitive and the pitch of the mixture was very insensitive to temperature changes. Although this mixture was fairly stable to begin with, the threshold voltage still changed by as much as 4.1% over a 15° temperature range as shown in Figure 6.3. A 4% change in threshold voltage is quite large considering that the available selection ratio for this type of display is only 1.066, leaving a 6.6% voltage margin. This means that a display that is fully off at 25° would be fully on at 55° when kept at the same voltage.

The first estimate for the desired temperature dependence of the pitch was as follows

$$\frac{1}{p} = -0.0833[\mu m^{-1}] - 2.0834\times10^{-4}[\mu m^{-1}{}^{\circ}C^{-1}](T)[^{\circ}C] \qquad (6.5)$$

so that p(0°) = 12μ and p(80°) = 10μ. We made this guess based on two considerations, first the pitch of the new mixture should be close to the pitch of the original mixture at the room temperature, secondly the pitch should become smaller as the temperature is increased as discussed before. This leave us with the two equations

$$(A_{+}c_{+} + A\_c\_) = -8.33\times10^{-2} \qquad (6.6)$$

and

$$(B_{+}c_{+} + B\_c\_) = -2.0834\times10^{-4} \qquad (6.7)$$

where A_+, A_-, B_+ and B_- are given in Table 6.1. These equations give us the solution $c_+ = 1.02\%$ and $c_- = 2.476\%$ for the right and left handed chirals respectively. This mixture was made and the characteristics of the mixture were measured. The measured temperature dependence of the pitch was as follows.

$$\frac{1}{p} = -0.087443[\mu m^{-1}] - 1.7103 \times 10^{-4}[\mu m^{-1} {}^{\circ}C^{-1}](T)[{}^{\circ}C] \qquad (6.8)$$

which has the correct sign in the temperature dependence but with an overall pitch considerably higher than the desired value.

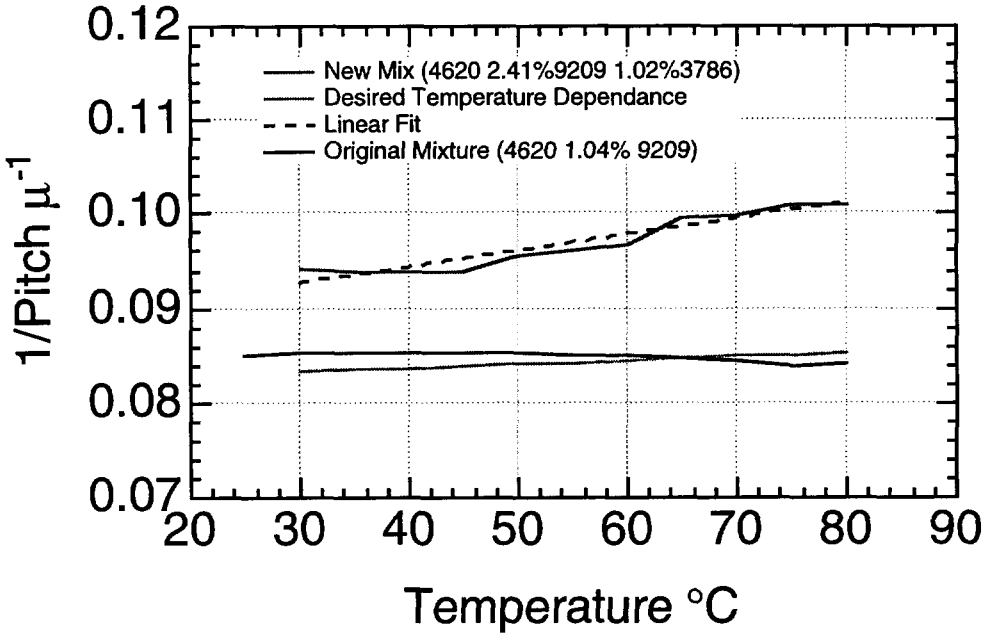

Figure 6.5 Temperature dependence of the inverse pitch for the new mixture compared to the original mix and the desired result.

Next the temperature dependence of the threshold voltage was measured. The cell was driven as a single pixel and the light output was measured as the voltage was varied over a range that included the threshold. This data is acquired for a range of temperature

values thereby giving a series of electro-optic curves from which the temperature dependence of the threshold voltage could be measured. The results of this measurement showed improvement over the original mixture but did not fully succeed in eliminating the temperature dependence effect. Over the range of operation of most TSTN projection displays which is typically 30-45°C, the new mixture showed a 29.6% improvement over the old mixture. For the old mixture, there is a 4.43% change in threshold voltage over the 25°C temperature range while the new mixture showed only a 3.12% change in threshold voltage.

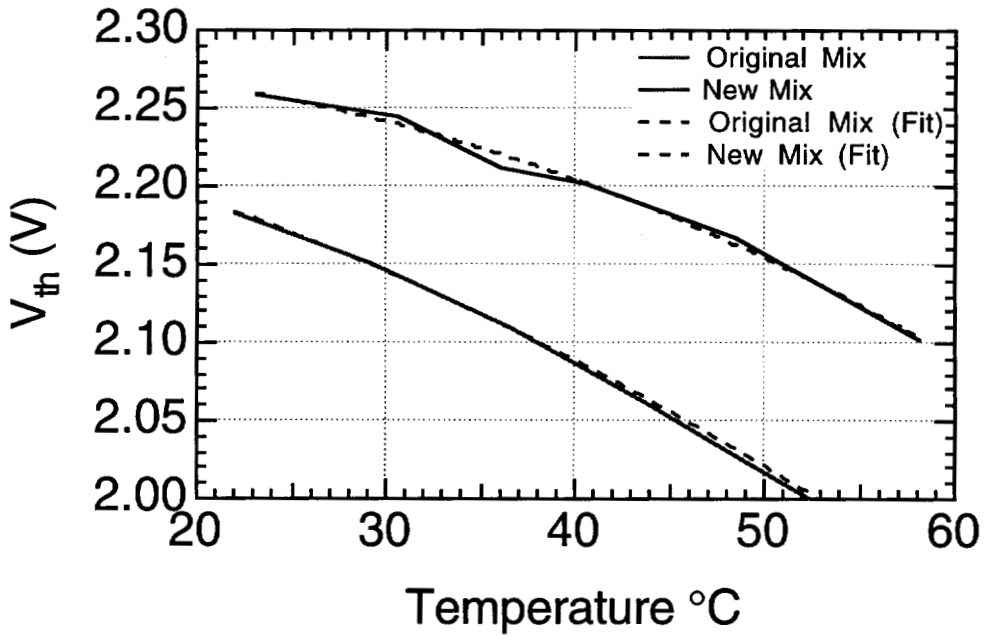

Figure 6.6 The temperature dependence of the threshold voltage in the new mixture as well as the original mix

6.4 Conclusions

Temperature compensation of the threshold voltage in TSTN displays is essential to maintain adequate performance. The previously described in-situ compensation

method in which left and right handed chiral dopants are mixed to cancel the underlying temperature dependence of the pitch is extremely promising. A 29% improvement in temperature dependence is especially good considering that these results represent a first pass attempt only. It is quite possible that these results could be significantly improved with a second or third pass.

7 CONCLUSION

The design and fabrication of TSTN displays requires a thorough understanding of many device parameters and techniques that are involved. The interrelation of the variables involved such as LC materials, color polarizers as well as the design considerations make modeling of STN devices essential to the development of this technology.

Investigations into the theoretical limits of subtractive color displays indicate that the technology is capable of very high transmission and extremely good color gamut although without better color polarizers, subtractive displays will continue to be plagued by poor performance in contrast as compared to additive systems. Analysis on the theoretical performance of the four different types of subtractive color TSTN shows that the currently popular design using a yellow cell in the center with birefringence colors and neutral polarizers offers the best contrast transmission and colors.

The Jones matrix approach to numerical simulation of non-depolarizing optical elements is a fast, accurate way to model LCDs. Integration of this type of simulation with the design of TSTN cells can be extremely useful as an aid to optimize the displays. We have designed a highly intuitive TSTN modeling program which can be used to easily change several variables simultaneously and give immediate visual response. Several designs were modeled and LCD devices were fabricated to verify the predicted display performance. The results indicate a very good match between modeled and measured results.

One effect that simulation is unable to predict is the temperature variation of device parameters. In the quest for better performing LCDs an investigation into the viability of *in-situ* temperature compensation was initiated. LCD temperature variations were documented and used to develop new LC mixtures whose temperature effects were predicted to be smaller. Display devices with the new mixtures were fabricated and the temperature variations were measured. The newly developed mixtures were successful in improving the performance somewhat, but procedure will need to be repeated for further improvements.

As the major LCD manufacturers continue to place most of their research money at active matrix LCDs, the TSTN will not likely develop at the same rate. There is, however opportunity to use the optimization procedure of this investigation for active matrix TN displays. The only obstacle being the availability of very good color polarizers. In the meantime, STN displays are still cheaper than active matrix displays and there is the possibility of improved performance with the implementation of Active Addressing technology. I look forward to seeing the first TSTN display with video rate performance and enhanced contrast when Active Addressing finally becomes commercially available.

REFERENCES

[1] W. F. Goede, "Status of Electronic Displays," *SID Seminar Lecture Notes,* **1**, M-0/1 (1994).

[2] C. N. King, "Electroluminescent Displays," *SID Seminar Lecture Notes*, **1**, M-9/1 (1994).

[3] N. O. Greenham and R. H. Friend, "Solid State Physics", **49**, p. 1, (1995).

[4] L. F. Weber, "Plasma Displays," *SID Seminar Lecture Notes*, **1**, M-9/1, (1995).

[5] T. J. Scheffer and J. Nehring, "SuperTwisted-Nematic (STN) LCDs," *SID Seminar Lecture Notes,* **1**, M-1/1, (1995).

[6] H. Amstutz, D. Heimgartner, M. Kaufmann and T. J. Scheffer, Swiss patent application no. 3819/83, July 12, (1983).

[7] L. E. Tannas, "Color in Electronic Displays," *Physics Today* p. 52, Dec. (1992).

[8] A. Connor, J. R. Biles and G. B. Kingsley, "Ultimate Limits for Subtractive Color Display Systems," *SID Application Notes* (1993).

[9] A. R. Connor, "Subtractive Color STN-LCD Display," *SID Application Notes (SID '92)* p. 83 May (1992).

[10] Sharp EL-8010 Pocket Calculator

[11] M. Schadt and W. Helfrich, "Voltage-Dependent Optical Activity of a Twisted Nematic Liquid Crystal," *Appl. Phys. Lett.*, **18**, p. 127, (1971).

[12] P. M. Alt and P. Pleshko, "Scanning limitations of Liquid-Crystal Displays", *IEEE Trans. Electron Devices*, **ED-21**, p. 146, (1974).

[13] M. G. Clark, J. L. Glasper, I. A. Shanks and C. J. T. Smith, "New Applications for Waveform Identity Addressing of LCDs" Proc. SID **26** p. 147 (1985).

[14] A. J. Lowe, "Active Matrix Development" *IEE Colloquium on Graphic Display Devices*, **71** p. 27 (1989).

[15] T. J. Scheffer, J. Nehring, M. Kaufmann, H. Amstutz, D. Heimgartner, and P. Eglin, " 24*80 Character LCD Panel Using the Supertwisted Birefringence Effect" *SID Digest of Technical Papers* p. 416, 120-3, (1985).

[16] B. Bahadur, *Liquid Crystals: Applications and Uses* Vols. I-III, World Scientific Singapore, (1990).

[17] E. Hecht and A. Zajac, *Optics*, Addison Wesley MA (1974).

[18] E. Jakeman and E.P. Raynes, "Electro-Optic Response Times In Liquid Crystals" *Physics Letters,* **39a,** No. 1, p. 69, (1972).

[19] Alt, P. M. and Pleshko, P., "Scanning limitations of Liquid-Crystal Displays", IEEE Trans. Electron Devices **ED-21**, pp. 146-155 (1974).

[20] J. Nehring and A. Kmetz, "Ultimate Limits for Matrix Addressing of RMS-Responding Liquid-Crystal Displays", IEEE Trans. Electron Devices, **ED-26**, pp. 795-802 (1979).

[21] T. J. Scheffer, (Personal Correspondence, Motif Inc. , 1994-1996)

[22] C. H. Gooch and H. A. Tarry, "The Optical Properties of Twisted Nematic Liquid Crystal Structures with Twist Angles ≤ 90°," *J. Appl. Phys.*, **8**, pp. 1575-1584 (1975).

[23] J. Nehring and T. J. Scheffer, "On the Electric Field Induced Stripe Instability Threshold of Twisted Nematic Layers," *Z. Naturforsch.* **45a**, pp. 867-872 (1990).

[24] Tannas, L. E., "Color in Electronic Displays", *Physics Today*, p. 52, Dec. (1992).

[25] D. L. MacAdam, *Color Measurement: Themes and Variations*, 2nd. ed., Springer Verlag, (1985).

[26] P. Keller, "1976 CIE - UCS Chromaticity Diagram With Color Boundaries," *Proceedings of the SID*, **24/4**, (1983).

[27] T. J. Scheffer, "Liquid Crystal Color Displays," *Non-Emissive Displays*, Ed. A. Kmetz and F. K. VonWillisen, Addison Wesley, pp. 45-79 (1975).

[28] A. R. Connor, "Evolution of the Stacked Color LCD," *SID Application Notes, SID '92*, pp. 109-112 May (1992).

[29] G. Wysecki and S. Stiles, *Color Science: Concepts and Methods, Qualitative Data and Formulae*, 2nd ed., Wiley, New York (1982).

[30] M. R. Pointer, "The Gamut of Real Surface Colours," *Color Research and Application*, **5**, No. 3, (1980).

[31] P. Candry, K. Henry, B. Verniest and W. Schorpion, "A High-Light-Output Active-Matrix TN-LC Projector for Video and Data-Graphics Applications," *Proceeding, SID 93* , pp. 291-294, May (1993).

[32] B. A. Loiseaux, C. Joubert, A. Delboulbé, J. P. Huignard and D. Battarel, "Compact Spatio-Chromatic Single-LCD Projection Architecture," *Asia Display Proceedings*, **S7-4** p. 87, (1995).

[33] D. W. Berreman, and T. J. Scheffer, "Reflection and Transmission by Single-Domain Cholesteric Liquid Crystal Films: Theory and Verification," *Mol. Cryst. Liq. Cryst.*, **11** (4), (1970).

[34] J. D. Jackson, *Classical Electrodynamics*, Wiley, New York, (1962).

[35] D. W. Berreman, "Optics in Smoothly Varying Anisotropic Planar Structures: Applications to Liquid Crystal Twist Cells," Jnl. Opt. Soc Amer., 63 (11), pp. 1374-1380 (1973).

[36] R.C. Jones, "A New Calculus For the Treatment of Optical Systems IV," *J. Opt. Soc. Am.* **32**, pp. 486-492 (1942).

[37] T. J. Scheffer and J. Nehring, "Optimization of Contrast Ratio in Reverse-Polarizer, Transmissive Type Twisted Nematic Displays," *J. Appl. Phys.* **56**, p. 908, (1984).

[38] E. P. Raynes, and R. J. A. Tough, "The Guiding of Plane Polarized Light By Twisted Liquid Crystal Layers," *Mol. Cryst. Liq. Cryst. Letters,* **2** (5), pp. 139-145, (1985).

[39] G. Baur, G. Windscheid and D. W. Berreman, "Optical Properties of a Nematic Twist Cell," Jnl Appl Phys. 8 (2), pp. 101-106 (1975).

[40] W. A. Shurcliff and S. S. Ballard, *Polarized Light*, Van Nostrand, Princeton, New Jersey (1964).

[41] M. C. Mauguin, "Sur les cristaux liquides de Lehmann," *Bull. Soc. franc. Miner.* **34**, pp. 71-117, (1911).

[42] Hl. de Vries, "Rotary Power and Other Optical Properties of Certain Liquid Crystals," *Acta Crystallographica,* **4**, pp. 219-226 (1951).

[43] E.P. Raynes, "The Optical Properties Of Supertwisted Liquid Crystal Layers," *Mol Cryst. Liq. Cryst. Letters,* **4**, pp. 69-75, (1986).

[44] A. Lien, "The General And Simplified Jones Matrix Representations For The High Pretilt Twisted Nematic Cell," *J. Appl. Phys.,* **67** (6), p. 2853, (1990).

[45] S. Chandrasekhar, G. S. Ranganath, U. D. Kini and K. A. Suresh, "Theory of the Optical Properties of Non-absorbing Compensated Cholesteric Liquid Crystals," *Mol. Cryst. Liq. Cryst.*, **24**, pp. 201-211, (1973).

[46] P. A. Breddels, H. A. van Sprang and J. Bruinink, "Influence of Dispersion on the Transmission Characteristics of Supertwisted Nematic Effects in Liquid-Crystal Displays," *J. Appl. Phys.,* **62** (5), p. 1964, (1987).

[47] T. J. Scheffer and B. Clifton, " Active Addressing for High-Contrast Video-Rate STN Displays," *Proceeding, SID "92* May (1992).

[48] R. A. Soref and M. J. Rafuse, "Electrically Controlled Birefringence Of Thin Nematic Films," *J. Appl. Phys.*, **43** (5) p. 2029 (1972).

[49] T.J. Scheffer and J. Nehring, "Investigation Of The Electro-Optical Properties Of 270° Chiral Nematic Layers In The Birefringence Mode," *J. Appl. Phys.*, **58** (8) pp. 3022-3031, (1985).

[50] Product Brochure, "Licristal, Liquid Crystal Mixtures for Electro-Optic Displays," Merck KGaA, Darmstadt, Germany, Update September 1997

[51] A. Conner and P. Gulick, "High Resolution Display System Based on Mutually Compensated STN-LCD Layers," *SID 1991 Digest of Technical Papers XXII*, pp. 755-757 (1991).

[52] K. Kathos, Y. Endo, M. Adatsuka, M. Ohgaara and K. Sawada, "Application of Retardation Compensation; A New Highly Multiplexable Black-White Liquid Crystal Display with Two Supertwisted Nematic Layers," *Jpn. J. Appl. Phys.* **26**, L1784, (1987).

[53] D.W. Berreman, "Dynamics of Liquid Crystal Twist Cells," *Appl. Phys. Lett.*, **25** (1) pp. 12-15, (1974).

[54] G. Weber, H. J. Plach, S. Naemura and B. Scheuble, " Influence of Material Parameters on the Temperature Dependence of the Electrooptic Characteristic of STN Displays," *Proc. 9Th International Display Research Conference (Japan Display '89)*, pp. 532-535, (1989).

[55] F. Moia, "How to Dope Liquid Crystal Mixtures in Order to Ensure Optimum Pitch and to Compensate the Temperature Dependence," F. Hoffmann- La Roche Ltd. Liquid Crystals Division (1990).

APENDIX 1 CODE LISTING FOR TSTN DEVICE SIMULATOR

This is the code listing without the graphical user interface. Icluding the subroutines which calculate both the trnasmission data as well as the CIE data.

```
C*********
C*********
c       The graf subroutine is the guts of the program, it does the transmission calculation
c       and plot the data in the windows.
      SUBROUTINE GRAF(IDELM1,IDELM2,IDELY1,IDELY2,IDELC1,IDELC2,
     1 ITWIM,ITWIY,ITWIC,IMLC,IYLC,ICLC,IRUBM,IRUBY,IRUBC,
     1 IRET1,IRET2,IRET3,IRET4,IGAM1,IGAM2,IGAM3,IGAM4,
     1 IRF1,IRF2,IRF3,IRF4,IMPSI,IAPSI,IPPSI,ICPSI,
     1 MTRPL,MTRPR,ATRPL,ATRPR,PTRPL,PTRPR,CTRPL,CTRPR,
     1 CON,TRANS,INL,TRANC,COL)
$INCLUDE:HLTBI.CON
$INCLUDE:LLTBI.CON
      COMPLEX*8 MA,MB,YA,YB,CA,CB,P1,P2,P3,P4,Q1,Q2,Q3,Q4
      COMPLEX*8 S1,T1,S2,T2,EX1,EY1,EX2,EY2
      COMPLEX*8 C11,C12,C21,C22,Y11,Y12,Y21,Y22,M11,M12,M21,M22
     COMPLEX*8 MAA,MBB,YAA,YBB,CAA,CBB
     REAL*4 TRANS(201,9),TTs(201,9),TRANSNS(201),TRANC(81,9)
     REAL*4 PTRPL(201),PTRPR(201),MTRPL(201),MTRPR(201)
     REAL*4 ATRPL(201),ATRPR(201),CTRPL(201),CTRPR(201)
      REAL*4 PTPL,PTPR,ATPL,ATPR,MTPL,MTPR,CTPL,CTPR
      REAL*4 MLP,CLP,ALP,PLP,PI
      REAL*4 CPOL11,CPOL12,CPOL21,CPOL22,APOL11,APOL12,APOL21,APOL22
      REAL*4 PPOL11,PPOL12,PPOL21,PPOL22,MPOL11,MPOL12,MPOL21,MPOL22
     INTEGER*2 CON,NX,INL,COL(9)
     INTEGER*4 BLACK,WHITE,RED,GREEN,BLUE,CYAN,MAGENTA,YELLOW
c     INTEGER*4 WNDPTR
     PARAMETER(BLACK=33,WHITE=30,RED=205,GREEN=341,BLUE=409)
     PARAMETER(CYAN=273,MAGENTA=137,YELLOW=69)
      PI=3.141592654
      SR2=SQRT(2.)
      DR=PI/180.0
      DISPMLC=0.01*REAL(IMLC)-1.0
      DISPYLC=0.01*REAL(IYLC)-1.0
      DISPCLC=0.01*REAL(ICLC)-1.0
      DISPRF1=0.01*REAL(IRF1)-1.0
      DISPRF2=0.01*REAL(IRF2)-1.0
      DISPRF3=0.01*REAL(IRF3)-1.0
      DISPRF4=0.01*REAL(IRF4)-1.0
      CONMLC=1.0+0.35206*DISPMLC
      CONYLC=1.0+0.35206*DISPYLC
      CONCLC=1.0+0.35206*DISPCLC
      CONRF1=1.0+0.35206*DISPRF1
      CONRF2=1.0+0.35206*DISPRF2
```

```
 CONRF3=1.0+0.35206*DISPRF3
 CONRF4=1.0+0.35206*DISPRF4
TWIM=REAL(ITWIM)*DR
CTWIM=COS(TWIM)
STWIM=SIN(TWIM)
TWIY=REAL(ITWIY)*DR
CTWIY=COS(TWIY)
STWIY=SIN(TWIY)
TWIC=REAL(ITWIC)*DR
CTWIC=COS(TWIC)
STWIC=SIN(TWIC)
 PSIM=REAL(IMPSI)*DR
 PSIA=REAL(IAPSI)*DR
 PSIP=REAL(IPPSI)*DR
 PSIC=REAL(ICPSI)*DR
 CPSIM=COS(PSIM)
 SPSIM=SIN(PSIM)
  CSPSIM=CPSIM*SPSIM
  CPSIM2=CPSIM*CPSIM
  SPSIM2=SPSIM*SPSIM
 CPSIA=COS(PSIA)
 SPSIA=SIN(PSIA)
  CSPSIA=CPSIA*SPSIA
  CPSIA2=CPSIA*CPSIA
  SPSIA2=SPSIA*SPSIA
  CPSIP=COS(PSIP)
  SPSIP=SIN(PSIP)
   CSPSIP=CPSIP*SPSIP
   CPSIP2=CPSIP*CPSIP
   SPSIP2=SPSIP*SPSIP
  CPSIC=COS(PSIC)
  SPSIC=SIN(PSIC)
   CSPSIC=CPSIC*SPSIC
   CPSIC2=CPSIC*CPSIC
   SPSIC2=SPSIC*SPSIC
RUBM=REAL(IRUBM)*DR
RUBY=REAL(IRUBY)*DR
RUBC=REAL(IRUBC)*DR
CRUBM=COS(RUBM)
SRUBM=SIN(RUBM)
CSRUBM=SRUBM*CRUBM
CRUBM2=CRUBM*CRUBM
SRUBM2=SRUBM*SRUBM
CRUBY=COS(RUBY)
SRUBY=SIN(RUBY)
CSRUBY=SRUBY*CRUBY
CRUBY2=CRUBY*CRUBY
SRUBY2=SRUBY*SRUBY
CRUBC=COS(RUBC)
SRUBC=SIN(RUBC)
CSRUBC=SRUBC*CRUBC
```

```
      CRUBC2=CRUBC*CRUBC
      SRUBC2=SRUBC*SRUBC
      GAM1R=(REAL(IGAM1)*DR-PI/2)
      GAM2R=(REAL(IGAM2)*DR-PI/2)
      GAM3R=(REAL(IGAM3)*DR-PI/2)
      GAM4R=(REAL(IGAM4)*DR-PI/2)
      CGAM1R=COS(GAM1R)
      SGAM1R=SIN(GAM1R)
      CGAM2R=COS(GAM2R)
      SGAM2R=SIN(GAM2R)
      CGAM3R=COS(GAM3R)
      SGAM3R=SIN(GAM3R)
      CGAM4R=COS(GAM4R)
      SGAM4R=SIN(GAM4R)
      T1M=TWIM/PI
      T11M=T1M*T1M
      T1Y=TWIY/PI
      T11Y=T1Y*T1Y
      T1C=TWIC/PI
      T11C=T1C*T1C
C
      DO 40 J=1,8
      IF (COL(J).EQ.0) GOTO 40
      IF (J.EQ.1) THEN
      CALL MACTBX(FORCOLOR,BLACK)
      IDELM=IDELM1
      IDELY=IDELY1
      IDELC=IDELC1
      ENDIF
      IF (J.EQ.2) THEN
      CALL MACTBX(FORCOLOR,BLACK)
      IDELM=IDELM2
      IDELY=IDELY2
      IDELC=IDELC2
      ENDIF
      IF(J.EQ.3)THEN
      CALL MACTBX(FORCOLOR,BLUE)
      IDELM=IDELM2
      IDELY=IDELY1
      IDELC=IDELC2
      ENDIF
      IF(J.EQ.4)THEN
      CALL MACTBX(FORCOLOR,GREEN)
      IDELM=IDELM1
      IDELY=IDELY2
      IDELC=IDELC2
      ENDIF
       IF (J.EQ.5)THEN
       CALL MACTBX(FORCOLOR,RED)
      IDELM=IDELM2
      IDELY=IDELY2
```

```
IDELC=IDELC1
 ENDIF
 IF (J.EQ.6)THEN
 CALL MACTBX(FORCOLOR,CYAN)
IDELM=IDELM1
IDELY=IDELY1
IDELC=IDELC2
 ENDIF
 IF (J.EQ.7)THEN
 CALL MACTBX(FORCOLOR,YELLOW)
 IDELM=IDELM1
IDELY=IDELY2
 IDELC=IDELC1
 ENDIF
 IF (J.EQ.8)THEN
 CALL MACTBX(FORCOLOR,MAGENTA)
 IDELM=IDELM2
IDELY=IDELY1
 IDELC=IDELC1
 ENDIF
DO 10 I=1,INL
IF (INL.EQ.21) THEN
 II = 10*I-9
 NX=290+12*(I-1)
 WL=380.+20.*(I-1)
ENDIF
IF (INL.EQ.41)THEN
 II = 5*I-4
 NX=290+6*(I-1)
 WL=380.+10.*(I-1)
ENDIF
IF (INL.EQ.201)THEN
 II = I
 NX=290+NINT(1.2*(I-1))
 WL=380.+2.*(I-1)
ENDIF
ATPL=SQRT(ATRPL(II))
ATPR=SQRT(ATRPR(II))
PTPL=SQRT(PTRPL(II))
PTPR=SQRT(PTRPR(II))
 PLP=PTPL-PTPR
 ALP=ATPL-ATPR
MTPL=SQRT(MTRPL(II))
 MTPR=SQRT(MTRPR(II))
CTPL=SQRT(CTRPL(II))
 CTPR=SQRT(CTRPR(II))
 MLP=MTPL-MTPR
 CLP=CTPL-CTPR
WL2=WL*WL
DELNDM=REAL(IDELM)*(1.0+0.74237*DISPMLC*
1 (445956.8/WL2-1.0))/CONMLC
```

```
      DELNDY=REAL(IDELY)*(1.0+0.74237*DISPYLC*
     1 (445956.8/WL2-1.0))/CONYLC
      DELNDC=REAL(IDELC)*(1.0+0.74237*DISPCLC*
     1 (445956.8/WL2-1.0))/CONCLC
      T2M=DELNDM/WL
      T22M=T2M*T2M
      T2Y=DELNDY/WL
      T22Y=T2Y*T2Y
      T2C=DELNDC/WL
      T22C=T2C*T2C
      ARGM=SQRT(T11M+T22M)
      BETAM=PI*ARGM
      SBM=SIN(BETAM)/ARGM
      IF (BETAM.EQ.0) SBM=PI
      ARGY=SQRT(T11Y+T22Y)
      BETAY=PI*ARGY
      SBY=SIN(BETAY)/ARGY
      IF (BETAY.EQ.0) SBY=PI
      ARGC=SQRT(T11C+T22C)
      BETAC=PI*ARGC
      SBC=SIN(BETAC)/ARGC
      IF (BETAC.EQ.0) SBC=PI
      CBM=COS(BETAM)
      CBY=COS(BETAY)
      CBC=COS(BETAC)
      MA=CMPLX( CTWIM*CBM+T1M*STWIM*SBM,-T2M*CTWIM*SBM)
      MB=CMPLX(-STWIM*CBM+T1M*CTWIM*SBM,-T2M*STWIM*SBM)
      YA=CMPLX( CTWIY*CBY+T1Y*STWIY*SBY,-T2Y*CTWIY*SBY)
      YB=CMPLX(-STWIY*CBY+T1Y*CTWIY*SBY,-T2Y*STWIY*SBY)
C
      CA=CMPLX( CTWIC*CBC+T1C*STWIC*SBC,-T2C*CTWIC*SBC)
      CB=CMPLX(-STWIC*CBC+T1C*CTWIC*SBC,-T2C*STWIC*SBC)
      RET1=REAL(IRET1)*(1.0+0.74237*DISPRF1*
     1 (445956.8/WL2-1.0))/CONRF1
      RET2=REAL(IRET2)*(1.0+0.74237*DISPRF2*
     1 (445956.8/WL2-1.0))/CONRF2
      RET3=REAL(IRET3)*(1.0+0.74237*DISPRF3*
     1 (445956.8/WL2-1.0))/CONRF3
      RET4=REAL(IRET4)*(1.0+0.74237*DISPRF4*
     1 (445956.8/WL2-1.0))/CONRF4
      TMP1=PI*RET1/WL
      TMP2=PI*RET2/WL
      TMP3=PI*RET3/WL
      TMP4=PI*RET4/WL
      CD1=COS(TMP1)
      CD2=COS(TMP2)
      CD3=COS(TMP3)
      CD4=COS(TMP4)
      SD1=SIN(TMP1)
      SD2=SIN(TMP2)
      SD3=SIN(TMP3)
```

```
      SD4=SIN(TMP4)
      P1=CMPLX(CD1,COS(2.0*GAM1R)*SD1)
      P2=CMPLX(CD2,COS(2.0*GAM2R)*SD2)
      P3=CMPLX(CD3,COS(2.0*GAM3R)*SD3)
      P4=CMPLX(CD4,COS(2.0*GAM4R)*SD4)
      Q1=CMPLX(0.0,SGAM1R*CGAM1R*2.0*SD1)
      Q2=CMPLX(0.0,SGAM2R*CGAM2R*2.0*SD2)
      Q3=CMPLX(0.0,SGAM3R*CGAM3R*2.0*SD3)
      Q4=CMPLX(0.0,SGAM4R*CGAM4R*2.0*SD4)
      MPOL11=MTPL*CPSIM2+MTPR*SPSIM2
      MPOL12=MLP*(CSPSIM)
      MPOL21=MLP*(CSPSIM)
      MPOL22=MTPL*SPSIM2+MTPR*CPSIM2
      APOL11=ATPL*CPSIA2+ATPR*SPSIA2
      APOL12=ALP*(CSPSIA)
      APOL21=ALP*(CSPSIA)
      APOL22=ATPL*SPSIA2+ATPR*CPSIA2
      PPOL11=PTPL*CPSIP2+PTPR*SPSIP2
      PPOL12=PLP*(CSPSIP)
      PPOL21=PLP*(CSPSIP)
      PPOL22=PTPL*SPSIP2+PTPR*CPSIP2
      CPOL11=CTPL*CPSIC2+CTPR*SPSIC2
      CPOL12=CLP*(CSPSIC)
      CPOL21=CLP*(CSPSIC)
      CPOL22=CTPL*SPSIC2+CTPR*CPSIC2
c
      MAA=(CRUBM2*MA)+(SRUBM2*CONJG(MA))+
     1    (CSRUBM*(CONJG(MB)-MB))
      MBB=(CRUBM2*MB)+(SRUBM2*CONJG(MB))+
     1    (CSRUBM*(MA-CONJG(MA)))
      YAA=(CRUBY2*YA)+(SRUBY2*CONJG(YA))+
     1    (CSRUBY*(CONJG(YB)-YB))
      YBB=(CRUBY2*YB)+(SRUBY2*CONJG(YB))+
     1    (CSRUBY*(YA-CONJG(YA)))
      CAA=(CRUBC2*CA)+(SRUBC2*CONJG(CA))+
     1    (CSRUBC*(CONJG(CB)-CB))
      CBB=(CRUBC2*CB)+(SRUBC2*CONJG(CB))+
     1    (CSRUBC*(CA-CONJG(CA)))
c
      M11=P1*(MAA*P2-CONJG(Q2)*MBB)-
     1   Q1*(P2*CONJG(MBB)+CONJG(MAA)*CONJG(Q2))
      M12=P1*(MAA*Q2+MBB*CONJG(P2))+
     1   Q1*(CONJG(MAA)*CONJG(P2)-Q2*CONJG(MBB))
      M21=-CONJG(M12)
      M22= CONJG(M11)
c
      Y11=APOL11*(YAA*PPOL11+YBB*PPOL21)+
     1   APOL12*(CONJG(YAA)*PPOL21-CONJG(YBB)*PPOL11)
      Y12=APOL11*(YAA*PPOL12+YBB*PPOL22)+
     1   APOL12*(CONJG(YAA)*PPOL22-CONJG(YBB)*PPOL12)
      Y21=APOL21*(YAA*PPOL11+YBB*PPOL21)+
```

```
     1   APOL22*(CONJG(YAA)*PPOL21-CONJG(YBB)*PPOL11)
         Y22=APOL21*(YAA*PPOL12+YBB*PPOL22)+
     1   APOL22*(CONJG(YAA)*PPOL22-CONJG(YBB)*PPOL12)
c
         C11=P3*(CAA*P4-CONJG(Q4)*CBB)-
     1   Q3*(P4*CONJG(CBB)+CONJG(CAA)*CONJG(Q4))
         C12=P3*(CAA*Q4+CBB*CONJG(P4))+
     1   Q3*(CONJG(CAA)*CONJG(P4)-Q4*CONJG(CBB))
         C21=-CONJG(C12)
         C22= CONJG(C11)
c
          S1= M11*(Y11*C11+Y12*C21)+
     1     M12*(Y21*C11+Y22*C21)
          T1= M11*(Y11*C12+Y12*C22)+
     1     M12*(Y21*C12+Y22*C22)
          T2= M21*(Y11*C11+Y12*C21)+
     1     M22*(Y21*C11+Y22*C21)
          S2= M21*(Y11*C12+Y12*C22)+
     1     M22*(Y21*C12+Y22*C22)

c         These are the computed electric field vectors
          EX1=(S1*CPOL11+T1*CPOL21)*(MPOL11)+
     1 (S2*CPOL21+T2*CPOL11)*(MPOL12)
          EY1=(S1*CPOL11+T1*CPOL21)*(MPOL21)+
     1 (S2*CPOL21+T2*CPOL11)*(MPOL22)
          EX2=(S1*CPOL12+T1*CPOL22)*(MPOL11)+
     1 (S2*CPOL22+T2*CPOL12)*(MPOL12)
          EY2=(S1*CPOL12+T1*CPOL22)*(MPOL21)+
     1 (S2*CPOL22+T2*CPOL12)*(MPOL22)

          TTs(I,J)= 0.5*REAL(EX1*CONJG(EX1)+EY1*CONJG(EY1)+
     1  EX2*CONJG(EX2)+EY2*CONJG(EY2))

          IF (TTs(I,J).LT.0.002) TTs(I,J) = 0.002

          IF(INL.EQ.41)THEN
          TRANS(5*I-4,J)=TTs(I,J)
          TRANC(2*I,J)=TTs(I,J)
          TRANC(2*I-1,J)=TTs(I,J)
          ENDIF
          IF(INL.EQ.21)THEN
          TRANS(10*I-9,J)=TTs(I,J)
          TRANC(4*I,J)=TTs(I,J)
          TRANC(4*I-1,J)=TTs(I,J)
          TRANC(4*I-2,J)=TTs(I,J)
          TRANC(4*I-3,J)=TTs(I,J)
          ENDIF
          IF(INL.EQ.201)THEN
          TRANS(I,J)=TTs(I,J)
          TRANC(IFIX(FLOAT(I)/2.5)+1,J)=TTs(I,J)
          ENDIF
```

```
      ICR=210-IFIX(2.0*TTs(I,1)/TTs(I,2))
      NY1=210-IFIX(400.0*TTs(I,J))
      IF (CON.EQ.0)THEN
     IF(I.EQ.1) CALL GRAFTB(MOVETO,NX,NY1)
     IF(I.GT.1) CALL GRAFTB(LINETO,1,NX,NY1)
      ENDIF
      IF (CON.EQ.1.AND.J.EQ.2)THEN
     CALL MACTBX(FORCOLOR,BLACK)
     IF(I.EQ.1) CALL GRAFTB(MOVETO,NX,ICR)
     IF(I.GT.1) CALL GRAFTB(LINETO,1,NX,ICR)
     IF(I.EQ.201)GOTO 41
     ENDIF
 10   CONTINUE
 40   CONTINUE
 41   CONTINUE
      RETURN
      END
C
c         this subroutine erases old transmission data and prepares the plot window for new
c         transmission data
    SUBROUTINE ERASE(CON)
$INCLUDE:HLTBI.CON
$INCLUDE:LLTBI.CON
     INTEGER*2 PAT1,PAT2,CON
     DIMENSION PAT1(4),PAT2(4)
    PAT1(1)=2#0101010110101010
    PAT1(2)=2#0101010110101010
    PAT1(3)=2#0101010110101010
    PAT1(4)=2#0101010110101010
    PAT2(1)=2#1111111111111111
    PAT2(2)=2#1111111111111111
    PAT2(3)=2#1111111111111111
    PAT2(4)=2#1111111111111111
     CALL GRAFTB(RECTAN,2,290,10,530,211)
     CALL GRAFTB(PENCHAR,4,PAT1,4)
     DO 10 I=1,4
    IY=40*I+10
    CALL MACTBX(LMOVETO,290,IY)
    CALL MACTBX(LLINETO,530,IY)
10   CONTINUE
     DO 20 I=0,3
    IX=60*I+302
    CALL MACTBX(LMOVETO,IX,10)
    CALL MACTBX(LLINETO,IX,210)
20   CONTINUE
     DO 30 I=0,18
    IX=12*I+302
    CALL MACTBX(LMOVETO,IX,10)
    CALL MACTBX(LLINETO,IX,20)
30   CONTINUE
     DO 40 I=0,18
```

```
      IX=12*I+302
      CALL MACTBX(LMOVETO,IX,210)
      CALL MACTBX(LLINETO,IX,200)
40    CONTINUE
      CALL GRAFTB(PENCHAR,4,PAT2,4)
      CALL GRAFTB(RECTAN,0,290,10,530,211)
      CALL MACTBX(TEXTSIZE,10)
      CALL MACTBX(LMOVETO,290,220)
      CALL MACTBX(DRAWSTRING,3,'400')
      CALL MACTBX(LMOVETO,350,220)
      CALL MACTBX(DRAWSTRING,3,'500')
      CALL MACTBX(LMOVETO,410,220)
      CALL MACTBX(DRAWSTRING,3,'600')
      CALL MACTBX(LMOVETO,470,220)
      CALL MACTBX(DRAWSTRING,3,'700')
      CALL MACTBX(LMOVETO,360,230)
      CALL MACTBX(DRAWSTRING,15,'WAVELENGTH (NM)')
      CALL MACTBX (LMOVETO,275,175)
      CALL MACTBX (DRAWSTRING,2,'10')
      CALL MACTBX (LMOVETO,275,135)
      CALL MACTBX (DRAWSTRING,2,'20')
      CALL MACTBX (LMOVETO,275,95)
      CALL MACTBX (DRAWSTRING,2,'30')
      CALL MACTBX (LMOVETO,275,55)
      CALL MACTBX (DRAWSTRING,2,'40')
      CALL MACTBX (LMOVETO,275,15)
      CALL MACTBX (DRAWSTRING,2,'50')
      CALL MACTBX(SETRECT,RECT,260,20,270,220)
      CALL MACTBX(ERASERECT,RECT)
      IF (CON.EQ.1) THEN
      CALL GRAFTB(DRBOX,8,'CONTRAST',260,50,270,220,1)
      ENDIF
      IF (CON.EQ.0)THEN
      CALL GRAFTB(DRBOX,12,'TRANSMISSION',260,20,270,220,1)
      ENDIF
      CALL MACTBX(TEXTSIZE,12)
      RETURN
      END

C         This subroutine erases the old Cie data and sets up the plot window for new cie data
      SUBROUTINE ERASE2
$INCLUDE:HLTBI.CON
$INCLUDE:LLTBI.CON
      REAL*4 TRIX(69),TRIY(69)
      INTEGER*2 I,II,III,ITRIX,ITRIY
      INTEGER*2 ITRIY0,ITRIX0,ITRIX1,ITRIY1,ITRIX2,ITRIY2
      INTEGER*2 ITRIY3,ITRIX3,ITRIX4,ITRIY4
      INTEGER*4 BLACK,WHITE,RED,GREEN,BLUE,CYAN,MAGENTA,YELLOW
      INTEGER*2 PATT1,PATT2
      DIMENSION PATT1(4),PATT2(4)
      PARAMETER(BLACK=33,WHITE=30,RED=205,GREEN=341,BLUE=409)
```

```
      PARAMETER(CYAN=273,MAGENTA=137,YELLOW=69)

      DATA (TRIX(I),I=1,69)/
     1.17722,.17188,.17213,.17273,.17312,
     1.17313,.17255,.17202,.17143,.17031,.16888,.16690,
     1.16422,.16122,.15644,.15099,.14396,.13550,.12414,
     1.10959,.09126,.06876,.04538,.02346,.00817,.00386,
     1.01387,.03885,.07434,.11415,.15472,.19284,.22962,
     1.26578,.30158,.33740,.37310,.40875,.44406,.47877,
     1.51247,.54479,.57515,.60293,.62704,.64823,.66578,
     1.68010,.69149,.70061,.70796,.71406,.71906,.72305,
     1.72599,.72827,.72997,.73100,.73199,.73272,.73354,
     1.73438,.73463,.73488,.73548,.73636,.73418,.73214,
    1.74359/

      DATA (TRIY(I),I=1,69)/
     1.00000,.00781,.00410,.00455,.00484,
     1.00448,.00476,.00488,.00510,.00579,.00690,.00854,
     1.01086,.01379,.01770,.02274,.02970,.03988,.05781,
     1.08684,.13268,.20071,.29495,.41270,.53842,.65482,
     1.75019,.81202,.83382,.82616,.80583,.78170,.75433,
     1.72432,.69237,.65885,.62445,.58962,.55471,.52020,
     1.48658,.45443,.42423,.39650,.37249,.35139,.33402,
     1.31976,.30835,.29930,.29204,.28594,.28094,.27695,
     1.27401,.27173,.27003,.26900,.26801,.26728,.26646,
     1.26563,.26537,.26512,.26452,.26364,.26582,.26786,
    1.25641/


      PATT1(1)=2#0101010110101010
      PATT1(2)=2#0101010110101010
      PATT1(3)=2#0101010110101010
      PATT1(4)=2#0101010110101010

      PATT2(1)=2#1111111111111111
      PATT2(2)=2#1111111111111111
      PATT2(3)=2#1111111111111111
      PATT2(4)=2#1111111111111111

      CALL GRAFTB(RECTAN,2,370,240,530,400)
      CALL GRAFTB(RECTAN,0,370,240,530,400,PAT2)
      CALL MACTBX(LMOVETO,424,347)
      CALL MACTBX(LLINETO,436,331)
      CALL MACTBX(LLINETO,458,319)
      CALL GRAFTB(PENCHAR,4,PATT1,0)
      DO 10 II=1,9
      IY=16*II+240
      CALL MACTBX(LMOVETO,370,IY)
      CALL MACTBX(LLINETO,530,IY)
10    CONTINUE
      DO 20 III=0,9
```

```
      IX=16*III+370
      CALL MACTBX(LMOVETO,IX,240)
      CALL MACTBX(LLINETO,IX,400)
20    CONTINUE

      DO 2 I=1,69
      CALL MACTBX(PENSIZE,2,2)
      CALL MACTBX(FORCOLOR,BLUE)
      CALL MACTBX(BAKCOLOR,BLUE)
      IF(I.GT.21) CALL MACTBX(BAKCOLOR,CYAN)
      IF(I.GT.22) CALL MACTBX(FORCOLOR,CYAN)
      IF(I.GT.23) CALL MACTBX(BAKCOLOR,GREEN)
      IF(I.GT.25) CALL MACTBX(FORCOLOR,GREEN)
      IF(I.GT.32) CALL MACTBX(BAKCOLOR,YELLOW)
      IF(I.GT.35) CALL MACTBX(FORCOLOR,YELLOW)
      IF(I.GT.41) CALL MACTBX(BAKCOLOR,RED)
      IF(I.GT.46) CALL MACTBX(FORCOLOR,RED)
      ITRIX=386+INT(TRIX(I)*160.0)
      ITRIY=384-INT(TRIY(I)*160.0)
      IF(I.EQ.1) CALL MACTBX(LMOVETO,ITRIX,ITRIY)
      IF(I.GT.1) CALL MACTBX(LLINETO,ITRIX,ITRIY)
2     CONTINUE
      ITRIX=386+INT(TRIX(69)*160.0)
      ITRIY=384-INT(TRIY(69)*160.0)
      ITRIX0=ITRIX-19
      ITRIY0=ITRIY+9
      ITRIX1=ITRIX0-19
      ITRIY1=ITRIY0+9
      ITRIX2=ITRIX1-19
      ITRIY2=ITRIY1+9
      ITRIX3=ITRIX2-19
      ITRIY3=ITRIY2+9
      ITRIX4=386+INT(TRIX(1)*160.0)
      ITRIY4=384-INT(TRIY(1)*160.0)
      CALL MACTBX(LLINETO,ITRIX0,ITRIY0)
      CALL MACTBX(FORCOLOR,MAGENTA)
      CALL MACTBX(LLINETO,ITRIX1,ITRIY1)
      CALL MACTBX(BAKCOLOR,MAGENTA)
      CALL MACTBX(LLINETO,ITRIX2,ITRIY2)
      CALL MACTBX(FORCOLOR,BLUE)
      CALL MACTBX(LLINETO,ITRIX3,ITRIY3)
      CALL MACTBX(BAKCOLOR,BLUE)
      CALL MACTBX(LLINETO,ITRIX4,ITRIY4)

      CALL MACTBX(PENNORMAL)
      CALL MACTBX(FORCOLOR,BLACK)
      CALL MACTBX(BAKCOLOR,WHITE)


      CALL MACTBX(LMOVETO,450,255)
      CALL MACTBX(DRAWSTRING,11,'1931 C.I.E.')
```

```
      CALL MACTBX(LMOVETO,460,271)
      CALL MACTBX(DRAWSTRING,7,'DIAGRAM')

      CALL MACTBX(LMOVETO,410,410)
      CALL MACTBX(DRAWSTRING,2,'.2')
      CALL MACTBX(LMOVETO,442,410)
      CALL MACTBX(DRAWSTRING,2,'.4')
      CALL MACTBX(LMOVETO,474,410)
      CALL MACTBX(DRAWSTRING,2,'.6')
      CALL MACTBX(LMOVETO,512,410)
      CALL MACTBX(DRAWSTRING,2,'.8')
      CALL MACTBX(LMOVETO,442,420)
      CALL MACTBX(DRAWSTRING,1,'x')

      CALL MACTBX (LMOVETO,355,354)
      CALL MACTBX (DRAWSTRING,2,'.2')
      CALL MACTBX (LMOVETO,355,322)
      CALL MACTBX (DRAWSTRING,2,'.4')
      CALL MACTBX (LMOVETO,355,290)
      CALL MACTBX (DRAWSTRING,2,'.6')
      CALL MACTBX (LMOVETO,355,258)
      CALL MACTBX (DRAWSTRING,2,'.8')
      CALL MACTBX (LMOVETO,345,322)
      CALL MACTBX (DRAWSTRING,1,'y')

      RETURN
      END
c
C       subroutine to get character from the integer variables to display in the windows as text
c
      SUBROUTINE INTCHR(X,M)
      CHARACTER*4 X
      N=IABS(M)
      N4=N/1000
      N3=(N-1000*N4)/100
      N2=(N-1000*N4-100*N3)/10
      N1=(N-1000*N4-100*N3-10*N2)
      X(1:1)=CHAR(N4+48)
      X(2:2)=CHAR(N3+48)
      X(3:3)=CHAR(N2+48)
      X(4:4)=CHAR(N1+48)
      IF(N4.NE.0) RETURN
      X(1:1)=CHAR(32)
      IF(N3.NE.0) THEN
      IF(M.GT.0) RETURN
      X(1:1)=CHAR(45)
      RETURN
      END IF
      X(2:2)=CHAR(32)
      IF(N2.NE.0) THEN
      IF(M.GT.0) RETURN
```

```
      X(2:2)=CHAR(45)
      RETURN
      END IF
      X(3:3)=CHAR(32)
      IF(M.LT.0) X(3:3)=CHAR(45)
      RETURN
      END
c
C     This is the routine which calls the graf program to redraw all or parts of the window
c
c
c          this is the subroutine to calculate the cie coordinates of the transmission
c          spectra.
      SUBROUTINE CIEGRAF(X,Y,COLOR)
$INCLUDE:LLTBI.CON
      REAL*4 X,Y
      INTEGER*2 RECT(4),COLOR
      INTEGER*4 BLACK,BLUE,GREEN,RED,CYAN,YELLOW,MAGENTA,WHITE
      PARAMETER(BLACK=33,WHITE=30,RED=205,GREEN=341,BLUE=409)
      PARAMETER(CYAN=273,MAGENTA=137,YELLOW=69)
      IX=386+INT(X*160)
      IY=384-INT(Y*160)
      CALL MACTBX(SETRECT,RECT,IX-1,IY-1,IX+1,IY+1)
       IF (COLOR.EQ.1)CALL MACTBX(FORCOLOR,BLACK)
       IF (COLOR.EQ.2)CALL MACTBX(FORCOLOR,BLACK)
       IF (COLOR.EQ.3)CALL MACTBX(FORCOLOR,BLUE)
       IF (COLOR.EQ.4)CALL MACTBX(FORCOLOR,GREEN)
       IF (COLOR.EQ.5)CALL MACTBX(FORCOLOR,RED)
       IF (COLOR.EQ.6)CALL MACTBX(FORCOLOR,CYAN)
       IF (COLOR.EQ.7)CALL MACTBX(FORCOLOR,YELLOW)
       IF (COLOR.EQ.8)CALL MACTBX(FORCOLOR,MAGENTA)
       CALL MACTBX(PAINTOVAL,RECT)
       CALL MACTBX(FORCOLOR,BLACK)
       RETURN
       END

C     computes normalized tristimulus values bigx,bigy,bigz for a given
C     transmission function over the wavelength range extending from
C     380 nm to 780 nm in 5 nm intervals
      SUBROUTINE FARBE1(LITE)
      REAL*4 TRI(81,3),T(81,9),SRCE(81,6),TEMP(81),XYZ(3)
      INTEGER*2 COL
      DATA (TRI(I,1),I=1,81)/
      1.0014,.0022,.0042,.0076,.0143,.0232,.0435,.0776,.1344,
      1.2148,.2839,.3285,.3483,.3481,.3362,.3187,.2908,.2511,.1954,.1421,
      2.0956,.0580,.0320,.0147,.0049,.0024,.0093,.0291,.0633,.1096,.1655,
      3.2257,.2904,.3597,.4334,.5121,.5945,.6784,.7621,.8425,.9163,.9786,
      41.0263,1.0567,1.0622,1.0456,1.0026,.9384,.8544,.7514,.6424,.5419,
      5.4479,.3608,.2835,.2187,.1649,.1212,.0874,.0636,.0468,.0329,.0227,
      6.0158,.0114,.0081,.0058,.0041,.0029,.0020,.0014,.0010,.0007,.0005,
      7.0003,.0002,.0002,.0001,.0001,.0001,.0000/
```

```
DATA (TRI(I,2),I=1,81)/.0000,.0001,.0001,.0002,
8.0004,.0006,.0012,.0022,.0040,.0073,.0116,.0168,.0230,.0298,.0380,
9.0480,.0600,.0739,.0910,.1126,.1390,.1693,.2080,.2586,.3230,.4073,
8.5030,.6082,.7100,.7932,.8620,.9149,.9540,.9803,.9950,1.000,.995,
7.9786,.9520,.9154,.8700,.8163,.7570,.6949,.6310,.5668,.5030,.4412,
6.3810,.3210,.2650,.2170,.1750,.1382,.1070,.0816,.0610,.0446,.0320,
5.0232,.0170,.0119,.0082,.0057,.0041,.0029,.0021,.0015,.0010,.0007,
4.0005,.0004,.0002,.0002,.0001,.0001,.0001,.0000,.0000,.0000,.0000/
DATA (TRI(I,3),I=1,81)/
3.0065,.0105,.0201,.0362,.0679,.1102,.2074,.3713,.6456,1.0391,
21.3856,1.6230,1.7471,1.7826,1.7721,1.7441,1.6692,1.5281,1.2876,
11.0419,.8130,.6162,.4652,.3533,.2720,.2123,.1582,.1117,.0782,
2.0573,.0422,.0298,.0203,.0134,.0087,.0057,.0039,.0027,.0021,.0018,
3.0017,.0014,.0011,.0010,.0008,.0006,.0003,.0002,.0002,.0001,31*0./
DATA (SRCE(I,1),I=1,81)/
1        9.8,10.9,12.09,13.35,14.71,16.15,17.68,19.29,20.99,22.79,
124.67,26.64,28.70,30.85,33.09,35.41,37.81,40.30,42.87,45.52,48.24,
251.04,53.91,56.85,59.86,62.93,66.06,69.25,72.50,75.79,79.13,82.52,
385.95,89.41,92.91,96.44,100.00,103.58,107.18,110.8,114.44,118.08,
4121.73,125.39,129.04,132.7,136.35,139.99,143.62,147.24,150.84,
5154.42,157.98,161.52,165.03,168.51,171.96,175.38,178.77,182.12,
6185.43,188.70,191.93,195.12,198.26,201.36,204.41,207.41,210.36,
7213.27,216.12,218.92,221.67,224.36,227.00,229.59,232.12,234.59,
8237.01,239.37,241.68/
DATA (SRCE(I,2),I=1,81)/
1                22.4,26.85,31.3,36.18,41.3,46.62,52.1,57.7,
763.2,68.37,73.1,77.31,80.8,83.44,85.4,86.88,88.3,90.08,92.,93.75,
895.2,96.23,96.5,95.71,94.2,92.37,90.7,89.65,89.5,90.43,92.2,94.46,
996.9,99.16,101.,102.2,102.8,102.92,102.6,101.9,101.,100.07,99.2,
898.44,98.,98.08,98.5,99.06,99.7,100.36,101.,101.56,102.2,103.05,
7103.9,104.59,105.,105.08,104.9,104.55,103.9,102.84,101.6,100.38,
699.1,97.7,96.2,94.6,92.9,91.1,89.4,88.,86.9,85.9,85.2,84.8,84.7,
584.9,85.4,85.4,85.4/
DATA (SRCE(I,3),I=1,81)/
1                33.,39.92,47.4,55.17,63.3,71.81,80.60,89.53,
498.1,105.8,112.4,117.75,121.5,123.45,124.,123.6,123.1,123.3,123.8,
3124.09,123.9,122.92,120.7,116.9,112.1,106.98,102.3,98.81,96.9,
296.78,98.,99.94,102.1,103.95,105.2,105.67,105.3,104.11,102.3,
1100.15,97.8,95.43,93.2,91.22,89.7,88.83,88.4,88.19,88.1,88.06,88.,
287.86,87.8,87.99,88.2,88.2,87.9,87.22,86.3,85.3,84.,82.21,80.2,
378.24,76.3,74.36,72.4,70.4,68.3,66.3,64.4,62.8,61.5,60.2,59.2,
458.5,58.1,58.,58.2,58.2,58.2/
DATA (SRCE(I,4),I=1,81)/     50.,52.3,54.6,68.7,82.8,87.1,91.5,
592.5,93.4,90.1,86.7,95.8,104.9,110.9,117.0,117.4,117.8,116.3,
6114.9,115.4,115.9,112.4,108.8,109.1,109.4,108.6,107.8,106.3,
7104.8,106.2,107.7,106.0,104.4,104.2,104.0,102.0,100.0,98.2,96.3,
896.1,95.8,92.2,88.7,89.3,90.0,89.8,89.6,88.6,87.7,85.5,83.3,83.5,
983.7,81.9,80.0,80.1,80.2,81.2,82.3,80.3,78.3,74.0,69.7,70.7,71.6,
873.0,74.3,68.0,61.6,65.7,69.9,72.5,75.1,69.3,63.6,55.0,46.4,56.6,
766.8,65.1,63.4/
DATA (SRCE(I,5),I=1,81)/81*1.0/
```

```
      DATA (SRCE(I,6),I=1,81)/
     1                  54.5,55.3,56.1,57.7,59.2,232.9,53.7,65.4,
     677.1,80.8,84.4,432.8,93.1,97.7,102.3,106.0,109.7,112.1,114.5,
     5115.4,116.2,112.8,109.3,108.0,106.6,106.0,105.4,106.2,106.9,
     4106.3,105.7,104.9,104.0,320.8,101.6,100.8,100.0,99.8,99.5,160.4,
     399.3,99.1,98.8,98.5,98.1,97.4,96.7,97.3,97.8,99.7,101.5,96.3,
     291.0,95.3,99.6,107.2,114.7,93.9,73.0,62.0,50.9,49.0,47.0,40.1,
     133.2,30.1,26.9,24.2,21.5,19.4,17.3,15.8,14.2,12.8,11.3,10.5,9.7,
     29.0,8.3,6.8,5.2/
C     TRI(81,3)=TRISTIMULUS VALUES (X,Y,Z) FOR CIE 1931 STANDARD COLOR-
C     IMETRIC OBSERVER EVERY 5 NM FROM 380 TO 780 NM
C     SRCE(81,6)=CIE STANDARD ILLUMINANTS A,B,C,D65,E,F(7) WHERE:
C           A=BLACKBODY RADIATOR AT 2856 K
C           B=DIRECT SUNLIGHT (CORRECTED COLOR TEMP. APPROX 4870 K)
C           C=AVERAGE DAYLIGHT (CORRECTED COLOR TEMP. APPROX 6500 K)
C         D65=DAYLIGHT (CORRECTED COLOR TEMP. APPROX. 6500 K)
C           E=EQUAL ENERGY ILLUMINATION
C        F(7)=FLUORESCENT LAMP F(7) DATA CONVERTED TO 5 NM INTERVALS
C     **********
C     WRITE OUT TABLE OF CIE DATA
C     WRITE(6,1)
C     FORMAT(1H1,1X,' WL    XBAR    YBAR    ZBAR       A       B',
C    1'       C      D65     F(7)'/)
C     WRITE(6,5)(I,TRI(I,1),TRI(I,2),TRI(I,3),SRCE(I,1),SRCE(I,2),
C    1SRCE(I,3),SRCE(I,4),SRCE(I,6),I=1,81)
C     FORMAT(3X,I2,8F9.4)
C     **********
C     COMPUTE NORMALIZATION FACTOR
      DO 10 I=1,81
      TEMP(I)=TRI(I,2)*SRCE(I,LITE)
 10   CONTINUE
      CALL QSF(5.0,TEMP,TEMP,81)
      XNORM=TEMP(81)
      RETURN
      ENTRY FARBE2(T,COL,XYZ,LITE)
C     T(I,COL)=TRANSMISSION CURVE
C     XYZ(I)=NORMALIZED TRISTIMULUS VALUES
C     LITE=SOURCE ILLUMINANT NUMBER (AS ABOVE)
C     **********
C     COMPUTE NORMALIZED TRISTIMULUS VALUES
      DO 30 J=1,3
      DO 20 I=1,81
      TEMP(I)=T(I,COL)*TRI(I,J)*SRCE(I,LITE)
 20   CONTINUE
      CALL QSF(5.0,TEMP,TEMP,81)
      XYZ(J)=TEMP(81)/XNORM
 30   CONTINUE
      RETURN
      END
C**********SIMPSONS RULE INTEGRATOR *************
      SUBROUTINE QSF(H,Y,Z,NDIM)
```

```
      DIMENSION Y(81),Z(81)
      HT=H/3.0
      L1=1
      L2=2
      L3=3
      L4=4
      L5=5
      L6=6
      IF(NDIM-5) 7,8,1
C     NDIM IS GREATER THAN 5, PREPARATIONS OF INTEGRATION LOOP
1     SUM1=Y(L2)+Y(L2)
      SUM1=SUM1+SUM1
      SUM1=HT*(Y(L1)+SUM1+Y(L3))
      AUX1=Y(L4)+Y(L4)
      AUX1=AUX1+AUX1
      AUX1=SUM1+HT*(Y(L3)+AUX1+Y(L5))
      AUX2=HT*(Y(L1)+3.875*(Y(L2)+Y(L5))+2.625*(Y(L3)+Y(L4))+Y(L6))
      SUM2=Y(L5)+Y(L5)
      SUM2=SUM2+SUM2
      SUM2=AUX2-HT*(Y(L4)+SUM2+Y(L6))
      Z(L1)=0.0
      AUX=Y(L3)+Y(L3)
      AUX=AUX+AUX
      Z(L2)=SUM2-HT*(Y(L2)+AUX+Y(L4))
      Z(L3)=SUM1
      Z(L4)=SUM2
      IF(NDIM-6) 5,5,2
C     INTEGRATION LOOP
2     DO 4 I=7,NDIM,2
      SUM1=AUX1
      SUM2=AUX2
      AUX1=Y(I-1)+Y(I-1)
      AUX1=AUX1+AUX1
      AUX1=SUM1+HT*(Y(I-2)+AUX1+Y(I))
      Z(I-2)=SUM1
      IF(I-NDIM) 3,6,6
3     AUX2=Y(I)+Y(I)
      AUX2=AUX2+AUX2
      AUX2=SUM2+HT*(Y(I-1)+AUX2+Y(I+1))
4     Z(I-1)=SUM2
5     Z(NDIM-1)=AUX1
      Z(NDIM)=AUX2
      RETURN
6     Z(NDIM-1)=SUM2
      Z(NDIM)=AUX1
      RETURN
C     END OF INTEGRATION LOOP
7     IF(NDIM-3) 12,11,8
C     NDIM IS EQUAL TO 4 OR 5
8     SUM2=1.125*HT*(Y(L1)+Y(L2)+Y(L2)+Y(L2)+Y(L3)+Y(L3)+Y(L3)+Y(L4))
      SUM1=Y(L2)+Y(L2)
```

```
      SUM1=SUM1+SUM1
      SUM1=HT*(Y(L1)+SUM1+Y(L3))
      Z(L1)=0.0
      AUX1=Y(L3)+Y(L3)
      AUX1=AUX1+AUX1
      Z(L2)=SUM2-HT*(Y(L2)+AUX1+Y(L4))
      IF(NDIM-5) 10,9,9
 9    AUX1=Y(L4)+Y(L4)
      AUX1=AUX1+AUX1
      Z(L5)=SUM1+HT*(Y(L3)+AUX1+Y(L5))
 10   Z(L3)=SUM1
      Z(L4)=SUM2
      RETURN
C     NDIM IS EQUAL TO 3
 11   SUM1=HT*(1.25*Y(L1)+Y(L2)+Y(L2)-0.25*Y(L3))
      SUM2=Y(L2)+Y(L2)
      SUM2=SUM2+SUM2
      Z(L3)=HT*(Y(L1)+SUM2+Y(L3))
      Z(L1)=0.0
      Z(L2)=SUM1
 12   RETURN
      END
```

VITA

The author was born on July 23, 1966 in Milwaukee, Wisconsin. In 1984, he enrolled in the department of Physics at the University of Wisconsin in Madison Wisconsin. He received his B.S. degree in Physics in May 1988.

The author then attended graduate school in the Department of Physics at the University of Wisconsin-Milwaukee in Milwaukee Wisconsin. He received his M.S. degree in Physics in May 1992.

The author came to Oregon Graduate Institute in 1992 and completed all of the requirements for the Doctor of Philosophy degree in Applied Physics in August 1997. During the course of study, he has received the Wilson Clark Fellowship as well as fellowship support from Motif, Inc. and In Focus Systems, Inc. He is currently employed at Clarity Visual Systems as a technologist and optical engineer.

The author has contributed to the following publications:

[1] J. Fogarty, W. Kong & R. Solanki, "Monte Carlo Simulation of High Field Electron Transport in ZnS," *Solid-State Electronics*, **38**, p. 653, (1995).

[2] W. Kong, J. Fogarty, R. Solanki & R. Tuenge, "White Light Emitting ZnS:PrSrS:Pr Electroluminescent Devices Fabricated via Atomic Layer Epitaxy," *Appl. Phys. Lett.*, **67**, p. 460, (1995).

[3] W. Kong, J. Fogarty & R. Solanki, "Atomic Layer Epitaxy of ZnS:Tb Thin Film Electroluminescent Devices," *Appl. Phys. Lett.*, **65**, p. 936, (1994).

[4] J. Fogarty, W. Kong, and R. Solanki, "Monte Carlo Simulation of Electrical Characteristics of High Field ACTFEL Devices," *SID symposium Digest of Technical Papers*, **P-37**, p. 569, (1994)